MITNE-63

MITNE-63
not extra

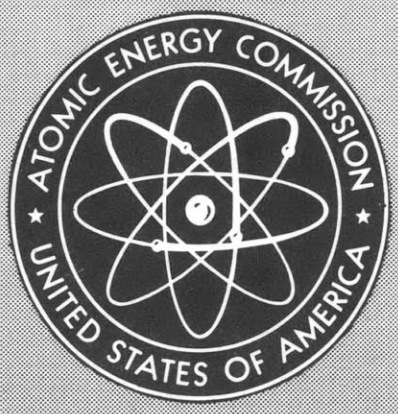

MIT-334-23

FRICTION FACTOR AND HEAT TRANSFER CORRELATION FOR IRRADIATED ORGANIC COOLANTS

By
A. H. Swan
E. A. Mason

September 1965

Department of Nuclear Engineering
Massachusetts Institute of Technology
Cambridge, Massachusetts

UNITED STATES ATOMIC ENERGY COMMISSION • DIVISION OF TECHNICAL INFORMATION

LEGAL NOTICE

Printed in USA. Price $5.00. Available from the Clearinghouse for Federal Scientific and Technical Information, National Bureau of Standards, U. S. Department of Commerce, Springfield, Virginia 22151.

USAEC Division of Technical Information Extension, Oak Ridge, Tennessee

MIT - 334 - 23
CHEMISTRY
(TID - 4500, 47th. Ed.)

FRICTION FACTOR AND HEAT TRANSFER CORRELATION FOR IRRADIATED ORGANIC COOLANTS

by

A. H. Swan
E. A. Mason
(Project Supervisor)

Contributors: W. N. Bley
J. C. Kim
D. T. Morgan

September, 1965

M.I.T. DSR PROJECT NO. 9819

Work Performed for the Savannah River Operations Office,
U. S. Atomic Energy Commission Under
Contract No. AT(38-1)-334

DEPARTMENT OF NUCLEAR ENGINEERING
MASSACHUSETTS INSTITUTE OF TECHNOLOGY
CAMBRIDGE, MASSACHUSETTS 02139

TABLE OF CONTENTS

LIST OF FIGURES

LIST OF TABLES

FRICTION FACTOR AND HEAT TRANSFER CORRELATION FOR IRRADIATED ORGANIC COOLANTS

ABSTRACT

Heat transfer data and friction factor data were taken on Santowax WR over the Reynolds Number range of $10^4 < Re < 10^5$ and it was found to fit the usual correlations, within an uncertainty of $\pm 10\%$.

A comparison was made of other investigators' organic coolant data as well as MIT's Santowax OMP data to try and resolve why some of these data show a Reynolds Number exponent greater than 0.8.

The Dittus-Boelter type equation suggested by McAdams

$$Nu_B = 0.023\ Re_B^{0.8}\ Pr_B^{0.4}$$

or a Colburn-type equation

$$j^* \equiv St\ Pr_B^{0.6} = 0.023\ Re_B^{-0.2} = \frac{f}{8}$$

is recommended to calculate heat transfer factors or friction factors for irradiated organic coolants.

1.0 SUMMARY

Because of the interest in organic coolants for nuclear reactors, extensive heat transfer data have been taken on various coolants at MIT and at other laboratories. Most of the correlations reported for these data have indicated that the Nusselt Number depends on the Reynolds Number to the 0.9 power rather than the 0.8 power, as normally used for heat transfer correlations.

To help to resolve this possible discrepancy, friction factor data were taken on Santowax WR with a newly designed test heater. These data were compared with the heat transfer data for Santowax WR, using a Colburn-type analogy to see if this discrepancy with heat transfer correlations on other coolants could be resolved.

For the data taken at MIT on Santowax WR, either a Dittus-Boelter type equation, for the heat transfer data

$$Nu_B = 0.023\ Re_B^{0.8}\ Pr_B^{0.4}$$

or Colburn-type equation, for both the heat transfer and friction factor data

$$j^* \equiv St\ Pr_B^{0.6} = 0.023\ Re^{-0.2} = \frac{f}{8}$$

were found to correlate the data quite well (within $\pm$10%).

This still left unresolved the MIT Santowax OMP data, which indicates a Reynolds Number dependence of 0.9.

Because of this, a survey of the literature was made to determine how the commonly quoted value of 0.8, for the Reynolds Number exponent, was arrived at.

From this survey and a consideration of the uncertainty in the physical properties and in the heat transfer measurements, the above correlations are recommended for irradiated organic coolants.

2.0 INTRODUCTION

2.1 Purpose of MIT Loop Experiment

The concept of an organic cooled and/or moderated nuclear reactor was proposed in a patent application by Fermi and Szilard dated December, 1944 (1). Since this time the United States Atomic Energy Commission, the AECL of Canada and Euratom of the European Community have financed research and development work to both select the best coolant and to design a reactor. Recent cost studies indicate that organic cooling of a heavy water-moderated reactor will result in a significant reduction of the cost of power generation (1).

Some of the advantages of an organic coolant are:

a. The low vapor pressure of these coolants results in lower capital equipment costs and the design of more compact reactors.

b. The compatibility with standard construction materials such as carbon steel.

c. The low specific activation of organic materials which reduces the shielding requirements of the primary coolant and makes maintenance comparatively simple.

d. The organic coolants provide greater neutron economy than light water.

The major disadvantages of organic coolants are:

a. Organic coolants undergo irreversible radiolytic and thermal degradation which means the coolant must be processed or fresh coolant added. As these materials degrade the heat transfer coefficient decreases and the viscosity increases.

b. The heat transfer characteristics of organic coolants are relatively poor.

c. The possibility of coking or fouling a heat transfer surface if temperature limitations are exceeded or if the coolant is allowed to become contaminated with inorganic particulates.

At MIT an inpile loop has been in operation since August of 1961 to study both the radiolytic and thermal degradation of organic coolants. The coolants that have been investigated at MIT are Santowax OMP and Santowax WR. Both of these are mixtures of ortho-, meta- and para-terphynel and are manufactured by the Monsanto Corporation. A description of these coolants, and similar coolants that are being studied, is presented in Table 1.

Although the inpile studies at MIT are principally to study the degradation rates of organic coolants, considerable work has been done on measuring the physical properties and the heat transfer coefficients of both Santowax OMP and Santowax WR (2) (3).

TABLE 1

COMPOSITION OF VARIOUS UNIRRADIATED ORGANIC COOLANTS

	Ortho	Meta	Para	Biphenyl & Degradation Products	Melting Point ^{o}F
Santowax OMP	~12%	~62%	~25%	< 2%	~350
Santowax WR	~15-20%	~75%	~ 5%	< 2%	~185
Santowax R	~10%	~55%	~20%	~15%	~300
Santowax OM	~62%	~32%	~ 4%	~ 5%	~125
Progil, OM_2	~20%	~76%	~4%	-	~185

2.2 Previous Organic Coolant Heat Transfer Data

Other investigators (4) (5) (6) (10) have also measured the heat transfer coefficient of irradiated organic coolants. The correlations for these data are summarized in Table 2, which also includes the range of important variables covered by each correlation. These same correlations are also plotted in Figure 1 for comparison. Previous data taken at MIT on irradiated Santowax OMP (3) are shown in Figures 2 and 3 for comparison with the usual correlations as summarized in Section 2.3.

While the data presented in Figures 1, 2 and 3 do fall within the uncertainty limits quoted on Equation (1) (presented in Section 2.3) of ±40% (7), it is interesting to note that a Reynolds Number exponent greater than 0.8 gives a better fit to each investigator's data as well as to all of the data grouped together as in Figure 1.

2.3 Usual Correlations of Heat Transfer Factor and Friction Factor Data

The usual heat transfer correlations for forced convection heat transfer are:

The Dittus-Boelter type of McAdams (7) (14)

$$Nu_B = 0.023\ Re_B^{0.8}\ Pr_B^{0.4} \qquad (1)$$

The Colburn type (7) (8)

$$j \equiv St\ Pr_f^{2/3} = 0.023\ Re_f^{-0.2} \qquad (2)$$

TABLE 2

A TABULATION OF HEAT TRANSFER CORRELATIONS FOR ORGANIC COOLANTS

Correlation	Coolants Used	Reynolds No. Range	Prandtl No. Range	Nominal Heat Flux BTU/hr-ft^2	Source
$Nu = 0.015\ Re^{.85}\ Pr^{.30}$ $\pm 9\%$	Unirradiated Biphenyl Santowax R Santowax OM	2×10^4 to 3×10^5	4.5 to 11	4×10^4 to 3×10^5	Atomics International (4)
$Nu = 0.0243\ Re^{.80} Pr^{.40}$ $\pm 20\%$	Unirradiated Santowax R Santowax OM Diphenyl, & Irradiated OMRE Coolant	2×10^5 to 5×10^5	-	-	Atomics International (28) (29)
$Nu = 0.0175\ Re^{.84}\ Pr^{.40}$ $\pm 6\%$	Biphenyl at 0% & 40% HB. A mixture of ortho- & meta-terphenyl & biphenyl at 0% & 30% HB.	1.2×10^4 to 4×10^5	-	4×10^4 to 3×10^5	NRL (5)
$Nu = 0.00835\ Re^{.90}\ Pr^{.40}$ $\pm 6\%$	OM_2 Mixtures of 10%, 20% & 30% HBR	2.6×10^4 to 3.7×10^5	5.5 to 12	1.6×10^5 to 3.2×10^5	Grenoble (6)
$Nu = 0.0079\ Re^{.90}\ Pr^{.40}$ $\pm 10\%$	Irradiated Santowax OMP from 0% to 35% HB	8×10^3 to 10^5	6 to 32	2×10^4 to 2×10^5	MIT (3)
$Nu = 0.0098\ Re^{.88}\ Pr^{.40}$ $\pm 6\%$	Unirradiated Santowax OMP and Santowax OM containing 24% HB	7.5×10^4 to 4×10^5	-	1.5×10^5 to 3.0×10^5	Grenoble (10)

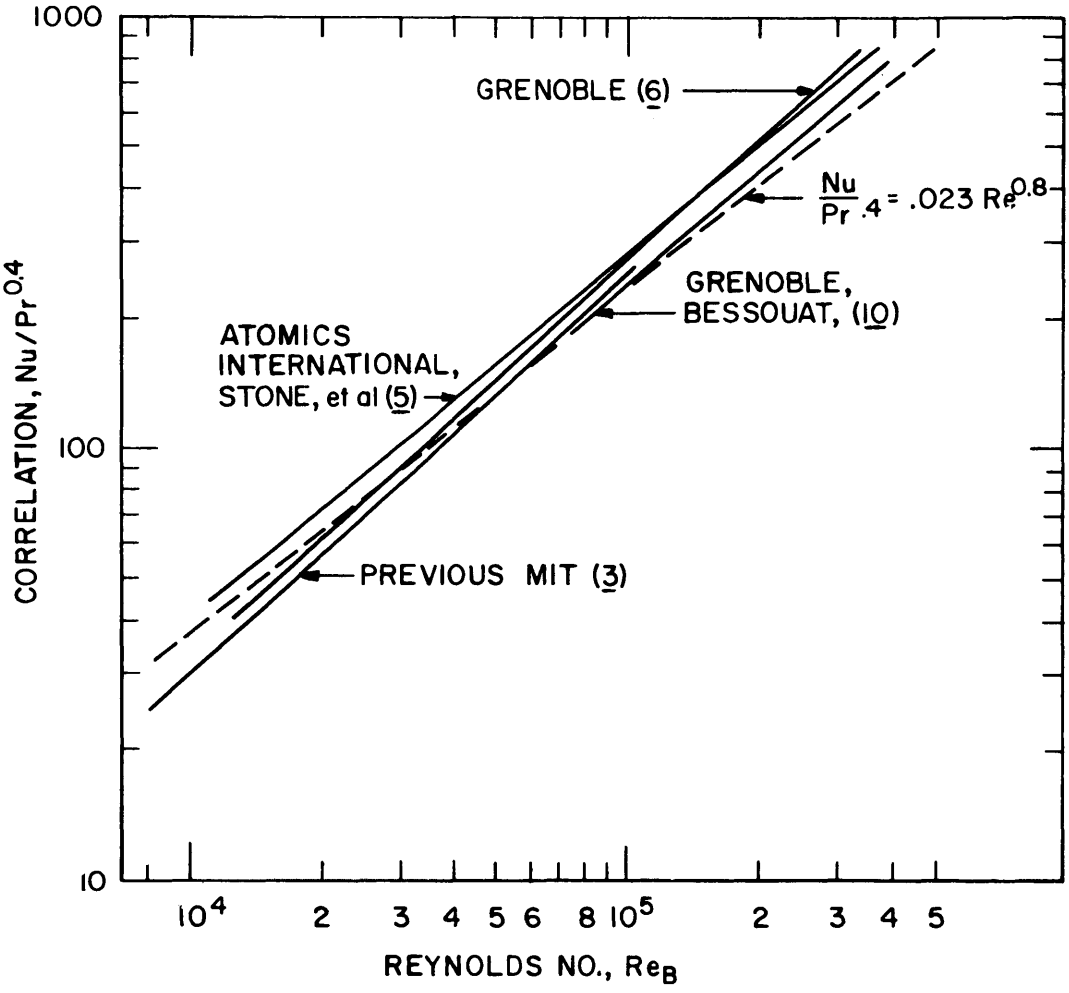

FIG. 1 COMPARISON OF HEAT TRANSFER CORRELATIONS FOR ORGANIC COOLANTS

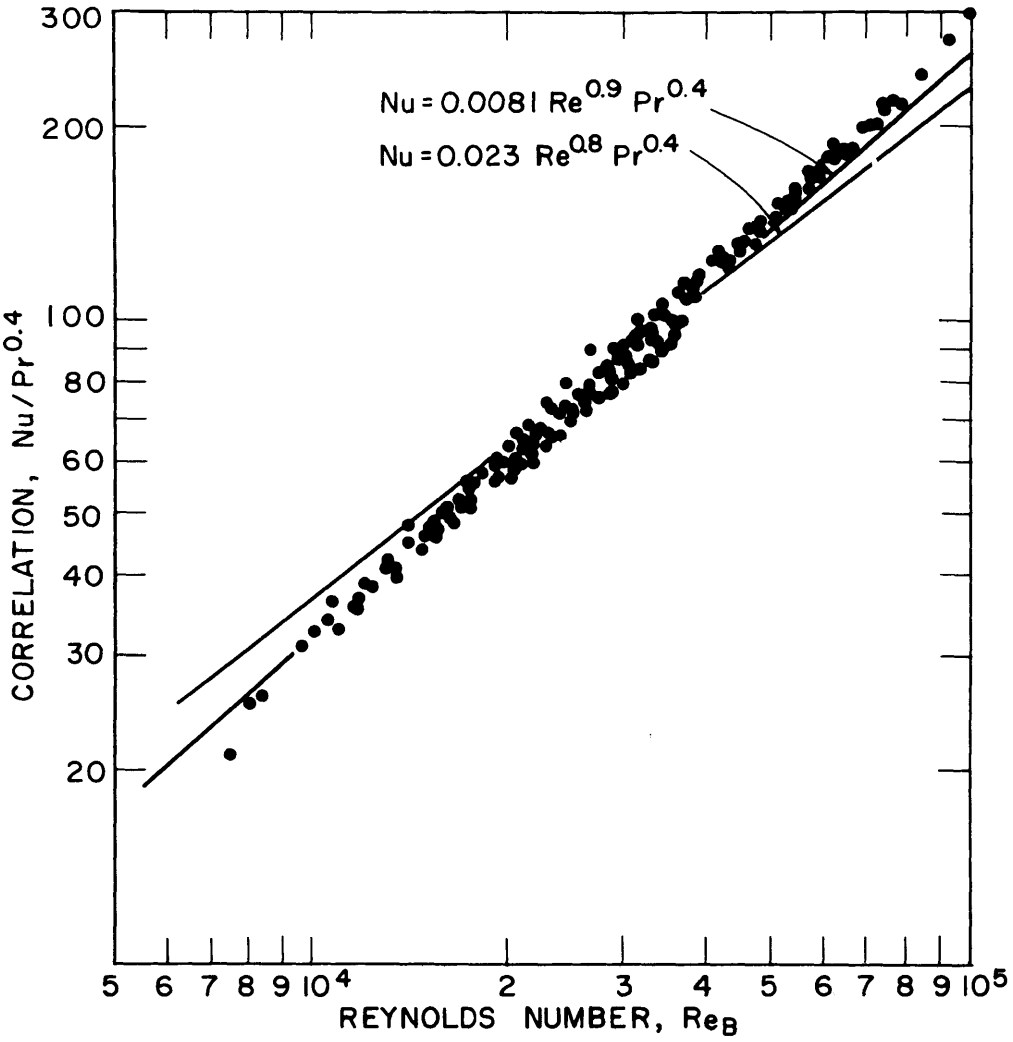

FIG. 2 MIT HEAT TRANSFER DATA FOR SANTOWAX OMP IRRADIATED AT 610°F, TH5 AND TH6

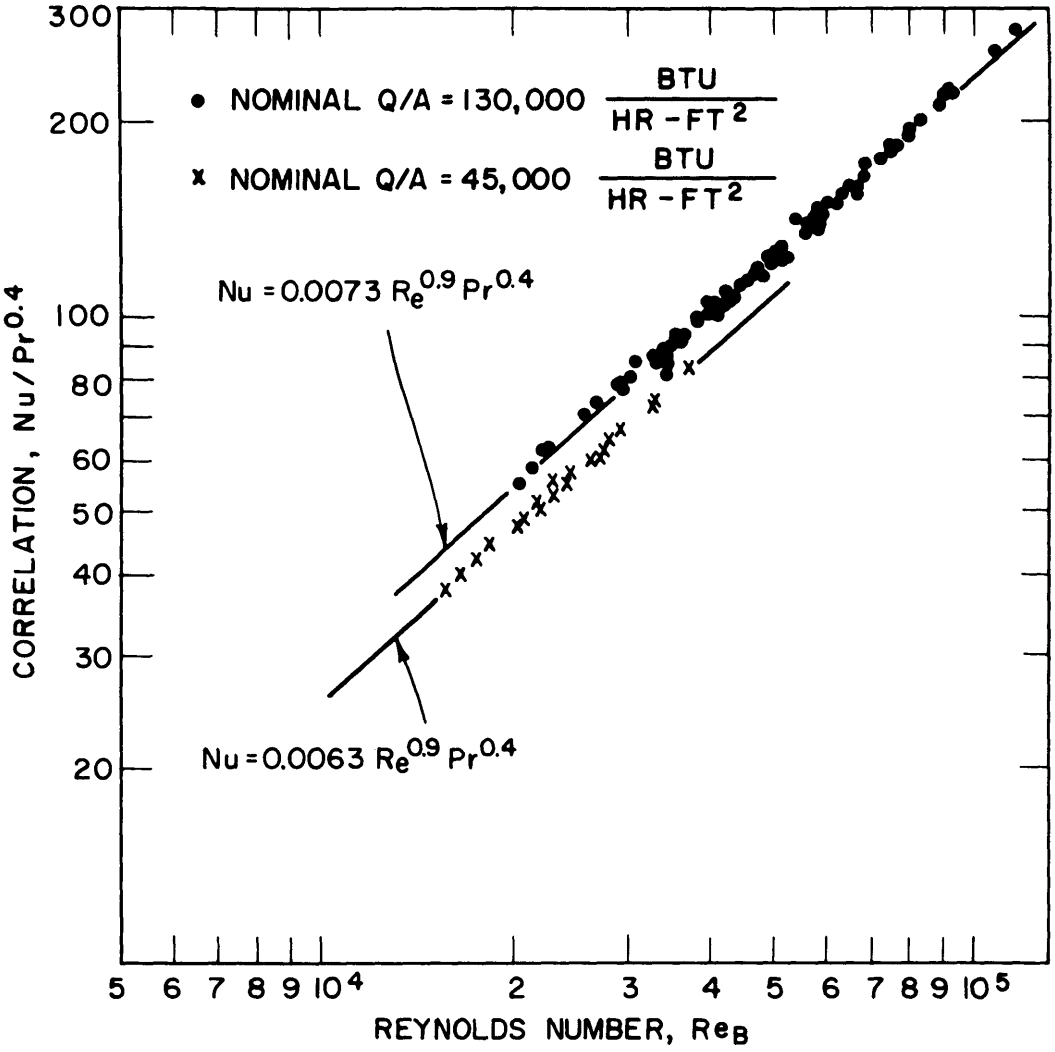

FIG. 3 MIT DATA FOR SANTOWAX OMP IRRADIATED AT 750° F, TH6

or the Seider-Tate type (7) (9)

$$St_B \; Pr_B^{2/3} \left[\frac{\mu_W}{\mu_B}\right]^{.14} = 0.023 \; Re_B^{-0.2} \qquad (3)$$

where $Nu \equiv hd/k$

$Re \equiv \rho VD/\mu$

$Pr \equiv c_p \, \mu/k$

$St \equiv Nu/Re \; Pr = U/\rho \, V \, c_p$

B indicates that properties are evaluated at bulk temperature.

f indicates that properties are evaluated at the film temperature, T_f. T_f is average of T_{bulk} and T_{wall} inside.

From the definition of the Stanton Number ($St \equiv Nu/Re \; Pr$), it can be shown that Equations (2) and (3) as well as Equation (1) indicate that the Nusselt Number, Nu, depends on the Reynolds Number to the 0.8 power. Equation (1) is plotted on Figures 1 and 2 for comparison with the organic coolant correlations.

Because most of the irradiated organic coolant data indicate a Reynolds Number dependence greater than 0.8, a literature survey was made to determine how previous investigators had finally decided on an exponent of 0.8.

Dittus and Boelter (14) were the first to suggest a correlation with an exponent of 0.8 on the Reynolds

Number after they had correlated their own data and surveyed all of the data taken to that time. The original correlations that they compared are presented in Figure 4. While their curve does fit the data quite well, considering the normal uncertainty limits quoted on heat transfer data, it should be noted that there is enough scatter in the data so that a line with a greater slope could be drawn. Dittus and Boelter did not use dimensionless units when they presented their data so appropriate scales have been added to the original figure to show the usual Nu, Re and Pr correlation.

McAdams (15) in his first edition of "Heat Transmission" surveyed all of the data taken to that time and concluded that the best general correlation for all fluids was that presented by Dittus-Boelter (14). The coefficient for the original Dittus-Boelter equation was 0.0243 instead of 0.023 as suggested by McAdams in Equation (1). In this edition McAdams also tabulated the values of exponents that were being used at that time for equations of the Nusselt type

$$Nu = a\ Re^{b}\ Pr^{c}\ \left[\frac{D}{L}\right]^{e} \qquad (4)$$

This tabulation is presented in Table 3 where it can be seen that the value of the Reynolds Number exponent varied between 0.75 to 0.83.

The final tabulation in Table 3 cites the data of Sherwood and Petrie (16) who took extensive heat transfer

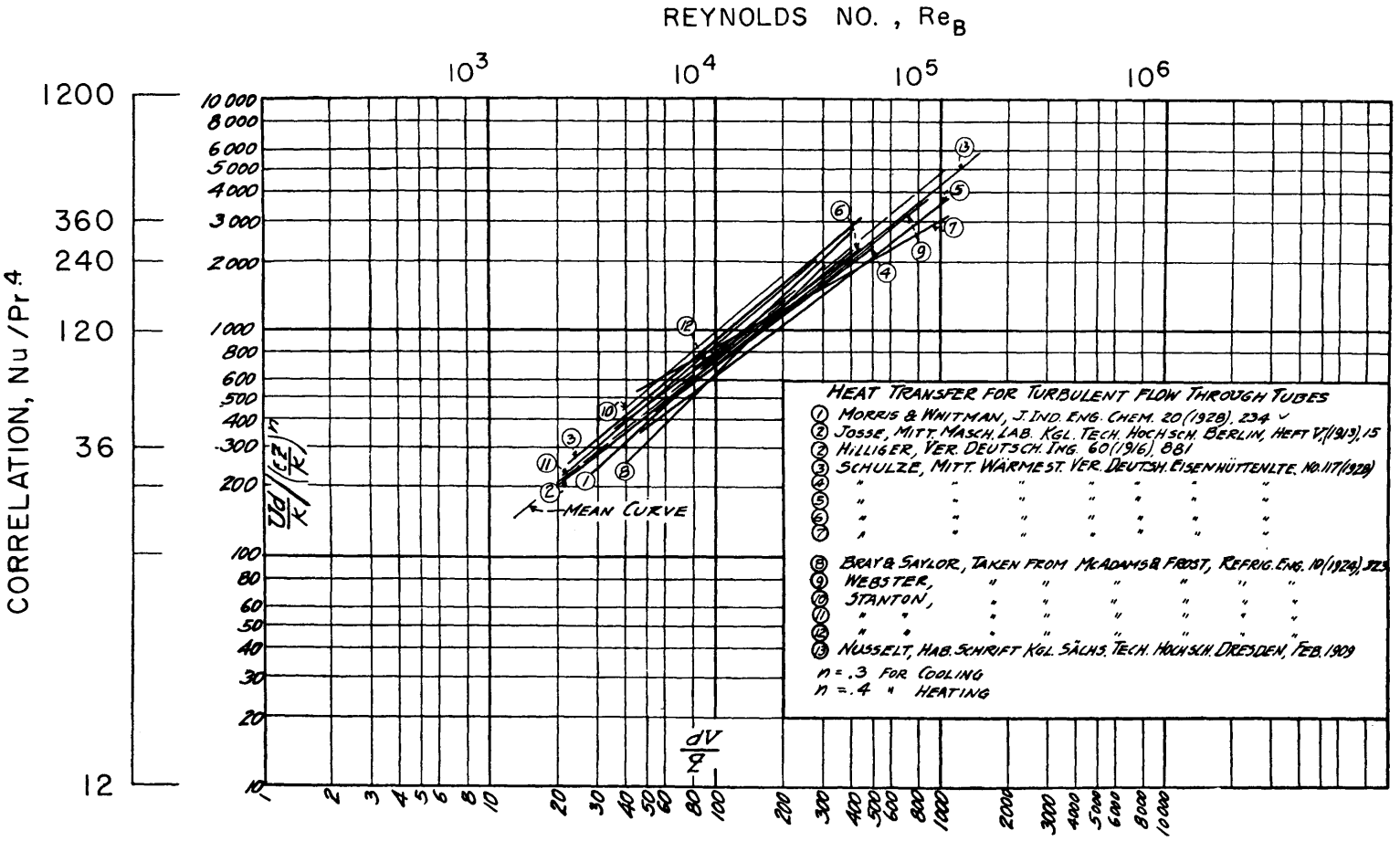

FIG. 4 ORIGINAL DATA USED BY DITTUS-BOELTER IN REFERENCE (14)

TABLE 3

VALUES OF "CONSTANTS" OF NUSSELT-TYPE EQUATION FROM MCADAMS (15)

Author	Date	a	b	c	e	Fluid Inside Pipe
Nusselt	1909	0.0255	0.786	0.786	0	Gases
Nusselt	1913	0.0302	0.786	0.786	0.054	Gases, water
Nusselt	1917	0.0362	0.786	0.786	0.054	
Grober	1921	0.0350	0.79	0.79	0.05	Gases
Rice	1923	0.0270	0.77	0	0	Gases
Rice	1924	0.0157	0.83	0.50	0	Gases, water
McAdams	1925	0.0178	0.83	0.38	0	Gases, water, oil
Purday	1927	0.026	(1)	(1)	0	Gases, water, oil
Morris & Whitman	1928	(2)	(2)	0.37	0	Water, oils
Cox	1928	0.0191	0.83	0.33	0	Gases, water, oils
Hinton	1928	0.0281	0.80	0.355	0	Gases, water, oils
Hinton	1928	0.0255	0.80	0	0	Gases
Keevil	1930	(3)	(3)	0.37	0	Water, oils
Dittus & Boelter	1930	(4)	0.80	(4)	0	Gases, water, oils
Nusselt	1930	(5)	0.75	1.0	0	Gases
Lawrence & Sherwood	1931	0.0561	0.70	0.50	0	Water
Sherwood & Petrie (16)	1932	0.024	0.80	0.40	0	Gases, water, oils, Acetone, n-Butyl alcohol

(1) $b = 0.792/(c_p\mu/k)^{0.051}$.

(2) A graphical function of DG/μ. For cooling, use 0.75h for heating.

(3) Function of (DG/μ).

(4) $a = 0.0243$ and $c = 0.4$, for heating; and $a = 0.0265$ and $c = 0.3$, for cooling.

(5) $a = 0.0396 \sqrt[3]{T_g/T_w}$, where T_g and T_w are absolute temperatures of gas and wall, respectively.

data on acetone, benzene, n-butyl alcohol, water and kerosene over a Reynolds Number range of 10^3 to 10^5 and Prandtl Number range of 2 to 20. These data are presented in Figure 5 and it can be seen that Equation (1) fits the data very well.

In summary, a Reynolds Number exponent of 0.8 was well established at this time and although other correlations have been proposed, they indicated that the Nusselt Number depends on the Reynolds Number to the 0.8.

There have been numerous analogies between heat transfer and momentum transfer proposed by Reynolds, Prandtl, Taylor, Von Karmen, Colburn, Martinelli and others (7). The analogies of Reynolds (7), Colburn (8) and Martinelli (11) (17) will be quoted here.

It is well established that turbulent flow in a tube consists of three zones or regions. These are: a laminar sublayer next to the wall, a transition zone and a turbulent zone in the center of the tube where eddies are always present. An expression for the heat transferred from the wall to the fluid can be written (7)

$$Q/A = -(k + \rho c_p E_H) \frac{dT}{dy} \qquad (5)$$

where E_H is the eddy diffusivity of heat. Equation (5) actually defines E_H. The first term in the parenthesis accounts for heat transfer by conduction while the second

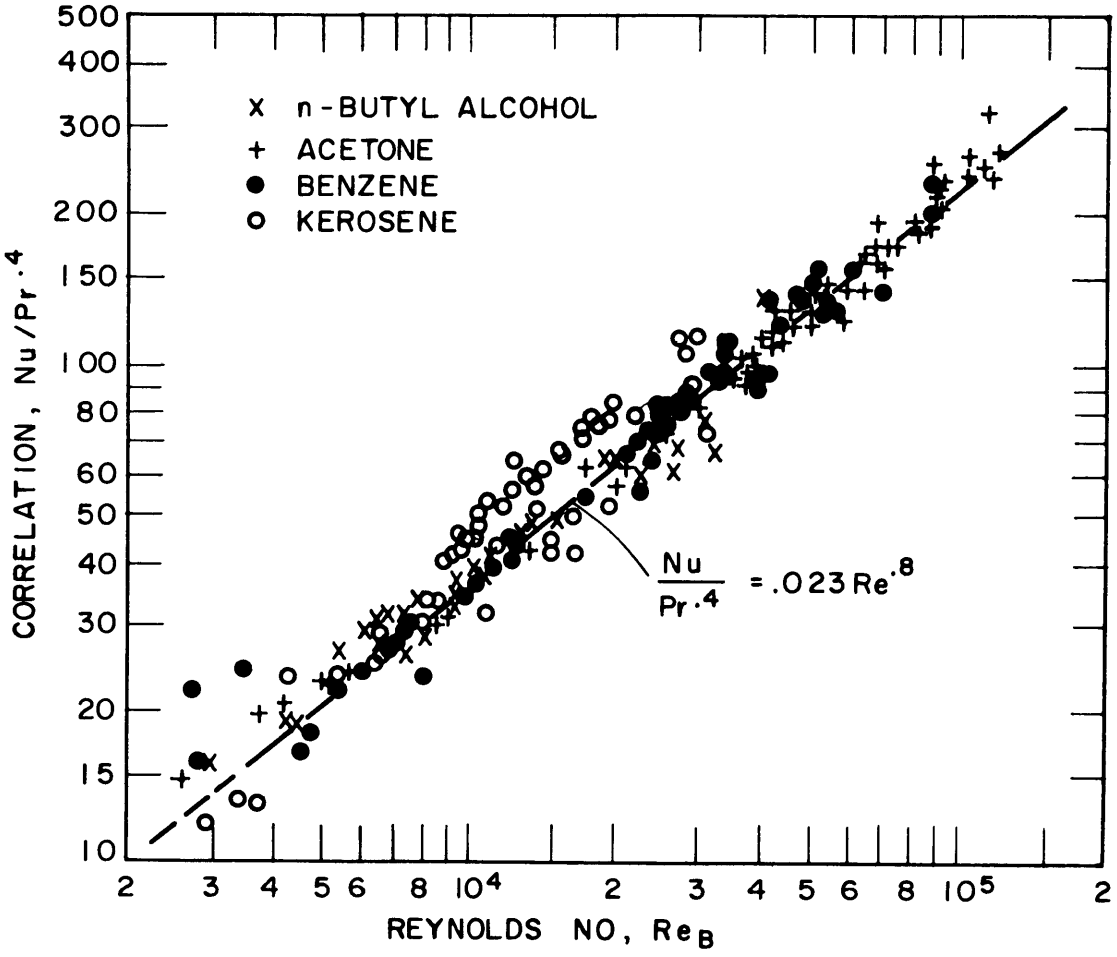

FIG. 5 HEAT TRANSFER DATA OF SHERWOOD AND PETRIE, REFERENCE (16)

term accounts for the heat transfer by diffusion or convection. In the laminar sublayer where $E_H = 0$, Equation (5) reduces to the normal equation for heat conduction.

A similar equation is used (7) to define the eddy diffusivity of momentum, E_M

$$\tau g_o = (\mu + \rho E_M) \frac{dV}{dy} \tag{6}$$

Assuming that both the shear stress and the heat flux are linear with respect to r, the above equations can be written

$$\frac{Q}{A}_W \frac{1}{\rho c_p} \left[1 - \frac{y}{r_w}\right] = - \left[\frac{k}{\rho c_p} + E_H\right] \frac{dT}{dy} \tag{5a}$$

$$\frac{g_o \tau}{\rho} \left[1 - \frac{y}{r_w}\right] = \left[\frac{\mu}{\rho} + E_M\right] \frac{dV}{dy} \tag{6a}$$

For the case when E_M is assumed equal to E_H and the Prandtl Number equals 1, Equations (5a) and (6a) can be integrated to:

$$\left(\frac{Q}{A}\right)_W \frac{V}{c_p g_o \tau_W} = (T_{Wi} - T_B) \tag{7}$$

But since by definition

$$h_f \equiv \left(\frac{Q}{A}\right)_W \Big/ (T_{Wi} - T_B) \tag{8}$$

and

$$\tau_w \equiv \frac{f \rho V^2}{8 g_o} \quad (9)$$

*

Equation (7) can be written as

$$\frac{h_f}{c_p V \rho} \equiv St = \frac{f}{8} \quad (10)$$

Equation (10) is known as Reynolds analogy and is quite valid for gases where $0.7 < Pr < 1.2$. However, it does not satisfactorily account for the influence of the Prandtl Number (7).

Colburn proposed plotting heat transfer data as in Equation (2)

$$j \equiv St\ Pr_f^{2/3} = 0.023\ Re_f^{-0.2} \cong 0.023\ Re_B^{-0.2} \quad (2)$$

Actual friction factor data for smooth tubes in the range of $5{,}000 < Re < 200{,}000$ can be represented by (7) (12) (13) (19)

$$f = 0.184\ Re_B^{-0.2} \quad (11)$$

Therefore, combining Equations (2) and (11)

$$j = \frac{f}{8} \quad (12)$$

which permits direct comparison of f and j data when both are plotted versus Re_B. Colburn also pointed out several other advantages of plotting heat transfer data in this manner. The more important reason is that when evaluating

---

*It should be noted that the friction factor used in this report is 1/4 of the Fanning friction factor, f_F.

the Stanton Number, St, from experimental data, the fluid properties do not enter the calculations because it can be shown that

$$St \equiv \frac{h}{c_p G} = \frac{S}{A} \frac{\left[T_{B_{out}} - T_{B_{in}}\right]}{\Delta T_f} \tag{13}$$

Martinelli (11) (17) directly integrated Equations (5a) and (6a) using measured profiles for the temperature and velocity and his final result was

$$St = \frac{E\sqrt{f/8}}{\frac{T_W - T_B}{T_W - T_C}(5)\left[E\ Pr + \ln(1 + 5\ Pr) + \frac{1}{2} F \ln \frac{Re}{60}\sqrt{\frac{f}{8}}\right]} \tag{14}$$

where E is defined $\equiv E_H/E_M$ (normally taken equal to 1 for $Pr \geq 1$). Values for $(T_W - T_B)/T_W - T_C)$ and F can be found in References (7), (12), (13) and (17).

Equation (14) is plotted versus Re_B in Figure 6 with $Nu/Pr^{0.4}$ selected as the ordinate. This was done so that a direct comparison could be made between Equation (1) and previous organic coolant data. As can be seen from Figure 6, Martinelli's analogy indicates that a correlation which involves $Nu/Pr^{0.4}$ does not account for variations in Pr when Pr becomes large ($Pr \geq 5$). It is very interesting to note that Equation (14) indicates an increasing value for the Reynolds Number exponent (or increasing slope) for increasing values of Prandtl Number.

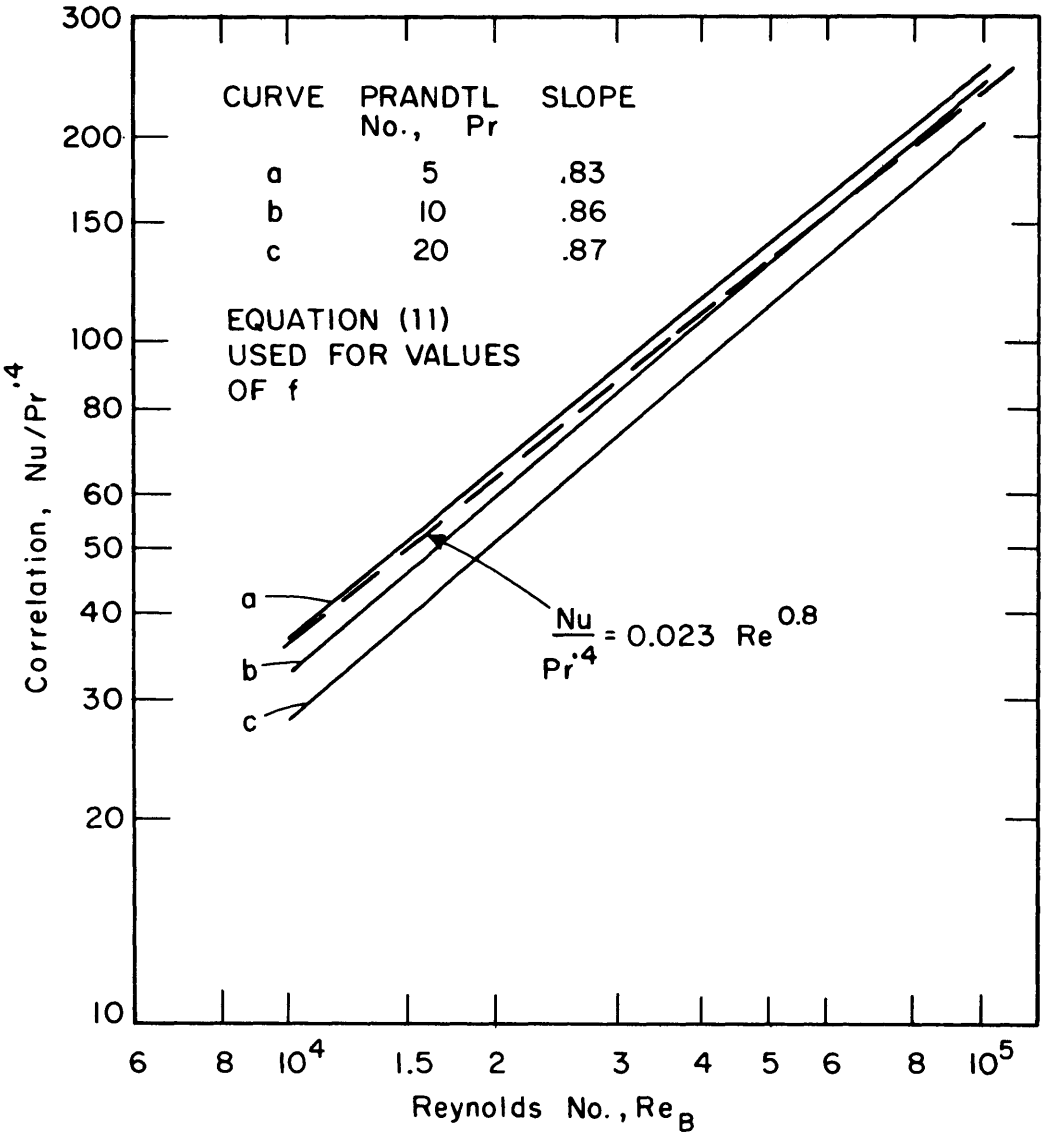

FIG. 6 PLOT OF MARTINELLI'S ANALOGY, EQUATION (14)

2.4 Goals of This Experiment

Because most of the correlations of organic coolant heat transfer data have an exponent on the Reynolds Number greater than 0.8, the following changes were made on the design of the MIT test heater to determine if this discrepancy, with the commonly used correlations, could be resolved.

Pressure taps were provided on Test Heater 7 so that the friction factor could be measured on the same test section. In addition to providing useful friction factor data, these measurements would help to determine if some of our physical properties data were correct. Specifically, the density and viscosity are used in the correlation of friction factor data, Equation (11), and therefore if the MIT measured values for these properties are in error, these errors would show up in the correlation.

These data could also provide a direct comparison of f and j factors taken on the same test section as indicated by Equation (12).

The test heater wall thermocouples were attached to the outside of the test heater wall in a different manner. Previous test heaters at MIT had the wall thermocouples spot-welded to the outside wall. While there was no doubt that these thermocouples were measuring the actual wall temperature, the readings

from these thermocouples were quite erratic and the resulting temperature profile data were quite scattered. For Test Heater 7 the thermocouples were insulated electrically from the wall by a thin sheet of mica ($\sim$.002 inch). These thermocouples were clamped to the test heater by small clamps and heat losses were minimized by asbestos insulation around the test heater and by an adiabatic oven surrounding the entire test heater section. Because the thermocouples were also thermally insulated from the test heater wall, it was necessary to provide this adiabatic oven. The adiabatic oven is provided with a separate heating control so that the inside wall temperature of the oven can be set equal to the outside wall temperature of the test heater (see Section 3.5). When these conditions exist, the test heater is adiabatic and hence the thermocouples indicate the actual outside wall temperature. From this measured outside wall temperature, the inside wall temperature is calculated using the equation for volumetric heating in a hollow cylinder (see Section 7.5). This significant change in the method of measuring the outside wall temperatures should help to determine the accuracy of the previous MIT heat transfer data.

3.0 DESCRIPTION OF EQUIPMENT AND PROCEDURES

3.1 Instruments at Loop Console

The MIT Organic Loop console has all the instrumentation necessary to measure flow rates, temperatures, voltage differences and pressure drops. A schematic of the MIT Organic Loop is presented in Figure 7. A more detailed description of this equipment is presented by Morgan and Mason (2). This section will just describe the instrumentation that is used in the measurement of heat transfer coefficients and friction factors.

The coolant velocity or flow rate is measured with a Potter turbine flowmeter*. This instrument measures the volumetric flow rate and is insensitive to changes in the density and viscosity of the coolant. This instrument was supplied with a calibration and was also calibrated at MIT using water at room temperature. These calibrations agree quite well and the maximum uncertainty in the absolute value of the velocity is estimated to be 2 to 3% (2) (3).

Voltage drops are measured with a precision voltmeter** that has a full range scale of 15 volts. This instrument has been calibrated several times and the maximum uncertainty in the voltage is estimated to be $\pm 1\%$.

---

*Potter Aeronautical Corporation, Union, New Jersey.

**General Electric Company, Model 8AP9V-Y261, Type AP9.

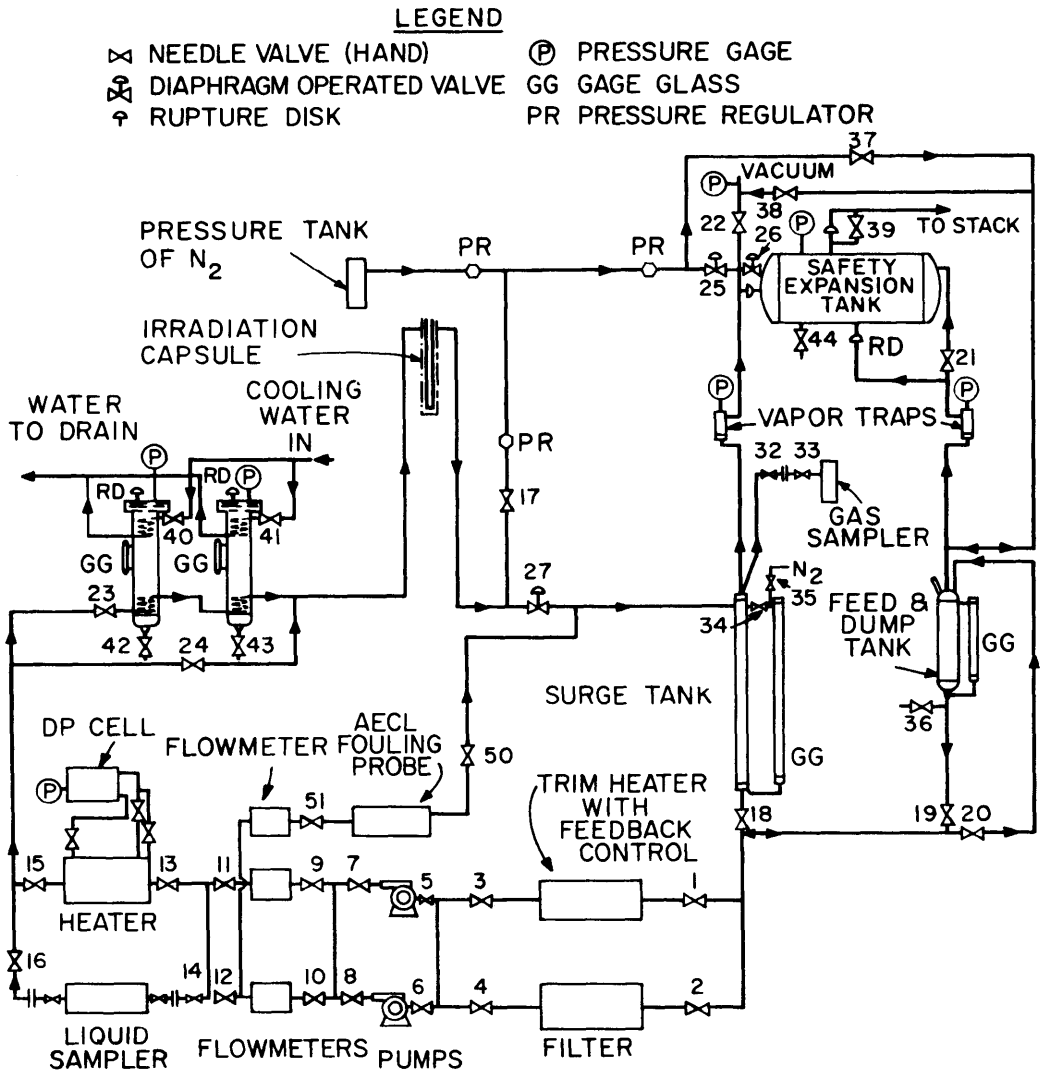

FIG. 7 SCHEMATIC FLOW DIAGRAM OF MIT ORGANIC LOOP

All temperatures are measured using chromel-alumel thermocouples. The millivolt reading of these thermocouples are measured with a precision potentiometer* which is accurate to ± 2 microvolts.

3.2 Description of Test Heater 6

This is a brief description of Test Heater 6 (also called TH6) since a complete description can be found in the report of Morgan and Mason (2) or Sawyer and Mason (3). What will be described here are the more important details and items that were changed in the design of Test Heater 7 (also called TH7).

Test Heater 6 is a 1/4" OD stainless steel tube with two heater sections each 12 inches long. An unheated inlet calming section with a L/D ratio of 40.5 was provided. The tube is resistance heated by the passage of large AC currents (up to 450 amperes) along the test heater wall and it is cooled by the organic coolant flowing through the tube at velocities up to 20 feet per second. The two outer electrodes are maintained at ground potential and a variable voltage (up to 12 volts) is applied to the center electrode. Each 12-inch section of the test heater has 7 chromel-alumel thermocouples spot-welded to the outside of the tube. With these thermocouples the temperature profile down the length

*Minneapolis-Honeywell Corporation, Model 105X11-P.

of the tube can be measured. Then with these measurements and the measured heat flux, the inside wall temperature can be calculated (see Section 3.5). The bulk organic temperature entering and leaving the test heater is measured with chromel-alumel immersion thermocouples. These are mounted at each end of the test heater in a mixing chamber to insure accurate measurement of the inlet and outlet bulk temperatures. The thermocouples are 1/8 of an inch in diameter and they are immersed approximately one inch into the organic. All of the thermocouples are calibrated and the appropriate corrections are applied during the calculations.

3.3 Description of Test Heater 7

Test Heater 7 is similar to Test Heater 6 except for the following design changes:

a. The test heater wall thermocouples are not spot-welded to the test heater section. Instead the thermocouples are clamped to the outside wall. They are also thermally and electrically insulated from the heater section by a thin sheet of mica.

b. Three pressure taps are provided for the measurement of friction factors. The first pressure tap is at the inlet to the unheated calming section, the second pressure tap is located upstream of the first heated section,

and the third pressure tap is located downstream of the second heated section. The pressure drop across these pressure taps is measured with a Foxboro differential pressure (DP) cell which is described in further detail in Section 3.4.

c. An adiabatic oven with separate heating control was provided so that the test sections could be run under adiabatic conditions.

A photograph of Test Heater 7 and a typical wall thermocouple is shown in Figure 8. Reference should also be made to Section 7.8 in the Appendix for a more detailed description of the construction of Test Heater 7.

3.3.1 Test Heater Wall Thermocouples

Fourteen chromel-alumel stainless steel-clad thermocouples are provided for the measurement of the test heater outside wall temperature. These thermocouples were purchased from the Conax Corporation* who also provided a special tip on each thermocouple so that they could be clamped to the test heater. The catalog number of these thermocouples is INC4K-G-T4-PJ-24 and details of the special tip are shown in Figure 9. These thermocouples were calibrated at MIT (27) and no significant errors were found.

*Conax Corporation, Buffalo, New York.

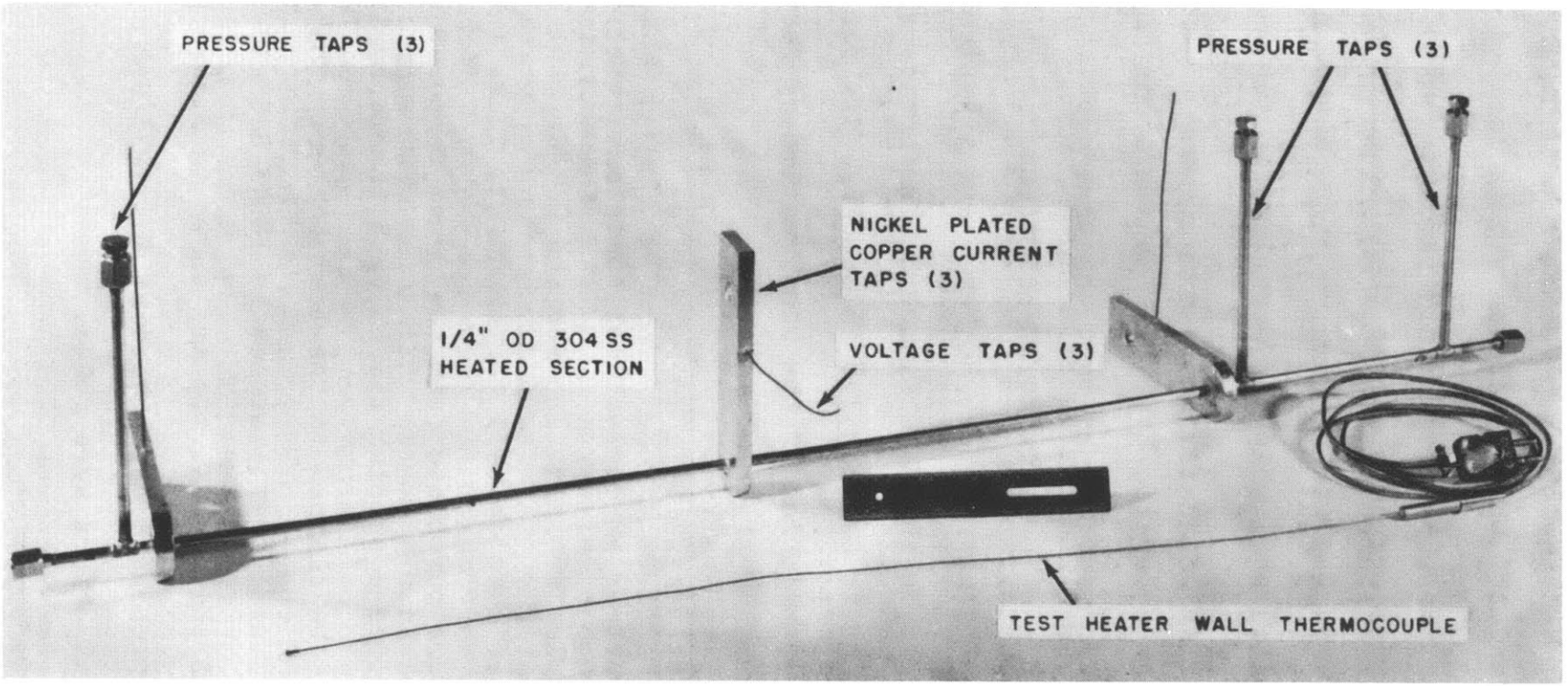

FIG. 8 TEST HEATER NO. 7 AND TYPICAL WALL THERMOCOUPLE

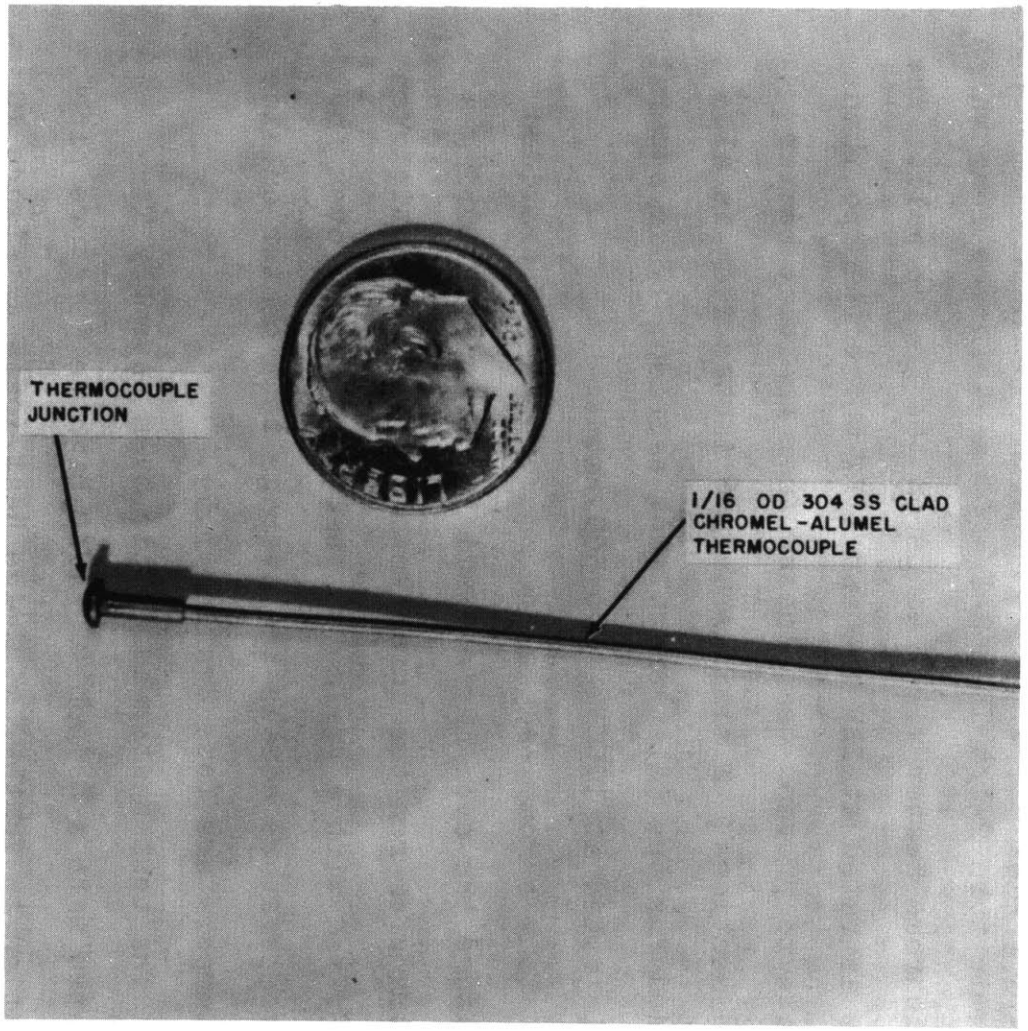

FIG. 9 TEST HEATER NO. 7 WALL THERMOCOUPLE

3.3.2 Adiabatic Oven

The adiabatic oven was purchased from the Hevi-Duty Corporation* and it is a slightly modified version of their Series 2700 ovens. This oven is essentially a ceramic tube 2-1/4 ID x 3-1/4 OD x 24 inches long which has Nichrome heater wires wound on the inside wall. The heater is rated at 115 VAC and 1 KW which is more than adequate to prevent heat losses from the test heater heated sections. A similar oven 6 inches long is also provided for the inlet or calming section. This separate oven is rated at 115 VAC and 500 watts.

Four chromel-alumel thermocouples are provided to measure the oven inside wall temperature. During a heat transfer run the input power to the adiabatic oven is adjusted with a variac so that the average oven inside wall temperature equals the average test heater outside wall temperature (see Section 3.5).

The test heater-adiabatic oven assembly is insulated with a 6 inch OD KAYLO high temperature pipe insulation to further minimize heat losses. Figure 10 shows how Test Heater 7 is mounted in the adiabatic oven. In order to show details of how the test heater wall thermocouples are mounted, the photograph in Figure 10 was taken before the asbestos insulation was applied

*Hevi-Duty Corporation, Watertown, Wisconsin.

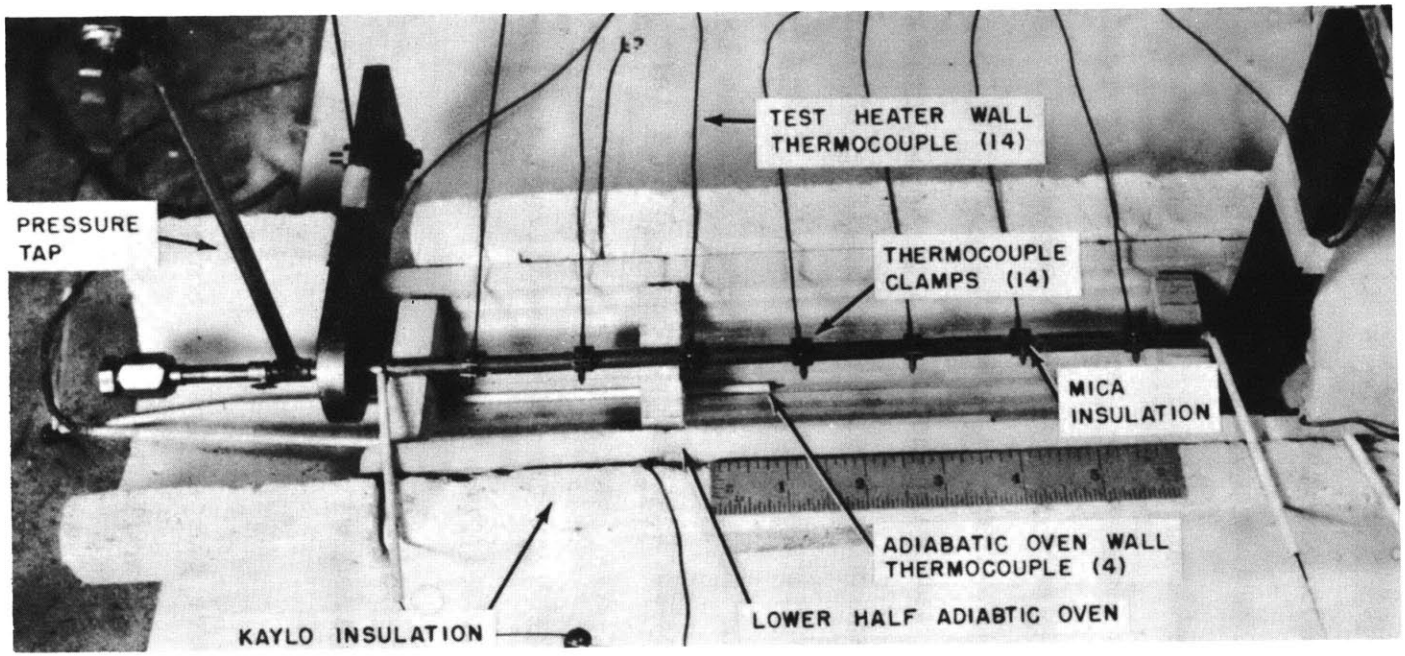

FIG. 10 TEST HEATER NO. 7 MOUNTED IN ADIABATIC OVEN
NO ASBESTOS INSULATION AROUND TEST HEATER

to the 1/4 inch OD heated section of the test heater.

3.3.3 Other Instrumentation

On previous test heaters used at MIT the heat input to the coolant was calculated from the voltage drop across the heated section, the resistance of that section and the measured heat loss (2). The test heater resistance was measured as a function of the test heater wall temperature before the test heater was installed in the loop console. Because of the way the previous test heaters were installed, it was not possible to measure the current in each half of the test heater. Test Heater 7 was provided with a method of measuring the total current to the test heater and of measuring the current to the left half or downstream half of the test heater. Therefore, with these measurements the heat input to each test heater section can be calculated from

$$Q = EI$$

and these values compared with the value obtained from

$$Q = \Delta E^2/R \quad .$$

Thermocouples were placed in the copper current lugs to determine if it would be possible to measure the temperature gradient and hence the heat loss along these lugs. Unfortunately, the temperature readings from these thermocouples were too scattered to give meaningful results.

3.4 DP Cell

Pressure drops were measured with a Foxboro, model 13A, DP cell*. This instrument converts the differential pressure to be measured to an air pressure reading which is directly proportional to the input ΔP. The instrument requires an air supply at approximately 30 psig and a read-out pressure gage with a range of 3 psig to 15 psig. Figure 11 is a photograph of the DP cell taken before it was mounted at the loop console. The readout gage shown was supplied by Foxboro and it reads from 0 to 100% of full scale rather than from 3 to 15 psig. This instrument has an adjustable range from approximately 10 psi ΔP to 1 psi ΔP. Whenever this operating range is changed, the DP cell must be calibrated. This cell was calibrated at MIT at various range settings and at various temperatures. A more detailed description of the calibration procedure and the results of these calibrations are presented in Appendix 7.3.

Because the organic coolants being tested have melting temperatures above room temperatures, it is necessary to heat the DP cell while it is in operation. A small one hundred watt heater was provided for heating the DP cell while the lines that transmit pressure to the cell were traced with a high temperature heating wire. For the

*Foxboro Corporation, Foxboro, Massachusetts.

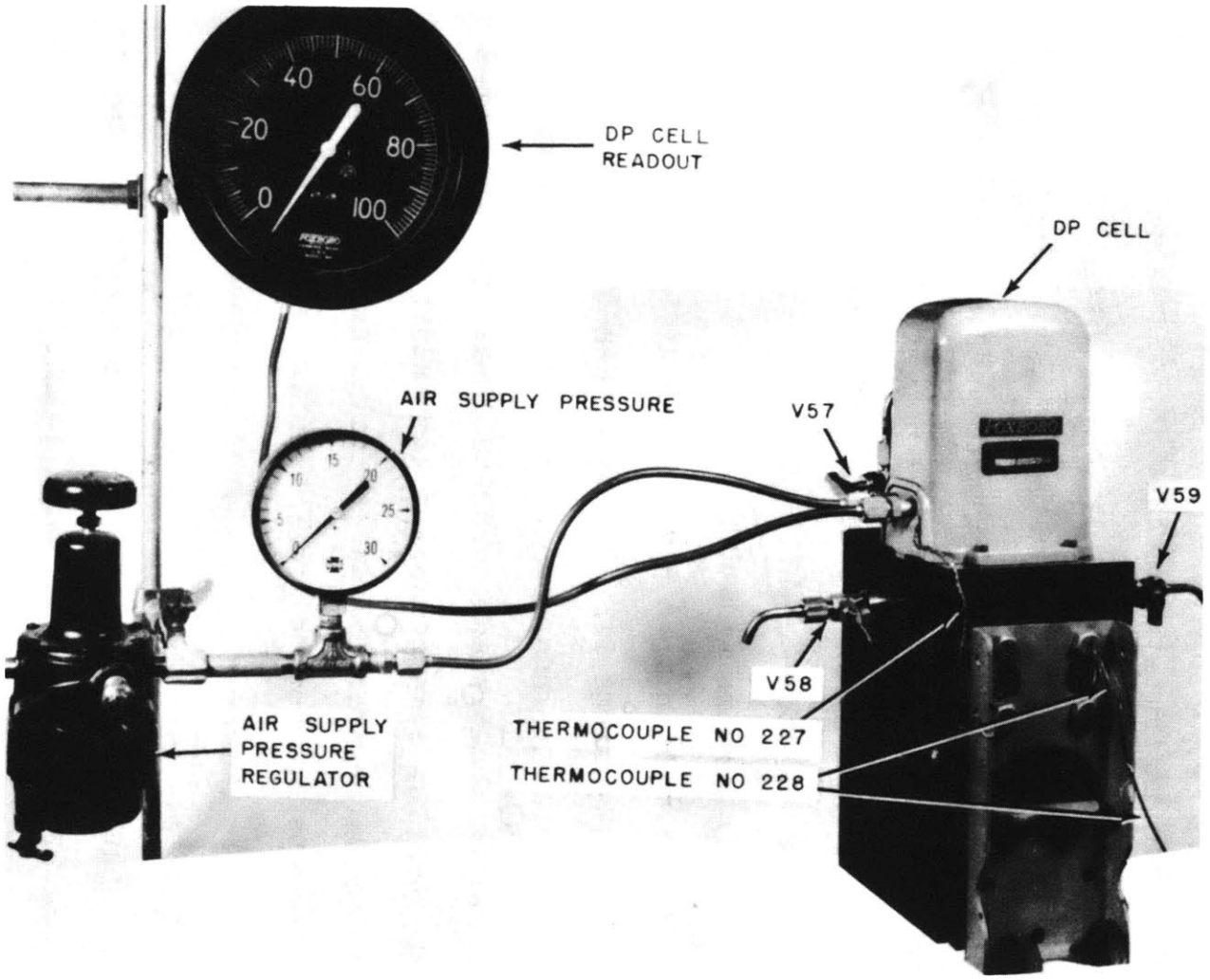

FIG II DP CELL

pressure drop data taken on Santowax WR it was necessary to heat the body of the DP cell to approximately 180°F. The body of the DP cell is all stainless steel and, therefore, temperatures even higher than this should not affect it. However, the upper section of the cell has some "O" rings which are used as seals so if higher melting coolants are ever tested, provisions should be made to cool and protect these seals.

3.5 Method of Operation

Normally it takes a full day to take a full set of heat transfer and friction factor data, which usually consists of measurements at five or six different velocities.

Before any data are taken certain safety procedures must be followed, the loop must be at thermal equilibrium and the DP cell must be vented and rezeroed (18). It is not necessary to recalibrate the DP cell unless the range of the instrument has been changed.

The measurements that are taken at each velocity are tabulated in Table 4. The location of the thermocouples, the voltage taps and the pressure taps are shown in Figure 12. Figures 13 and 14 are schematics of the Test Heater 7 wiring and the Test Heater 7 DP cell respectively.

TABLE 4

VARIABLES MEASURED DURING A HEAT TRANSFER AND PRESSURE DROP RUN

Variable	Description
Thermocouple 211	Test Heater Outside Wall at Inlet Section
Thermocouple 212	Test Heater Outside Wall at Outlet Section
Thermocouple 228	DP Cell, Body Temperature
Thermocouple 227	DP Cell, Upper Chamber Temperature
Thermocouple 213-217	Adiabatic Oven, Inside Wall Temperatures
Thermocouple 1-14	Test Heater Outside Wall Temperatures
Thermocouple 68	Coolant Bulk Temperature, Inlet
Thermocouple 69	Coolant Bulk Temperature, Outlet
Voltage Drop ΔE_3	Upstream Half Test Heater, Voltage Drop
Voltage Drop ΔE_4	Downstream Half Test Heater, Voltage Drop
Voltage Drop ΔE_5	Upstream Half Test Heater, Voltage Drop
Voltage Drop ΔE_6	Downstream Half Test Heater, Voltage Drop
Flow Rate GPM	Coolant Flow Rate
I_{total}	Total Test Heater Current
I_4	Downstream Half Test Heater Current
Percent Full Scale, DP Cell	Pressure Drop Across Test Heater

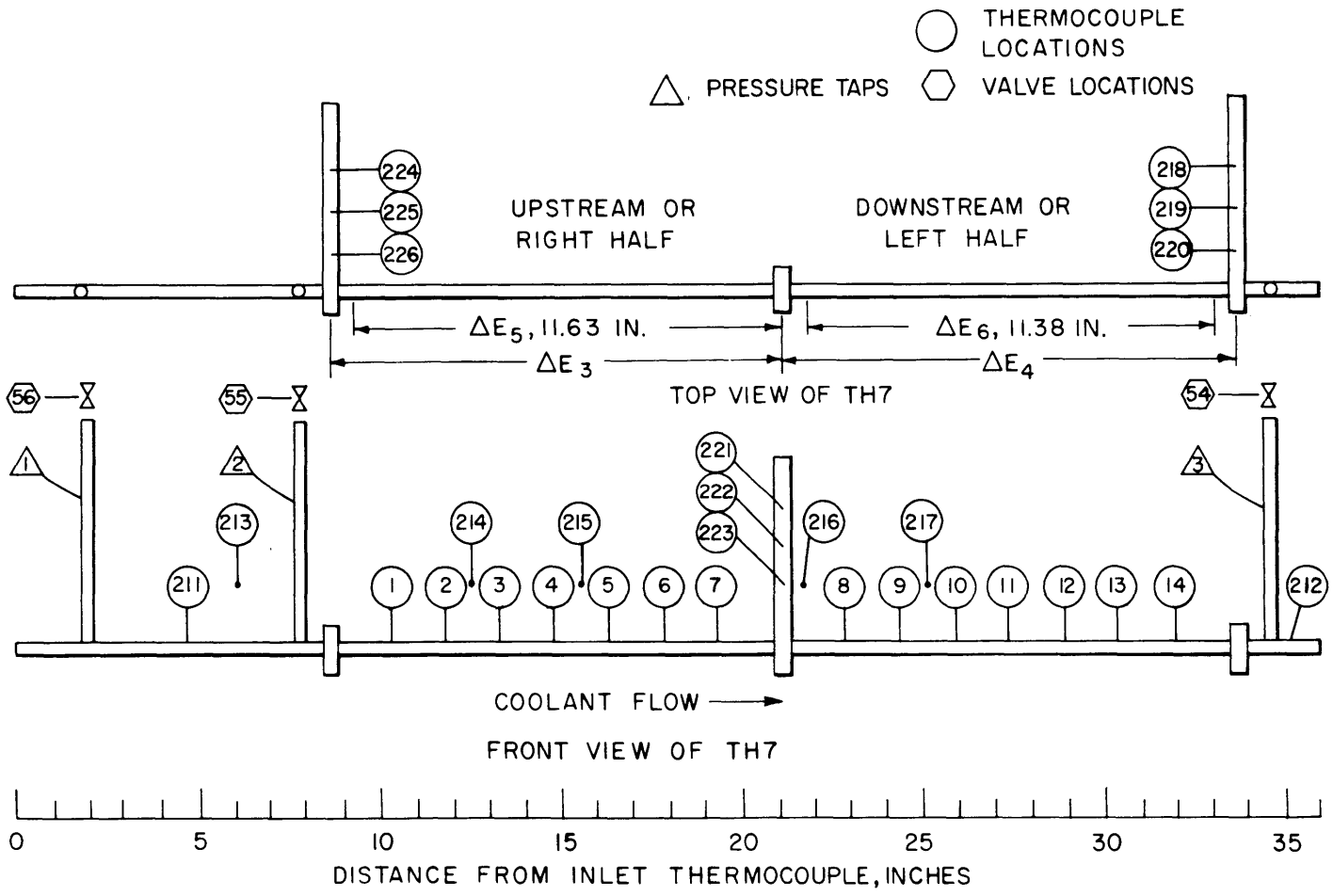

FIG. 12 LOCATION OF THERMOCOUPLES AND VOLTAGE TAPS, TEST HEATER 7

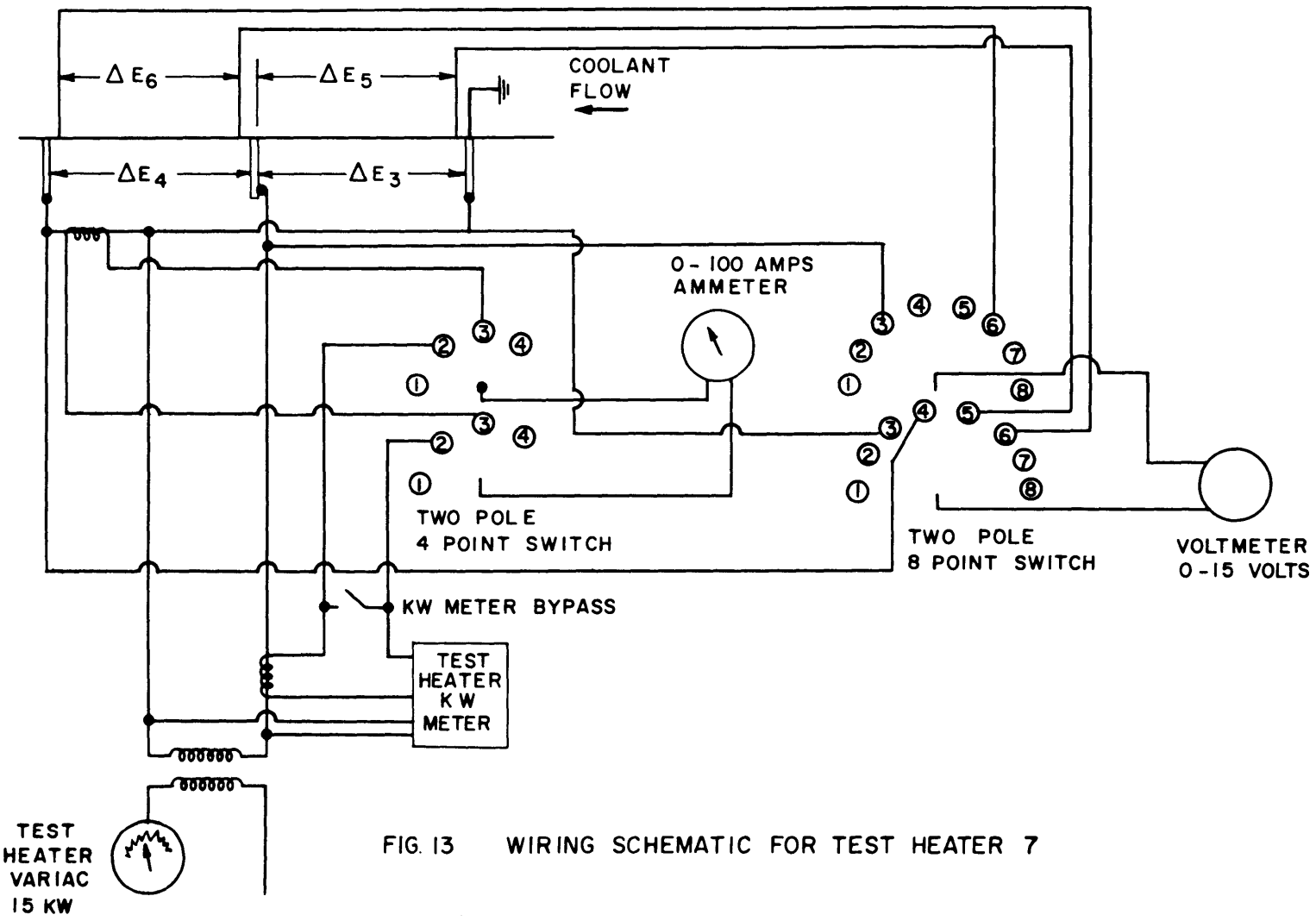

FIG. 13 WIRING SCHEMATIC FOR TEST HEATER 7

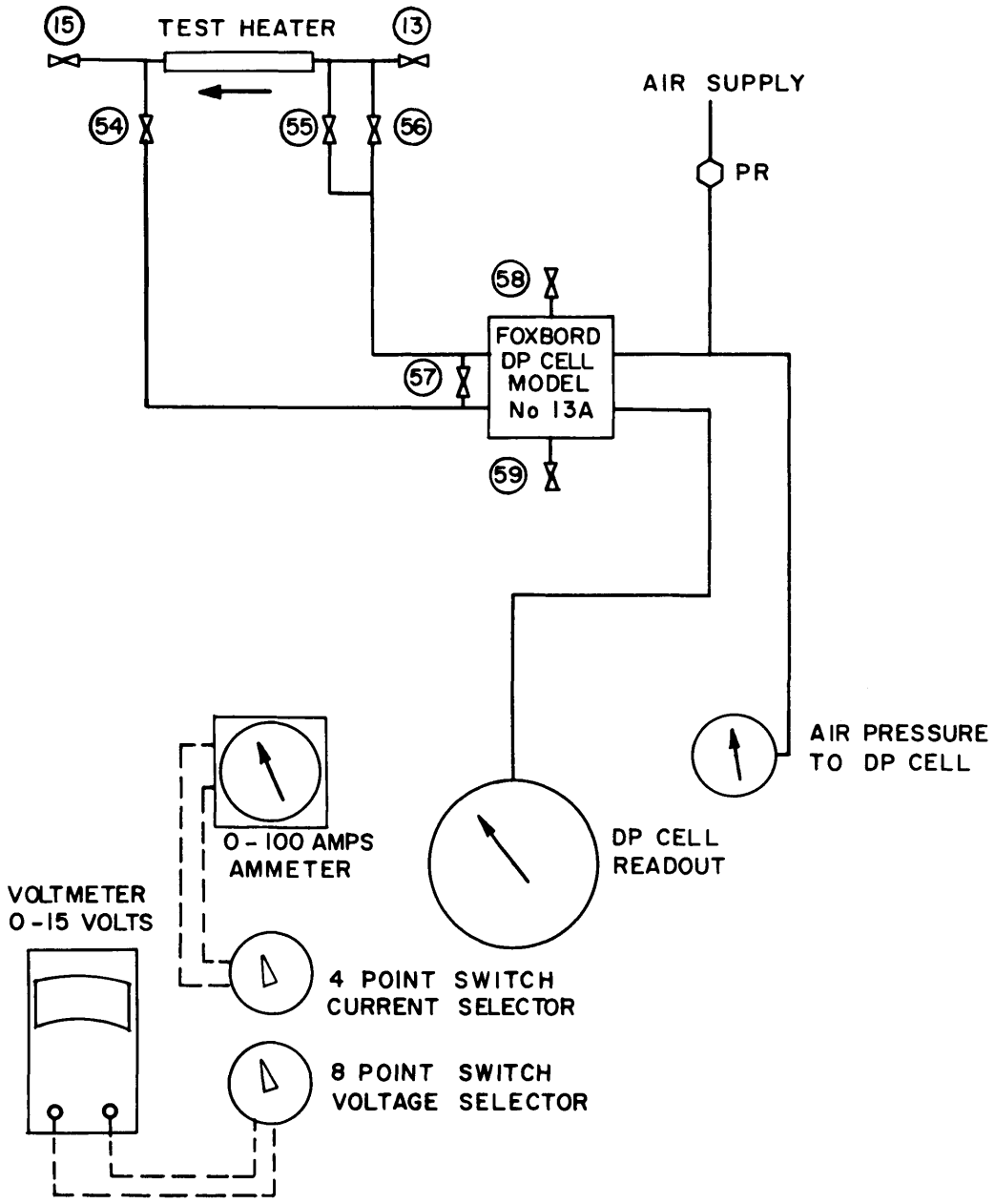

FIG. 14 SCHEMATIC OF DP CELL AND INSTRUMENT PANEL

A brief outline of the procedure will be presented here. For the actual taking of the data, Reference (18) should be read and followed step by step.

The test heater is set at the appropriate heat flux, the heater to the DP cell is turned on and then the system is allowed to come to thermal equilibrium. The appropriate valves between the test heater and the DP cell are then opened to select the section that will be tested. It has been found that valves 54 and 55, which open the DP cell to section 2-3, give the best results. Pressure tap 1 is located too close to the inlet of Test Heater 7 and the resulting pressure readings cannot be correlated with the normal friction factor correlations. The DP cell is vented and rezeroed at the start of a day's run and rezeroed occasionally during the day to make sure that the zero point has not changed.

The adiabatic oven variac is adjusted so that the average inside wall temperature of the oven is equal to the average outside wall temperature of the test heater. It has been found that the upstream half of Test Heater 7 gives a better fit to Equation (1) than the downstream half (see Figures 18 and 19 presented in Section 5.2). This is probably due to the fact that the temperature profiles of the adiabatic oven and the test heater are approximately the same shape on the upstream half, whereas this is not true for the downstream half.

This can be seen from a typical temperature profile for Test Heater 7 as shown in Figure 15. In future heat transfer runs it is suggested that the average of the upstream temperatures be set equal to each other, since the averaging of all the thermocouples gives a high inside oven wall temperature.

When thermal equilibrium has been reached, two sets of consecutive readings as outlined in Table 4 are taken. If the bulk inlet and outlet thermocouple readings do not vary by more than ± 0.005 millivolt between these two readings, then the average of these two sets of data are considered as a valid set of data.

Then the flow rate is lowered with valve 15 to the next selected value. This procedure is followed until the test heater's outside wall temperature reaches approximately $900^{\circ}F$, the maximum recommended wall temperature.

Then all valves to the DP cell are closed and the loop console is returned to its normal operating condition.

3.6 Equipment for Measurement of Physical Properties

Viscosity and density measurements were made at MIT on organic coolant samples removed from the MIT organic loop. The samples are removed in stainless steel capsules and are handled very carefully to prevent contamination (2) (3). In general, these

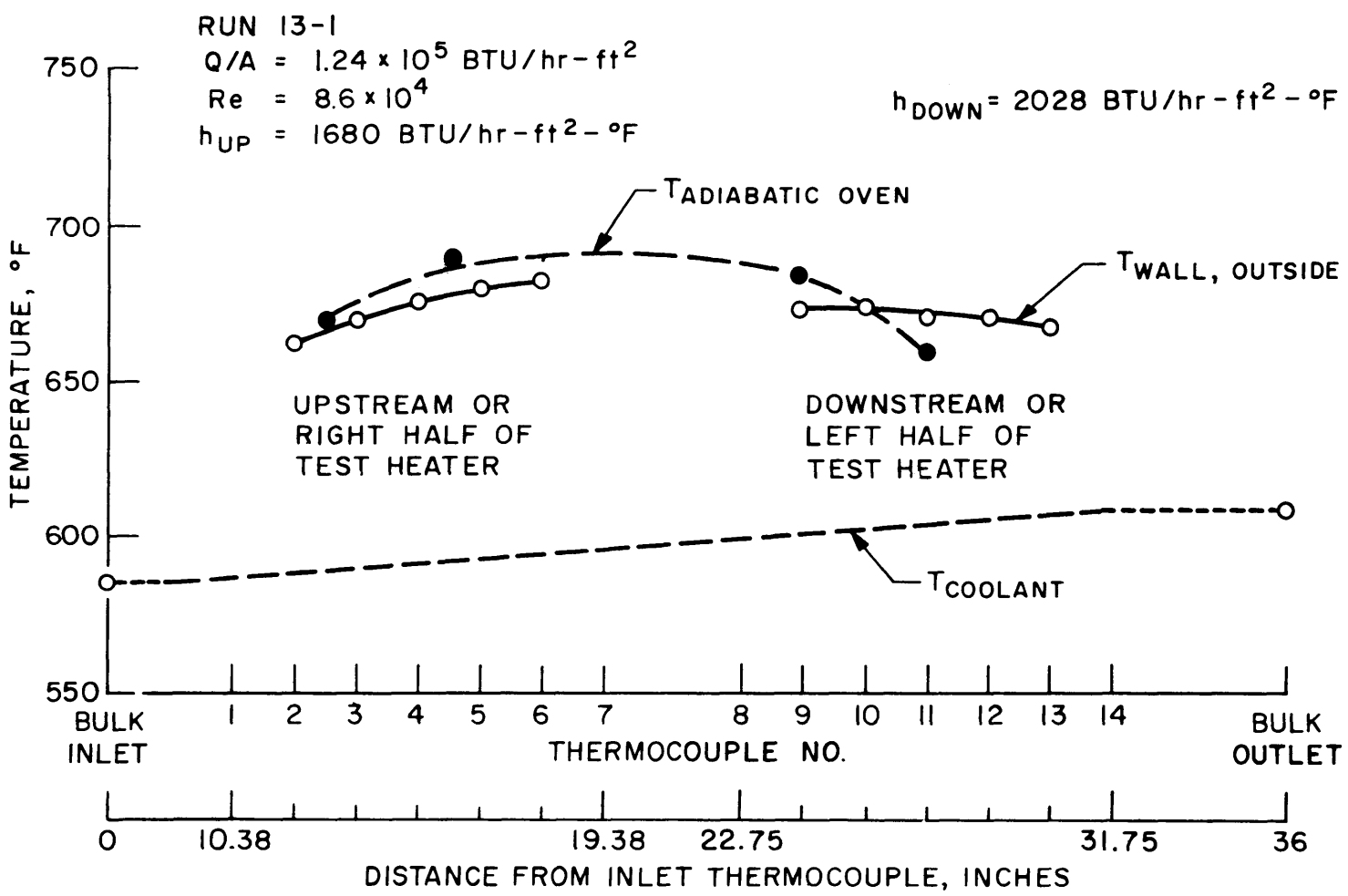

FIG. 15 TYPICAL TEMPERATURE PROFILE FOR TH7

measurements are reproducible and they agree with measurements made, on the same samples, at other laboratories (3). Thermal conductivity and specific heat measurements were not made at MIT, so data from other laboratories were used in the heat transfer correlations.

A complete description of the equipment and procedures for the density and viscosity measurements are presented by Morgan and Mason (2) and for the specific heat and thermal conductivity measurements by Elberg (20).

3.6.1 Viscosity Measurements

The kinematic viscosity of the irradiated organic coolants were determined by measuring the efflux time in a semi-micro capillary viscometer of the Ostwald type. The viscometer constant was determined as a function of the liquid volume in the viscometer, using water at 25°C as a calibration liquid. An analysis of the change in the calibration constant with temperature due to thermal expansion of the viscometer glass indicated this change was negligible. The viscosity was calculated from the efflux time by means of appropriate equation of calibration.

In performing the viscosity measurements on the coolant samples, the viscometer containing the organic was suspended in a molten salt bath. The bath was well-stirred to insure a uniform temperature and was equipped with a temperature controller which maintained the

temperature constant to within ± 1 to 2°F. To prevent boiling of the organic coolant at the higher temperatures, the viscometer was pressurized with nitrogen to approximately 40 psig. A more detailed description of the equipment and procedure used is given by Morgan and Mason (2). With the technique used it is estimated that the viscosity measurements are accurate to ±1 percent at the lower temperatures, to ±4 percent at 800°F.

3.6.2 Density Measurements

The density of irradiated organic coolants were determined by use of a pycnometer in which the volume of a known mass of organic was determined by measuring the liquid height in two capillary tubes connected to a small reservoir of fluid. The volume of the pycnometer at different capillary heights was determined by measuring the height in the capillaries when the pycnometer contained a known volume of mercury (determined from the mercury mass and density). All calibrations were performed at a temperature of 25°C. Calculations indicate that the volume change of the pycnometer with temperature due to thermal expansion of the glass can be neglected.

The constant temperature salt bath used for the viscosity measurements was also used for the density measurements; the pycnometer was similarly pressurized with nitrogen gas to prevent boiling of the organic.

3.6.3 Specific Heat and Thermal Conductivity Measurements

Specific heat and thermocouple data taken at Grenoble (20) on the organic coolant, OM_2, were used in this report, since OM_2 is similar to Santowax WR.

Specific heat measurements were made in an adiabatic calorimeter, in which the sample container has a small heat capacity relative to the sample. The container was closed tightly, and heated electrically while the temperature rise was measured with a platinum-resistance wire. The vapor pressure in the container was balanced by an equal outer pressure to avoid destruction of the container's thin wall. The container was kept under adiabatic conditions by differential thermocouples which regulate the outside container temperature to that of the sample. The scatter in the data was about 0.5% and the systematic error is estimated to be on the same order.

For the measurement of thermal conductivity, a non-stationary wire method was used. Readings were taken automatically during the test to minimize errors during the short test period (only a few seconds). A very thin resistance wire was immersed in the sample and a temperature rise was caused by a step change in the current to the wire. This temperature rise of the sample, multiplied by the time increment, is inversely proportional to the thermal conductivity of the liquid sample. Toluene was used to calibrate the instrument, and the estimated uncertainty is $\sim$1.5%.

4.0 UNCERTAINTY IN MEASUREMENTS

4.1 Estimated Uncertainty on Measurements of Variables

The estimates of the uncertainty on all of the measurements made to calculate heat transfer and friction factor data are presented in Table 5. These estimates are based on those quoted by Morgan and Mason (2), Sawyer and Mason (3), and on a review of the actual data taken.

At this point definitions will be given for some of the operational terms used in this report. Heat transfer data are taken at the organic loop console while the coolant is circulating through the MIT reactor core, during which time there is a small change in properties as the organic coolant degrades. These changes are quite small during a given day and, therefore, are assumed constant during a set (5 to 6 different velocities) of heat transfer data. The period of time during which the degradation products (DP) build up in the circulating loop is called the transient of a particular irradiation. The steady state part of a run refers to that period of time when the coolant is processed and returned to the loop at a rate such that the percent of degradation products and high boilers remains constant. Degradation products and high boilers are defined as:

Weight Percent Degradation Products (% DP) ≡

100 - weight percent total terphenyls (% OMP).

TABLE 5

ESTIMATED UNCERTAINTY ON VARIABLES USED IN HEAT TRANSFER AND FRICTION FACTOR CORRELATIONS

Variable	ΔP lb_f/in^2	Velocity ft/sec	Nominal Heat Flux, Q/A BTU/hr-ft^2 $<10^5$	10^5	2×10^5	During Steady State Portion of Irradiation	During Transient Portion of Irradiation
ρ						$\pm$1%	$\pm$1.5%
μ						$\pm$3%	$\pm$4%
c_p						$\pm$5%	$\pm$6%
k						$\pm$5%	$\pm$6%
ΔT_f		10$\pm$3%	$\pm$5%	$\pm$3%	$\pm$2%		
		20$\pm$2%	$\pm$10%	$\pm$8%	$\pm$4%		
Q/A, calculated from $\Delta E^2/R$		10$\pm$3%	$\pm$8%	$\pm$6.5%	$\pm$6.5%		
		20$\pm$2%	$\pm$8%	$\pm$6%	$\pm$6%		
ΔP	10$\pm$2%						
	5$\pm$3%						
	1$\pm$5%						
L,D,A	negligible						

High Boilers (HB) ≡ materials having boiling points higher than that of para-terphenyl. They have molecular weights ranging from 230 to about 3,000.

Low and Intermediate Boilers (LIB) ≡ materials with boiling points less than or equal to those of the terphenyls.

From these definitions it can be seen that % DP = % LIB + % HB.

The transient portion of a run, where the % DP goes from ~2% to ~50%, lasts a minimum of ten weeks while the steady state portion of a run lasts from ten to twenty weeks.

The nomenclature, DP, is also used in this report for Differential Pressure when referring to the Foxboro DP cell. However, it should be clear from the text which definition is to be used.

Density (ρ) and viscosity (μ) measurements are made at MIT on samples taken from the organic loop as described in Section 3.6. Samples are taken as the irradiation run proceeds and, therefore, actual measurements of ρ and μ are used in the heat transfer correlations. Samples from MIT have been sent to other laboratories for analysis and in general the agreement on density and viscosity data has been within $\pm$1% and $\pm$3% respectively (3). The uncertainty limits on density and viscosity data taken during the transient portion of the irradiation are higher than the

limits on the steady state data since during the transient the physical properties must be correlated as a function of both % DP and temperature while during steady state the % DP is fixed. The actual data taken during a run (3) show that there is more scatter in the transient data than the steady state data.

Specific heat and thermal conductivity measurements in general must be obtained from the available literature (1) (2) (3) (6) (20) (25) (26) or from measurements made at other laboratories. Several samples of coolant irradiated at MIT have been sent to other laboratories for analysis and the results have agreed, within the uncertainty limits, with published data. Since c_p and k measurements are not made at MIT and in general such data is difficult to obtain, the estimate of the uncertainty on both of these measurements is $\pm 5\%$ during steady state and $\pm 6\%$ during the transient portion of the run.

All temperatures are measured with calibrated chromel-alumel thermocouples and the appropriate corrections are applied when the data are reduced. The coolant bulk inlet and outlet temperatures are measured with 1/8" OD chromel-alumel immersion thermocouples that extend 1" into the coolant mixing chambers. The inside wall temperatures are calculated (2) (3) (Section 7.5) from the measured outside wall temperature and the calculated

temperature drop through the test heater wall. The temperature drop across the film (ΔT_f) is calculated from the definition

$$\Delta T_f \equiv (T_{Wi} - T_B) \quad .$$

The error limits on ΔT_f are those reported by Morgan and Mason (3).

The heat input to the test heater is calculated from

$$Q = \Delta E^2/R$$

which is then corrected for the heat losses to the current lugs to determine the heat input to the coolant. This heat input is compared with a heat balance on the coolant

$$Q = m\ c_p\ (T_{B_{out}} - T_{B_{in}})$$

and in general the difference between these two values is less than 7%.

The errors in the velocity measurement are those quoted by Morgan and Mason (2) (see Section 3.1).

Pressure drop measurements were made with a Foxboro, model 13A, Differential Pressure (DP) cell as described in Section 3.3. The instrument can be read to within approximately $\pm$0.25 percent at full scale and $\pm$0.5 percent at half scale. This is confirmed by the reproducibility of the calibrations (Section 7.3) and the excellent agreement with the usual friction factor correlations when measurements were made on distilled water (Section 7.4). However, when data were taken on organic coolants,

it was necessary to heat the DP cell to keep the coolant liquid. Also, to avoid erroneous readings, it is imperative that the DP cell be vented so that there is no gas in either line leading to the cell or in the chamber itself. When venting with water at room temperature, the cell could be vented for a long period to be certain that no gas was entrapped. When venting hot organic this may not have been true (see Section 5.3). These considerations led to the uncertainty limits quoted in Table 5.

The errors in the measurement of lengths or diameters are considered negligible compared to the uncertainty in the other variables.

4.2 Calculated Uncertainty on Final Correlations

Based on the estimated uncertainty of Table 5, the Root Mean Square (RMS) uncertainty was calculated on the variables used in the correlations. These estimates are presented in Table 6. In summary, the RMS uncertainty on the heat transfer correlation (finally fixed at $Nu/Pr^{0.4}$) is on the order of $\pm$10% to $\pm$12% and the RMS uncertainty on the Reynolds Number is estimated at $\pm$5%. The estimated uncertainty on the friction factor measurement is $\pm$5% to $\pm$10% depending on the Reynolds Number range.

TABLE 6

CALCULATED ROOT MEAN SQUARE (RMS) UNCERTAINTY ON FINAL CORRELATIONS

Variable	Calculated From	Remarks	Estimated Uncertainty RMS
Nu	$\frac{UD}{k} = \frac{\Delta E^2 D}{RA\ \Delta T_f\ k}$	$Q/A = 10^5$ BTU/hr-ft^2	
		Steady State	
		V_m = 10 ft/sec	9%
		V_m = 20 ft/sec	11%
		Transient	
		V_m = 10 ft/sec	9%
		V_m = 20 ft/sec	12%
Re	$\frac{\rho VD}{\mu}$	Steady State	
		V_m = 10 ft/sec	4%
		V_m = 20 ft/sec	4%
		Transient	
		V_m = 10 ft/sec	5%
		V_m = 20 ft/sec	5%
Pr	$\frac{c_p \mu}{k}$	Steady State	7%
		Transient	9%
f	$\frac{\Delta P}{\frac{\rho}{2g_o} V^2 \frac{L}{D}}$	Steady State Only	
		Re = 10^4	10%
		Re = 10^5	5%

5.0 HEAT TRANSFER AND FRICTION FACTOR DATA FOR SANTOWAX WR

5.1 Heat Transfer Data Measured With Test Heater 6

The heat transfer data taken with Test Heater 6 by Sawyer and Mason (3), on Santowax OMP, were presented in Section 2.2, Figures 2 and 3. Heat transfer measurements were not taken as frequently during the Santowax WR runs because of a temporary manpower shortage during that period and also it was felt that sufficient data had been taken on organic coolants.

The data taken with Test Heater 6 on Santowax WR is presented in Figures 16 and 17. It should be noted that the Dittus-Boelter type equation of McAdams (7) gives a very good fit to these data. Figure 16 presents all of the data taken during the 750°F irradiation of Santowax WR (Run No. 3). Figure 17 presents the steady state data from Run No. 3 and the steady state data from the 700°F (Run No. 5) and the 610°F (Run No. 11) irradiations. Data were taken only during the steady state portions of Runs 5 and 11.

Tabulated values of these data are presented in Section 7.7 of the Appendix.

5.2 Heat Transfer Data Measured With Test Heater 7

A large number of pressure drop runs were made with Test Heater 7 but because of time limitations only a few heat transfer runs were made. The factor

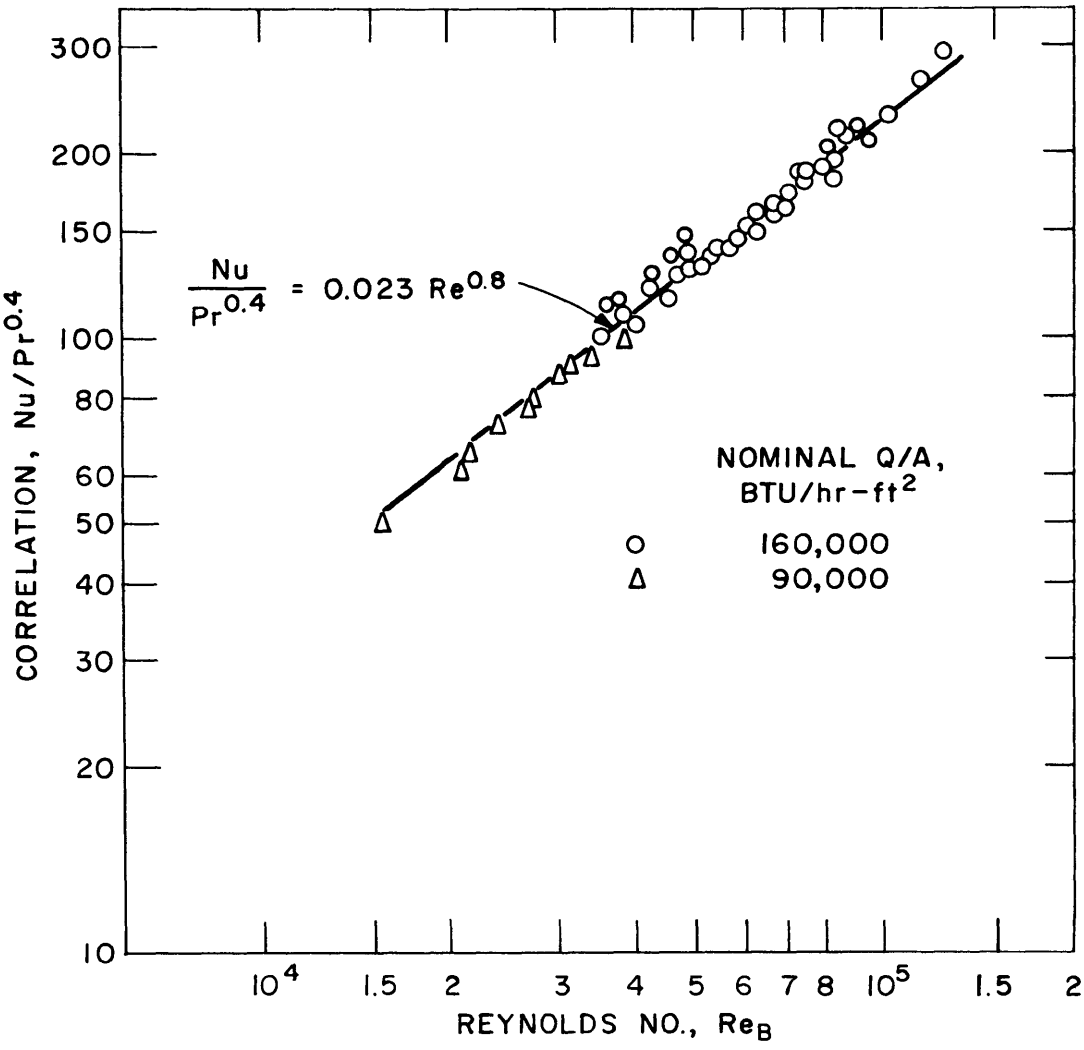

FIG. 16 UPSTREAM HALF OF TH6 DATA FOR SANTOWAX WR IRRADIATED AT 750°F (ALL RUN NO. 3 DATA)

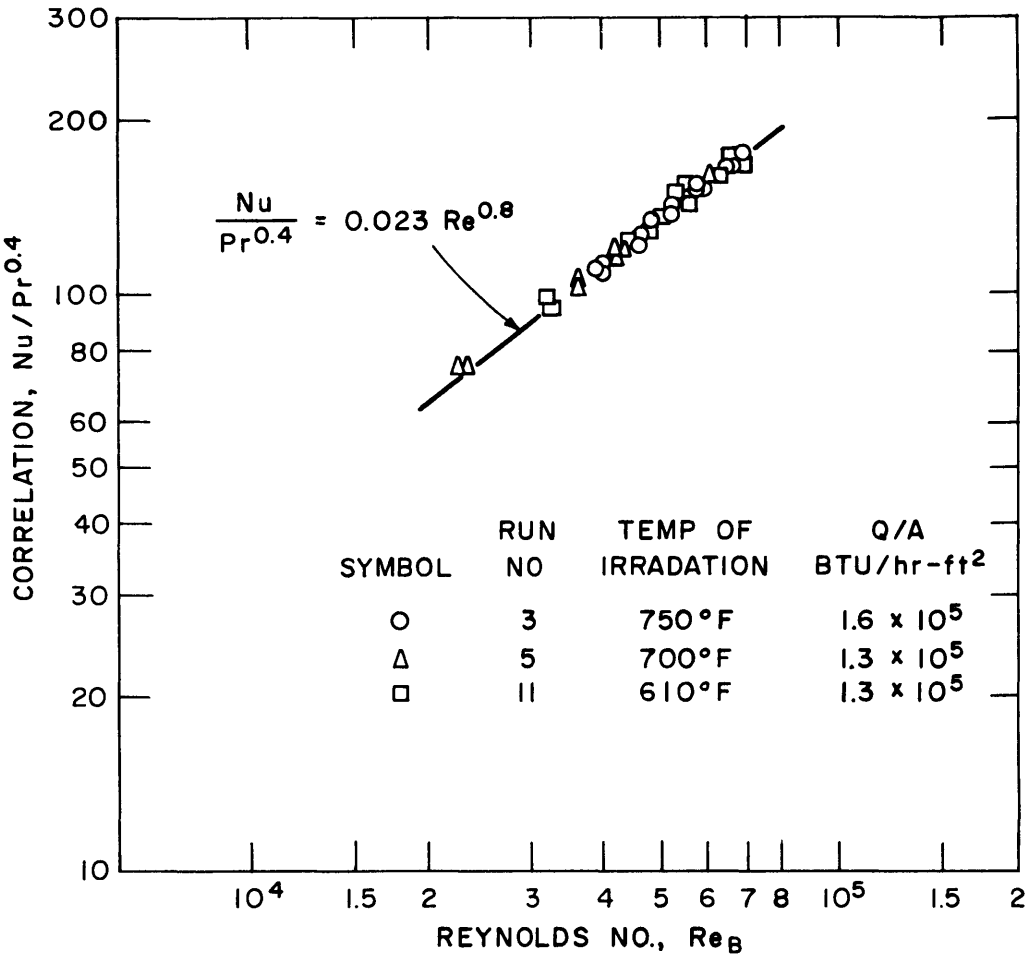

FIG. 17 UPSTREAM HALF OF TH6 DATA FOR SANTOWAX WR IRRADIATED AT VARIOUS TEMPERATURES, STEADY STATE DATA

that increased the time to take heat transfer data was waiting for the adiabatic oven wall temperature to reach equilibrium with the test heater outside wall temperature.

During the period of time when most of the friction factor data and heat transfer were taken, the organic loop was not circulating coolant through the reactor core. Therefore, in order to take measurements on irradiated coolant, it was necessary to make a mixture of HB and fresh coolant to get irradiated coolant. This was done by taking high boilers (HB), which had been separated from the irradiated coolant of Run No. 9 by distillation, and adding these HB to fresh Santowax WR. This charge of coolant to the organic loop was called Run No. 12 and analysis of samples taken from the loop (see Section 7.6) indicates that it was $\sim$33% DP.

Heat transfer data taken during Run No. 12 and the first few days of Run No. 13 (Santowax WR at 572°F and approximately 10% DP) are presented in Figures 18, 19 and 20. Data shown in Figure 18 were taken on the upstream half of Test Heater 7 while data shown in Figure 19 were taken on the downstream half of the test heater. Because of the better temperature profile on the upstream half of the heater (Figure 15) and the better fit to the Dittus-Boelter type correlation, it is recommended that the upstream half of TH7 be used for

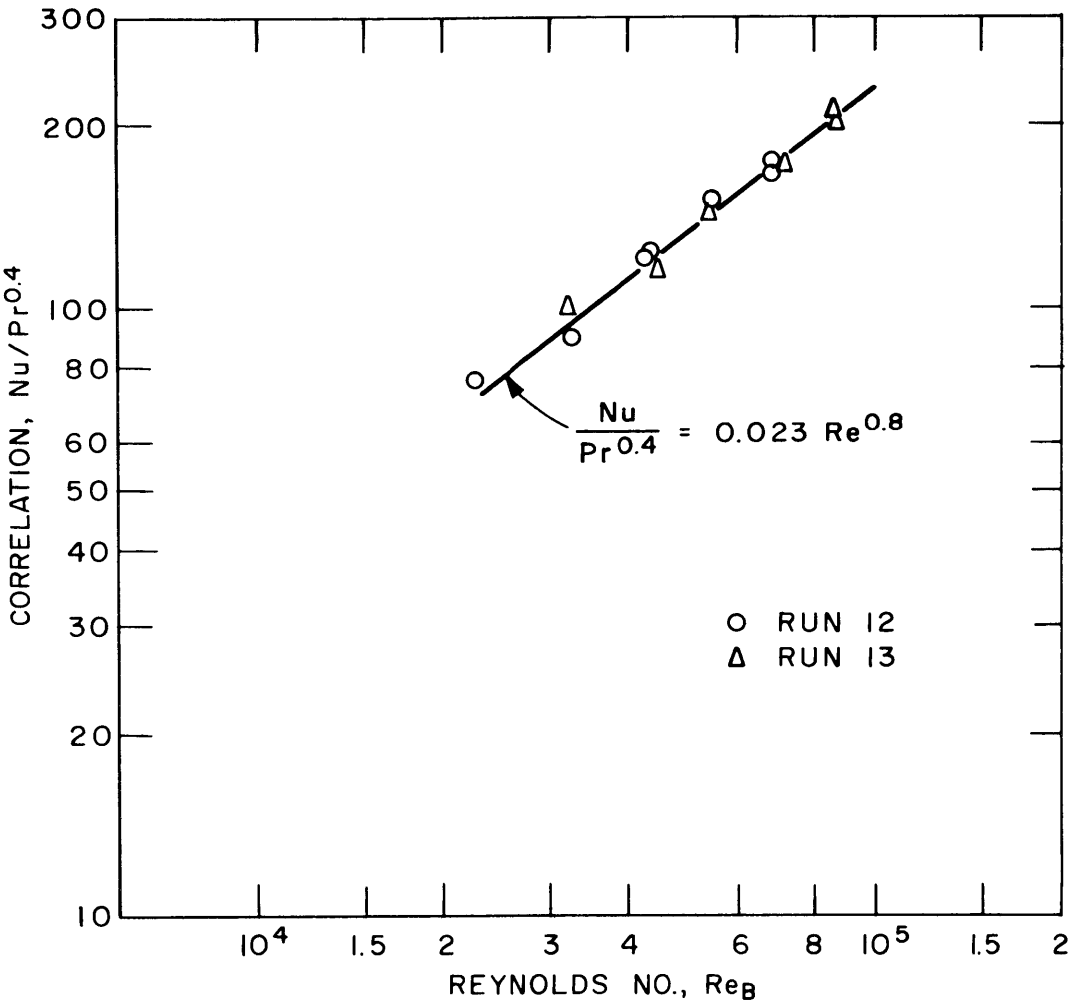

FIG. 18 UPSTREAM HALF OF TH7 DATA FOR IRRADIATED SANTOWAX WR

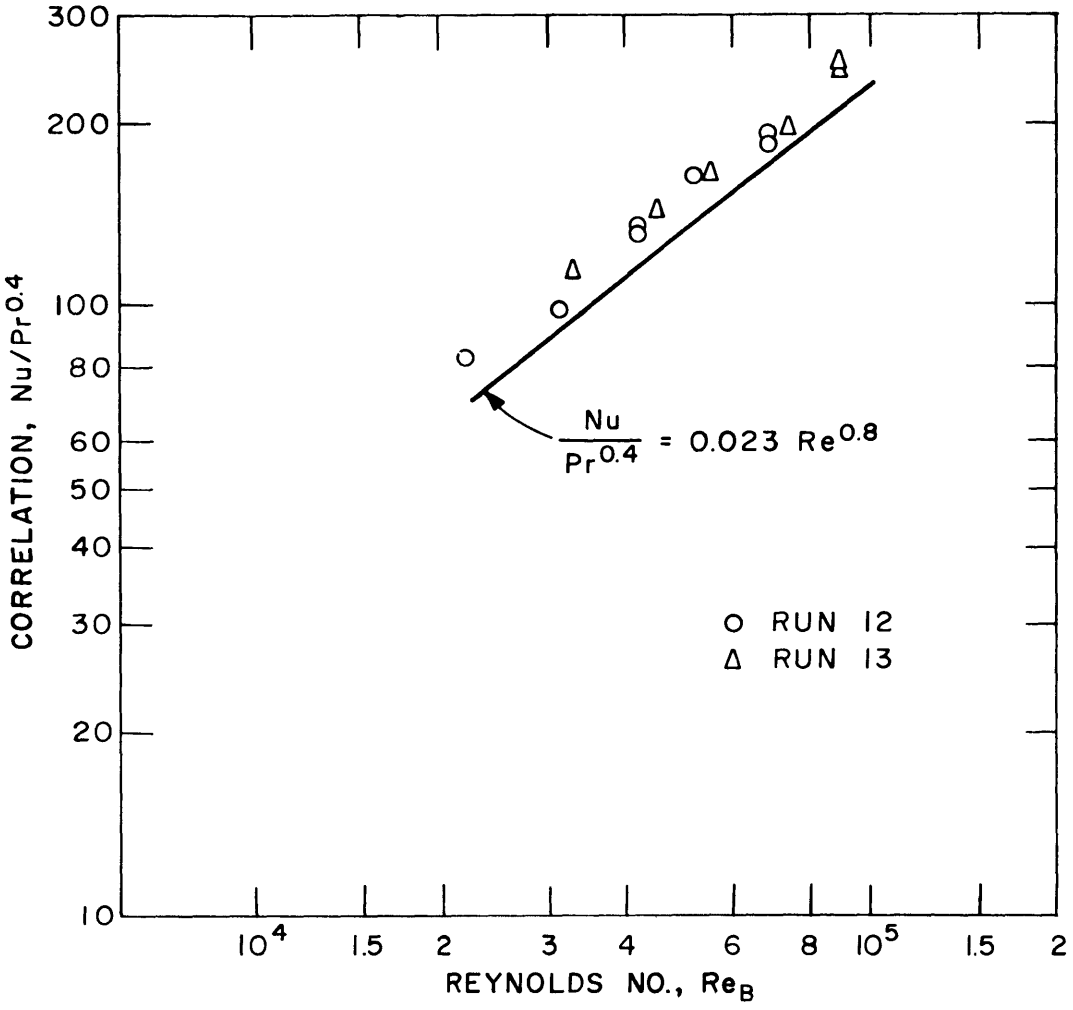

FIG. 19 DOWNSTREAM HALF OF TH7 DATA FOR IRRADIATED SANTOWAX WR

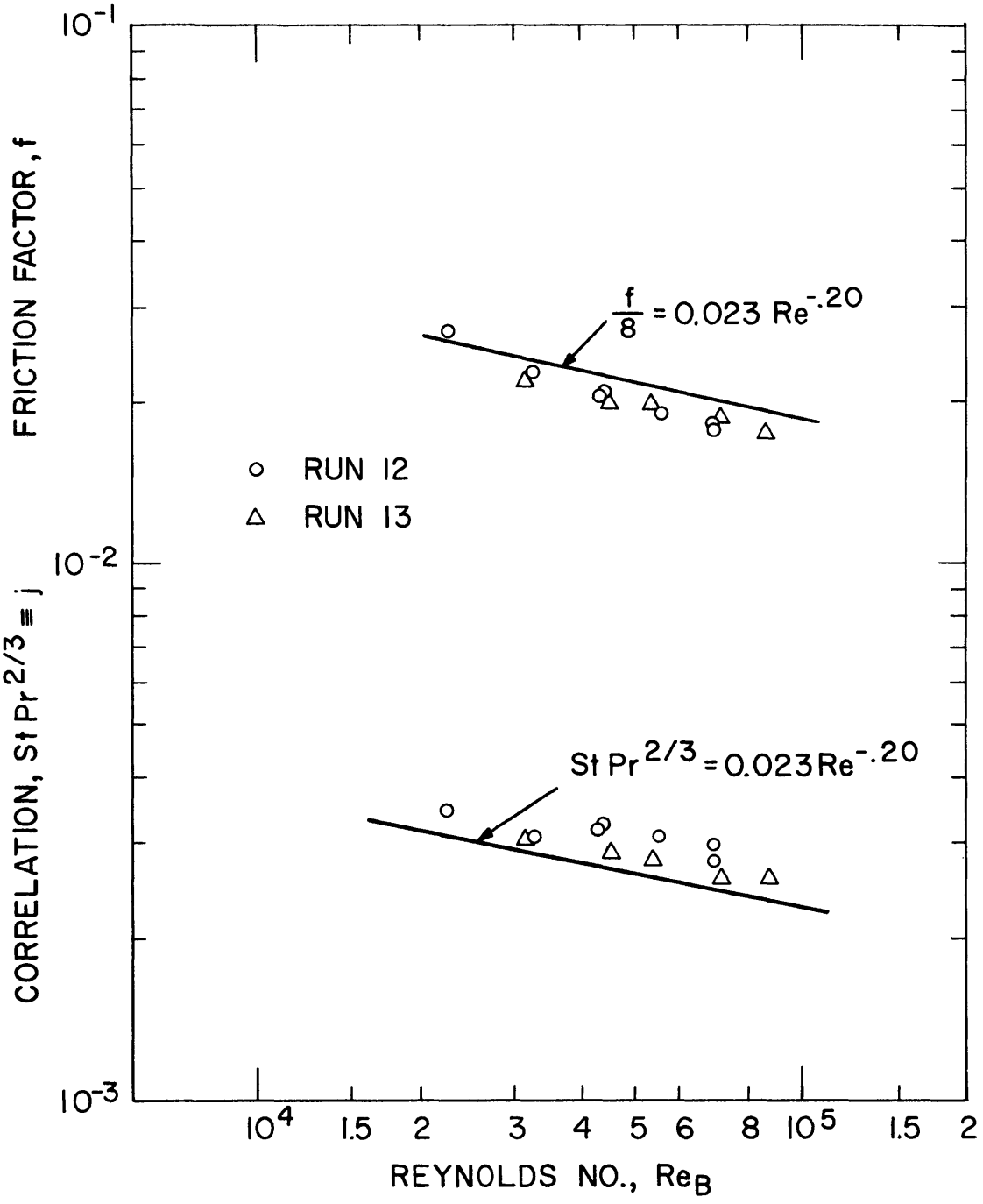

FIG. 20 FRICTION FACTOR AND HEAT TRANSFER FACTOR FOR IRRADIATED SANTOWAX WR, UPSTREAM HALF OF TEST HEATER 7

future correlations. It should be noted that even though the data from the downstream half of TH7 fall above Equation (1), the slope of the data is 0.8.

Figure 20 presents friction factor data and heat transfer data as suggested by the Colburn Relation, Equation (2). It should be noted that the slope of -0.2 on the Reynolds Number fits both the j factor and f factor data quite well.

5.3 Friction Factor Data Measured With Test Heater 7

A large number of friction factor data points were taken with Test Heater 7, using Santowax WR at 12%, 17% and 33% DP. A histograph is presented in Appendix 7.1 which shows the order in which these runs were taken, when particular samples were taken for analysis, and when the coolant was changed in the loop.

Figure 21 presents all the data taken on so-called low % DP ($12 \leqslant \%\ DP \leqslant 17$) which are compared with the usual correlation of friction factor data for smooth tubes (Equation 11).

All of the friction factor data taken on Santowax WR arepresented in Figure 22. These data are compared with the following correlation

$$f = 0.175\ Re_B^{-0.20} \qquad (15)$$

because it was found to give a better fit to all of the TH7 data than Equation (11).

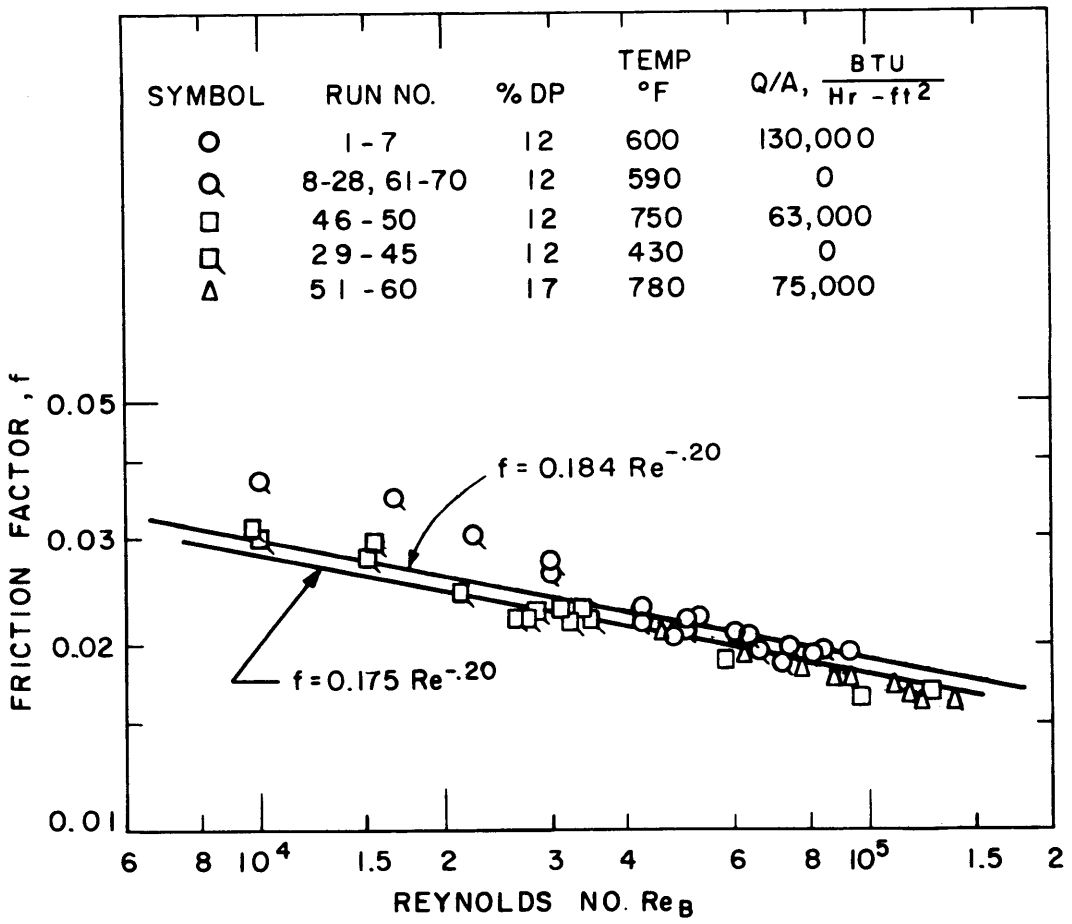

FIG. 21 FRICTION FACTOR DATA FOR IRRADIATED SANTOWAX WR, LOW % DP

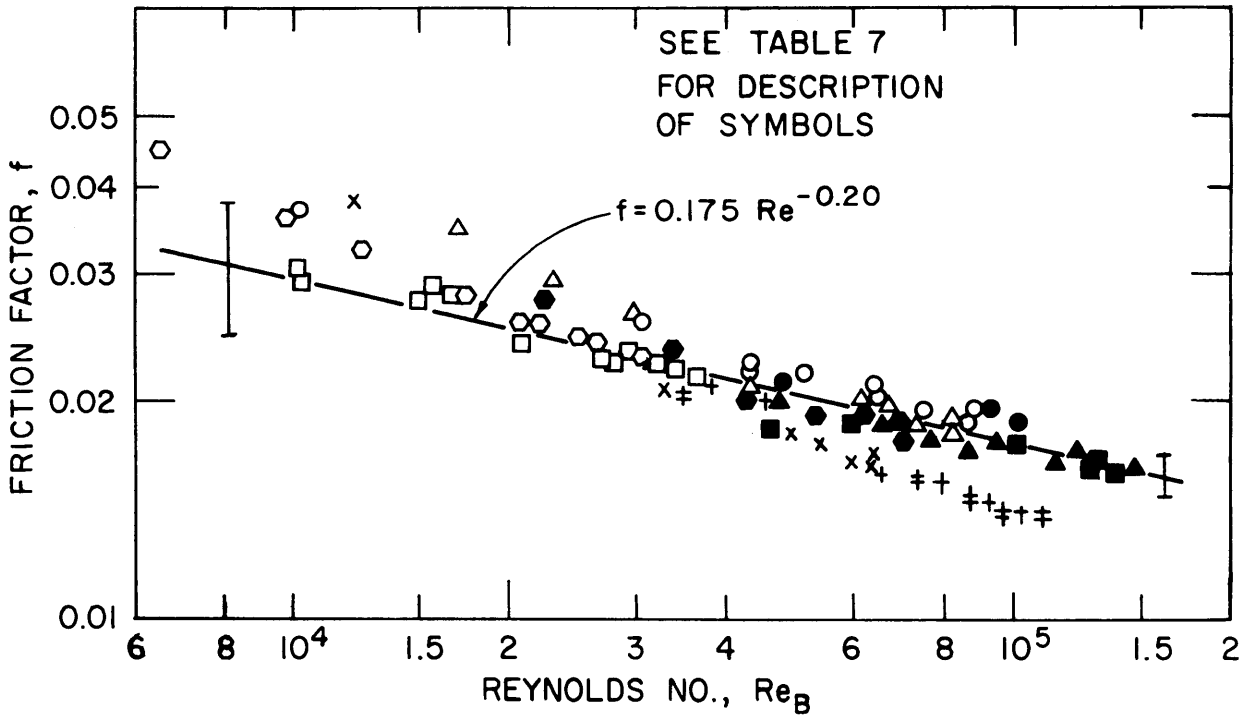

FIG. 22 ALL SANTOWAX WR FRICTION FACTOR DATA

TABLE 7

DESCRIPTION OF SYMBOLS FOR FIGURES 22, 23 AND 24
(Friction Factor Data)

Symbol	Run No.	% DP	Temp. ^{o}F	Q/A BTU/hr-ft^2
●	1-7	12	600	130,000
○	8-28	12	590	0
□	29-45	12	430	0
■	46-50	12	750	63,000
▲	51-60	17	780	75,000
△	61-70	17	590	0
×	71-80	33	600	0
+	81-89	33	750	75,000
‡	90-96	33	780	75,000
⬡	97-109	33	430	0
⬢	110-122	33	630	110,000
⊘	Water Runs 1-61	-	71 to 104	0

It should be noted that the data taken on 33% DP coolant appears to have a steeper slope than the low % DP data; however, for the following reasons it was decided that these data do not confirm such a correlation.

a. These data (Runs 71 to 96) were taken soon after the loop was charged with new coolant and it is quite possible that the DP cell was not vented properly. It is not possible to visually inspect the lines to the DP cell or the DP cell itself to be certain that there is not gas present. Coolant is bled through the DP cell until only liquid comes out, but it is possible that for these runs this procedure did not work.

b. Runs 97 to 122 which were taken the following week do fit Equation (15) quite well. The DP cell was vented before each series of runs.

c. During Runs 110 to 120 heat transfer data were taken, see Figure 20, which indicate that both the j factor data and f factor data have a slope of -0.2 on the Reynolds Number. Unfortunately, no heat transfer data were taken during Runs 71 to 96, therefore, Runs 110 to 120 were given greater weight in this evaluation.

Figure 23 shows selected Santowax WR data, where Runs 71 to 96 were deleted on the basis of the above

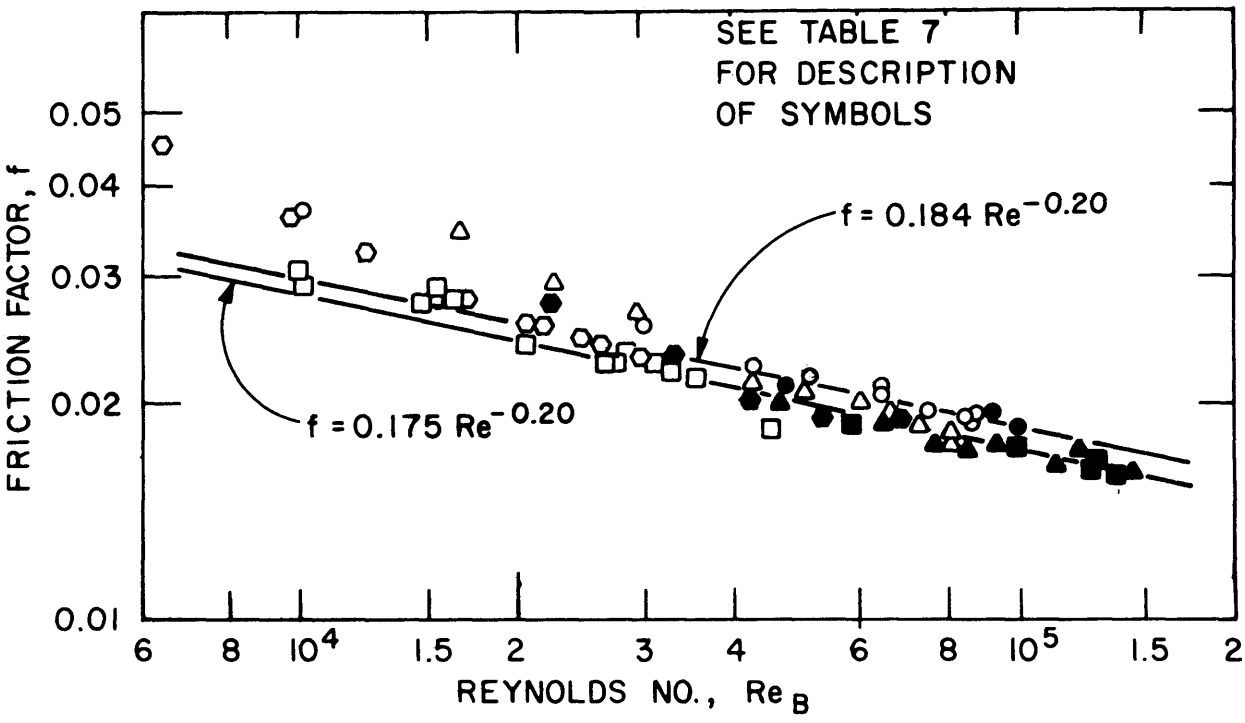

FIG. 23 FRICTION FACTOR FOR IRRADIATED SANTOWAX WR, SELECTED DATA

evaluation. These data are compared with Equations (11) and (15), and it can be seen that the lower curve gives a better fit.

Finally, to show that Equation (15) gives a better fit on all the friction factor data taken, Figure 24 presents selected Santowax WR data and all of the water friction factor data (see Appendix 7.4).

The vertical lines on Figures 22 and 24 represent the calculated uncertainty on each measurement as outlined in Section 4.

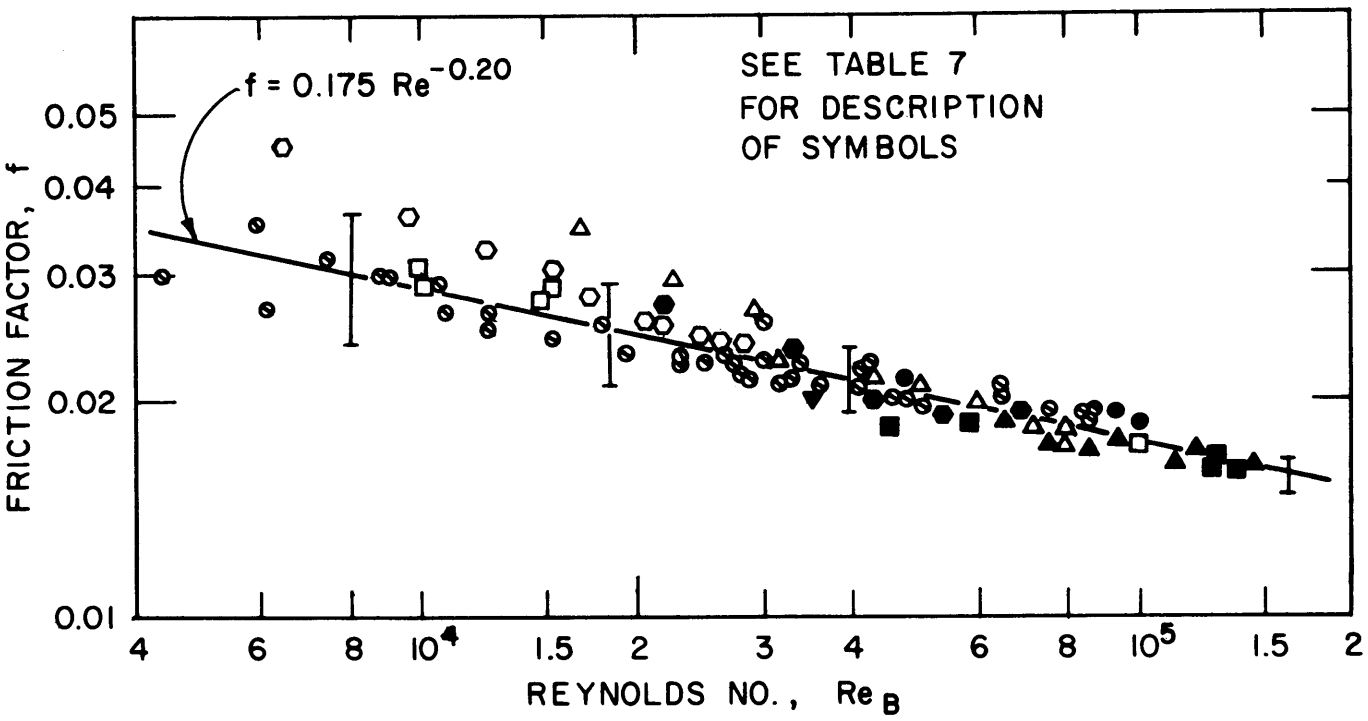

FIG. 24 FRICTION FACTOR DATA FOR TH7, SELECTED SANTOWAX WR DATA AND WATER DATA

6.0 DISCUSSION AND CONCLUSIONS

6.1 Correlation of Heat Transfer Data

A tabulation of the "best" correlations for all of the MIT organic coolant data is presented in Table 8. The "best" correlations quoted here were obtained from the computer program MNHTR (3), (Appendix 7.5) which calculates the best least square fit to all of the data taken during a particular run.

The method of data reduction is outlined in detail in Appendix 7.5, but a brief outline of how the best correlations were obtained will be presented here. It was found that including the viscosity ratio, (μ_B/μ_W), in the correlations did not improve the fit of the data so a Dittus-Boelter type correlation was selected. For the MIT data the "best" value of the Prandtl Number exponent was finally fixed at 0.4. This value represents a rounded-off value of the "best least square" value selected by the computer program, MNHTR, for each set of data. It should be mentioned that the best value selected by the computer program was generally quite close to 0.4, and that it was fixed at this value for convenience in plotting and comparing the final correlations.

The program (MNHTR) was then programmed to find the "best least square" value for the Reynolds Number exponent and coefficient a (see Appendix 7.5, Equation (40)) and these results are presented in Table 8.

TABLE 8

SUMMARY OF MIT ORGANIC COOLANT HEAT TRANSFER DATA

"Best" or Recommended Correlation*	Coolant	Irradiation Run No.	Reynolds No. Range	Prandtl No. Range	Nominal Heat Flux BTU/hr-ft^2	No. of Data Points	Test Heater Used
$Nu_B = .0079\ Re_B^{.92} Pr_B^{.35}$ or $Nu_B = .0081\ Re_B^{.9} Pr_B^{.40}$	Santowax OMP	1	9×10^3 to 10^5	7-32	10^5 to 2×10^5	267	TH5, TH6
$Nu_B = .0069\ Re_B^{.9} Pr_B^{.4}$	Santowax OMP	2	2×10^4 to 10^5	6-19	1.3×10^5	102	TH6
**$Nu_B = .0079\ Re_B^{.9} Pr_B^{.4}$	Santowax OMP	1,2	9×10^3 to 10^5	6-32	10^5 to 2×10^5	369	TH5, TH6
$Nu_B = .016\ Re_B^{.83} Pr_B^{.4}$	Santowax OMP	2	2.2×10^4 4 to 6.7×10^4	8.6-12	1.3×10^5	steady state data, 50	TH6
$Nu_B = .026\ Re_B^{.79} Pr_B^{.4}$	Santowax WR	3	2×10^4 to 1.2×10^5	5.5-10	9×10^4 to 1.6×10^5	58	TH6
$Nu_B = .033\ Re_B^{.77} Pr_B^{.4}$	Santowax WR	5,11	2×10^4 4 to 8×10^4	7.3-8.9	1.3×10^5 to 1.6×10^5	26	TH6
$Nu_B = .041\ Re_B^{.75} Pr_B^{.4}$	Santowax WR	12,13	3×10^4 to 10^5	7.4-10	1.3×10^5	13	TH7

*For all except the first correlation, the Prandtl Number exponent was fixed at 0.4.

**Recommended by Sawyer and Mason (3).

One of the purposes of building Test Heater 7 was to measure friction factors and then compare these data with the usual correlations. Because of the previous heat transfer data obtained on Santowax OMP, which has a Reynolds Number dependence of 0.9, it was expected that Santowax WR would behave the same way and hence f and j factors could be compared on a coolant whose Reynolds Number dependence was different than that usually quoted. However, the recent Santowax WR data taken at MIT are correlated quite well by the Dittus-Boelter type equation or the Colburn type analogy (see Figure 16 or Table 8) and therefore the friction-factor data did not help to explain this discrepancy in the previous heat transfer data on Santowax OMP.

To help evaluate the anomaly of the Santowax OMP data, the following facts are noted:

a. Santowax OMP data cover a more extensive range of both Reynolds Number and Prandtl Number.

b. There were more data points taken on Santowax OMP than Santowax WR (369 to 97).

c. Other investigators of organic coolants (4) (5) (6), (Section 2.2) have found that a correlation with an exponent on the Reynolds Number greater than 0.8 gives the best fit to their data.

d. The calculated Root Mean Square (RMS) uncertainty limits on a particular measurement of the Nusselt Number are estimated to be $\sim \pm 10\%$ during the steady state portion of a run and $\sim \pm 11\%$ during the transient. The RMS deviation of the data from a given correlation is on the order of these calculated values (generally less than $\pm 10\%$). If the data are compared with the Dittus-Boelter type equation with a slope of 0.8, the data at the high and the low values of the Reynolds Number lie outside of these uncertainty limits.

e. A change in test heaters took place during Run 1 so that the following Reynolds Number range was covered for the two heaters:

$2 \times 10^4 < Re < 10^5$ for TH5

$9 \times 10^3 < Re < 4 \times 10^4$ TH6

f. Heat transfer data taken at high Reynolds Number are in general taken at the beginning of the transient portion of the irradiation run, while the low Reynolds Number data are taken at the end of the transient when the % DP or % HB is highest. Therefore, errors in the physical properties could influence these particular measurements which have a large influence on the "best fit" selected.

g. A large number of data were taken during the steady state portion of an irradiation where errors in the physical properties should not influence the slope of the "best" correlation. In general, these data fit Equation (1) fairly well. Also, note the change in Reynolds Number exponent (Table 8) from 0.9 to 0.83 when the data taken during Run 2, steady state, was correlated by itself on the computer program, MNHTR.

   The exponents calculated by the program, MNHTR, have one standard deviation (one σ) on the order of .02 to .05, depending on the number of data points. Therefore, for 95% confidence ($\pm 2\sigma$) these exponents should be written 0.9 ± 0.1, and hence such a change is significant.

h. Error limits usually quoted on heat transfer data are on the order of $\pm$40%.

i. Santowax WR is similar in composition to the Euratom reference coolant OM_2 (Table 1) for which considerable data are available on the physical properties (20) that are not measured directly at MIT. For the correlations reported here on Santowax WR, MIT values for the density and viscosity were used and specific heat and thermal conductivity values were taken from

Reference (20). The same laboratories that measured c_p and k for OM_2 provided the values used for Santowax OMP, but fewer measurements were made on OMP (3) (30). Also, for the correlations quoted here and in Reference (3), it was assumed that c_p did not vary with % HB but Atomics International (28) (29) reports a 10% decrease for the value of c_p for the OMRE coolant at 40% HB.

j. Wilson plots can also be used as an aid to determine the best exponent on the Reynolds Number. The results of plotting the heat transfer data in this manner indicate that an exponent on the Reynolds Number of 0.8 is to be slightly preferred (Appendix 7.9).

Items a, b, c and d indicate that there is a dependence on the Reynolds Number greater than 0.8. Items e through j indicate that perhaps too much emphasis is being placed on this deviation, considering the errors involved.

It has also been suggested that this discrepancy could be due to one of the following:

a. A natural circulation or Grashof Number effect because of the high temperature differences between the test heater wall and the coolant. A study (22) was made to see if any such effect could be noted and the results were

negative. A Grashof Number (Gr) was defined

$$Gr \equiv \frac{g_o \beta \Delta T_f D^3 \rho_B^2}{\mu_f^2} \qquad (16)$$

and values of a normalized Nusselt Number were plotted as a function of this parameter. For a range of $6 \times 10^4 < Gr < 2 \times 10^6$ no effect could be seen.

b. The effect of (μ/μ_w) or the viscosity ratio. This parameter was considered by Sawyer and Mason (3) and, in general, they found that when the viscosity ratio was included in the correlation, its influence was to raise the exponent on the Reynolds Number (see Table 12, Appendix 7.5).

c. A buildup of scale on the test heater inside wall during the period of time that data are taken. The heat exchanger used for heat transfer measurements is also used to maintain the organic coolant being tested at the specified irradiation temperature so it is possible that a scale could build up on this surface.

The heat transfer coefficient measured at MIT is actually the over-all coefficient, U. Where U is defined as follows

$$1/U \equiv 1/h_f + 1/h_s \tag{17}$$

and where h_f is the usual film coefficient of heat transfer and h_s is a scale coefficient of heat transfer. The heat transfer program (MNHTR) can be programmed to account for the influence of h_s but because all of the measurements at MIT, over a period of three years, indicate that there has been no measurable scale buildup on heat transfer surfaces, h_s was set equal to zero for all of the quoted correlations (Appendices 7.5.1 and 7.9). Sawyer and Mason (3) also considered this possibility and they were able to show that any buildup of scale would raise the exponent on the Reynolds Number to a higher value.

To help to determine what the best Reynolds Number exponent is for Santowax OMP, some of these data were replotted in Figure 25 using a Colburn-type analogy. For this correlation the Stanton Number was calculated directly from Equation (13)

$$St = \frac{S}{A} \left[\frac{T_{B_{out}} - T_{B_{in}}}{\Delta T_f} \right] \tag{13}$$

where the above temperatures can be read directly from the computer output of MNHTR. A modified j factor, j^*, defined as

$$j^* \equiv St \; Pr_B^{0.6} \tag{18}$$

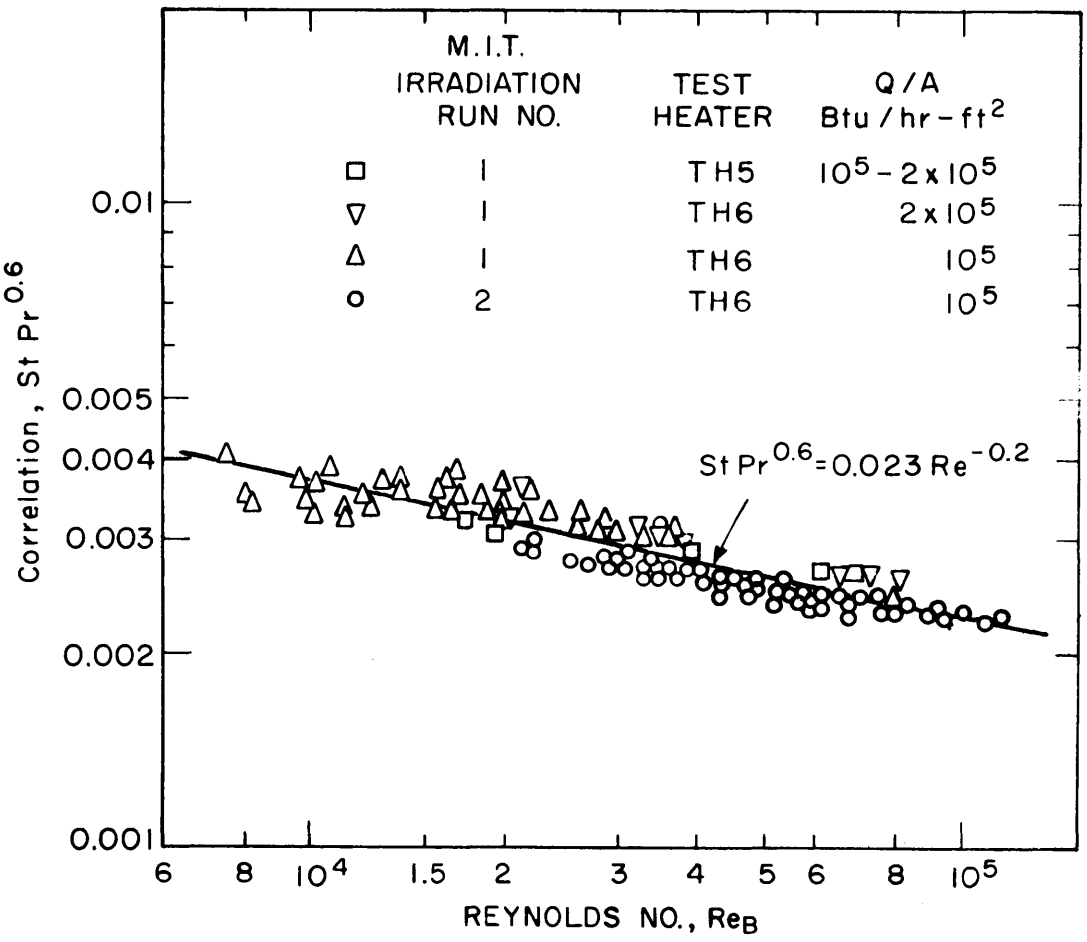

FIG. 25 COLBURN ANALOGY FOR M.I.T., IRRADIATED SANTOWAX OMP, HEAT TRANSFER DATA

was used as the correlation because of the following considerations. Equation (1) can be rearranged to a Colburn-type equation from the definition of the Stanton Number

$$j^* \equiv St\ Pr_B^{0.6} = 0.023\ Re_B^{-0.2} \quad . \tag{19}$$

If the best fit to all of the MIT Santowax OMP data (3) (Table 2) (Table 8)

$$Nu_B = 0.0079\ Re_B^{0.9}\ Pr_B^{0.4} \tag{20}$$

is rearranged in the same manner, the resulting equation is

$$St\ Pr_B^{0.6} = 0.0079\ Re_B^{-0.1} \quad . \tag{21}$$

Therefore, if the "best correlation" for Santowax OMP, Equation (20), is not a function of the physical properties, then the data plotted in such a manner should fit Equation (21). If the correlation is a function of the physical properties used, then some deviation would be expected. Figure 25 indicates that Equation (19) is to be preferred to correlate these data. When making such an evaluation by eye, it should be noted that the error limits are much higher on data taken below a Reynolds Number of 10^4.

Another consideration is that all of the above correlations are correlated by the heat transfer program, MNHTR, one irradiation run at a time. For example, Run 1 (267 data points) is least squared separately from Run 2 (102 data points) and, therefore, separate "best least

square fit" correlations are tabulated for each group. The data are correlated this way because MNHTR can only least square 300 data points at a time, due to the limit of a 32K storage on the IBM 709/7090 computer.

To aid in the final conclusions, all of the MIT heat transfer data (466 data points) taken on irradiated coolants are plotted in Figure 26. It can be seen that the Dittus-Boelter type equation of McAdams (7), with error limits of ±10%, correlates all of the data.

Of course, Equation (20) will also fit all of the data in this range, but Equation (1) or (19) is recommended because of the following considerations:

a. Equation (1) is well established for a large number of coolants over a considerable Prandtl Number and Reynolds Number range (7) (16) (Section 2.3).

b. For the MIT Santowax OMP data, the high Reynolds Number and the low Reynolds Number data were taken during the transients of the irradiation run, when the physical properties are probably not as well known.

c. With reasonable uncertainty limits of ±10%, compared to the usual limits quoted of ±40%, Equation (1) fits all of the MIT data.

d. Santowax WR is correlated very well by Equation (1). Also, the friction factor data taken with

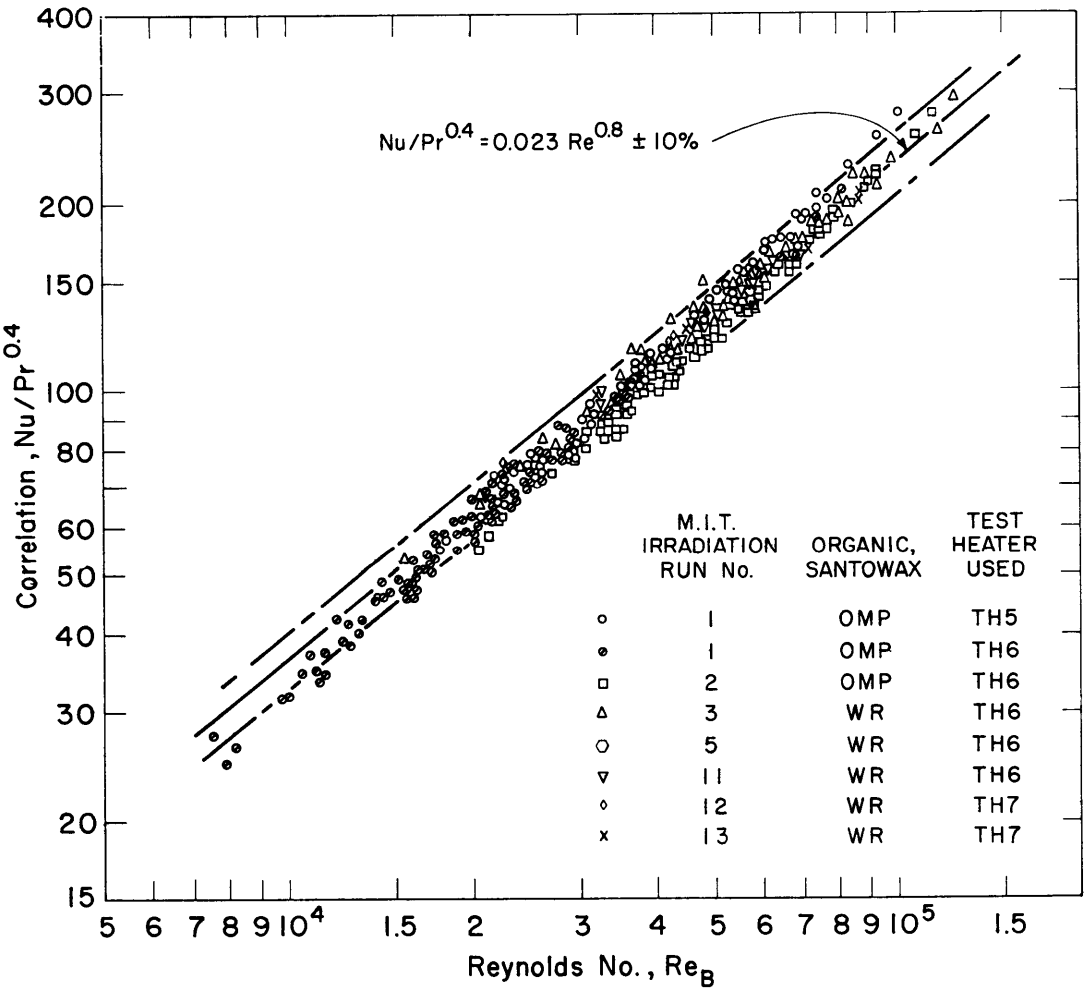

FIG. 26 ALL M.I.T., IRRADIATED ORGANIC COOLANT, HEAT TRANSFER DATA

TH7 on Santowax WR is correlated quite well by

$$j^* \equiv St\ Pr_B^{0.6} = 0.023\ Re_B^{-0.2} = \frac{f}{8} \quad . \qquad (22)$$

e. Martini, et. al. (28) (29) plotted their data (4) along with the data of Stone, et. al. (5) and recommended

$$Nu_B = 0.0243\ Re_B^{0.8}\ Pr_B^{0.4} \qquad (23)$$

for the Reynolds Number range of $2 \times 10^4 < Re < 5 \times 10^5$. These data cover a greater range of Reynolds Number than the MIT data. These data, as plotted by Martini, et. al., are presented in Figure 27.

f. Equation (19) gives a good fit to the Santowax OMP data as plotted in Figure 25.

Therefore, the following correlations are recommended for irradiated organic coolants in the Reynolds Number range, $10^4 < Re < 5 \times 10^5$

$$Nu_B = 0.023\ Re_B^{0.8}\ Pr_B^{0.4}\ \pm 10\% \qquad (1)$$

or

$$St\ Pr_B^{0.6} = 0.23\ Re_B^{-0.2}\ \pm 10\% \qquad (19)$$

6.2 Correlation of Santowax WR Friction Factor Data

From Figures 19, 20, 21, 22 and 23 it can be seen that all of the friction factor data fits Equation (15) quite well. This correlation gives values of the friction factor, f, 5% lower than the usual correlation for smooth tubes

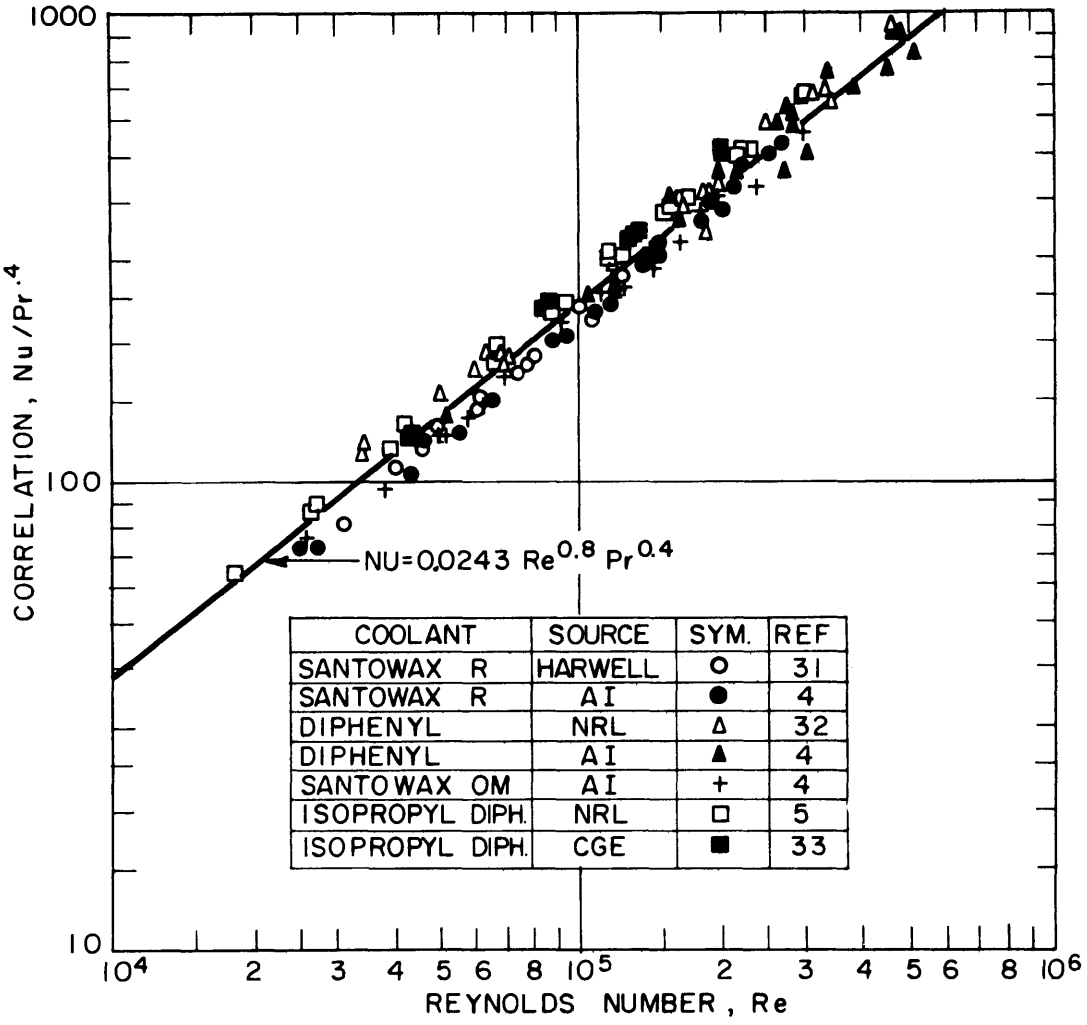

FIG. 27 COMPARISON OF UNIRRADIATED ORGANIC COOLANT HEAT TRANSFER DATA BY GERKE AND MARTINI, ET AL (28)

but this is within the normally quoted uncertainty limits (of ±5%) on such data.

Since it gives more conservative values for f, and it is difficult to evaluate the effect of roughness, the following Equation (11) is recommended for irradiated organic coolants in smooth tubes for the Reynolds Number range, $10^4 < Re < 10^5$

$$f = 0.184\ Re_B^{-0.2} \tag{11}$$

It should be mentioned again that this value of f is equal to 1/4 of the Fanning friction factor, f_F. The f used in this report can be defined as in Equation (9) or as

$$f \equiv \frac{\Delta P}{\frac{1}{2g_o}\ \rho V^2\ \frac{L}{D}} \tag{23}$$

The major reasons for the installation of Test Heater 7 and the DP cell were (Section 2.4): to aid in the determination of the best Reynolds Number exponent on the heat transfer data and to provide useful friction factor data. Useful friction factor data are reported (Equation (11)) and these data did help to resolve the Reynolds Number exponent discrepancy, since all the friction factor and heat transfer data taken with TH7 on Santowax WR can be correlated by

$$\frac{f}{8} = 0.023\ Re_B^{-0.2} = St\ Pr_B^{0.6} \equiv j^* \quad . \tag{22}$$

7.0 APPENDICES

7.1 Histograph for End of Run 11 and Run 12

Figure 28 presents a profile of the organic loop surge tank temperature as a function of time. During this period, November 1964 to February 1965, the organic loop was not being run inpile. The inpile section of the loop had been removed from the reactor core so a bypass line was installed at the rear of the hydraulic console to permit the taking of heat transfer and friction factor data. Figure 28 also shows when pressure drop or heat transfer data were taken and when samples were taken for analysis.

7.2 Resistance Measurements of Test Heater 7

The heat input to the test heater is calculated from

$$Q = \triangle E^2/R$$

so it is necessary to know the resistance of heater as a function of temperature. These measurements were made before the heater was installed in the hydraulic console.

Two techniques (27) were used for this measurement. A precision Wheatstone Bridge was used to measure the actual resistance of the heater while it was heated in the adiabatic oven. Temperature profiles were taken along the heater and the total resistance of TH7 was plotted as a function of the average of this temperature profile. Because these resistances were so low, and

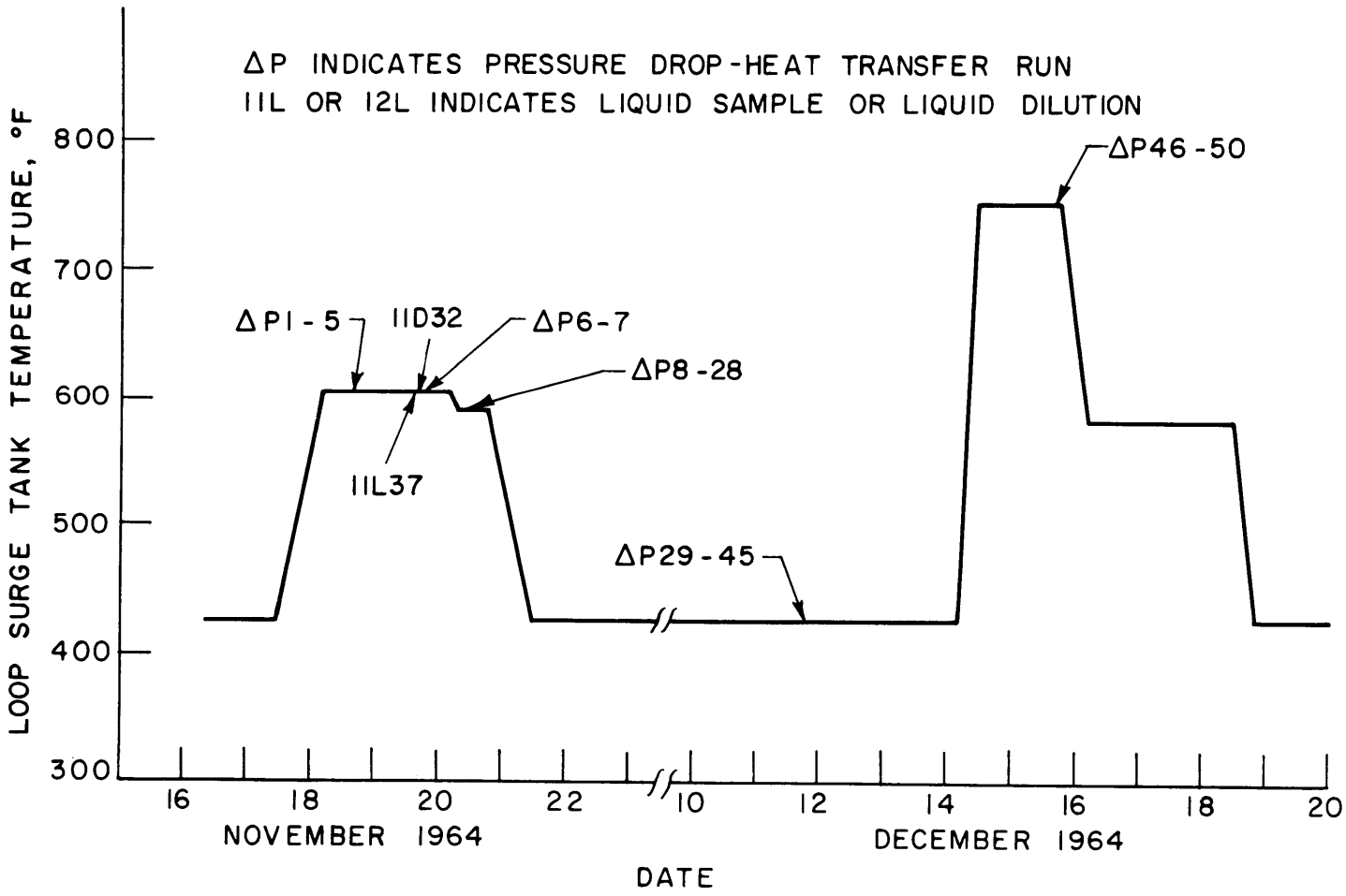

FIG. 28a HISTOGRAPH DURING FRICTION FACTOR AND HEAT TRANSFER RUNS

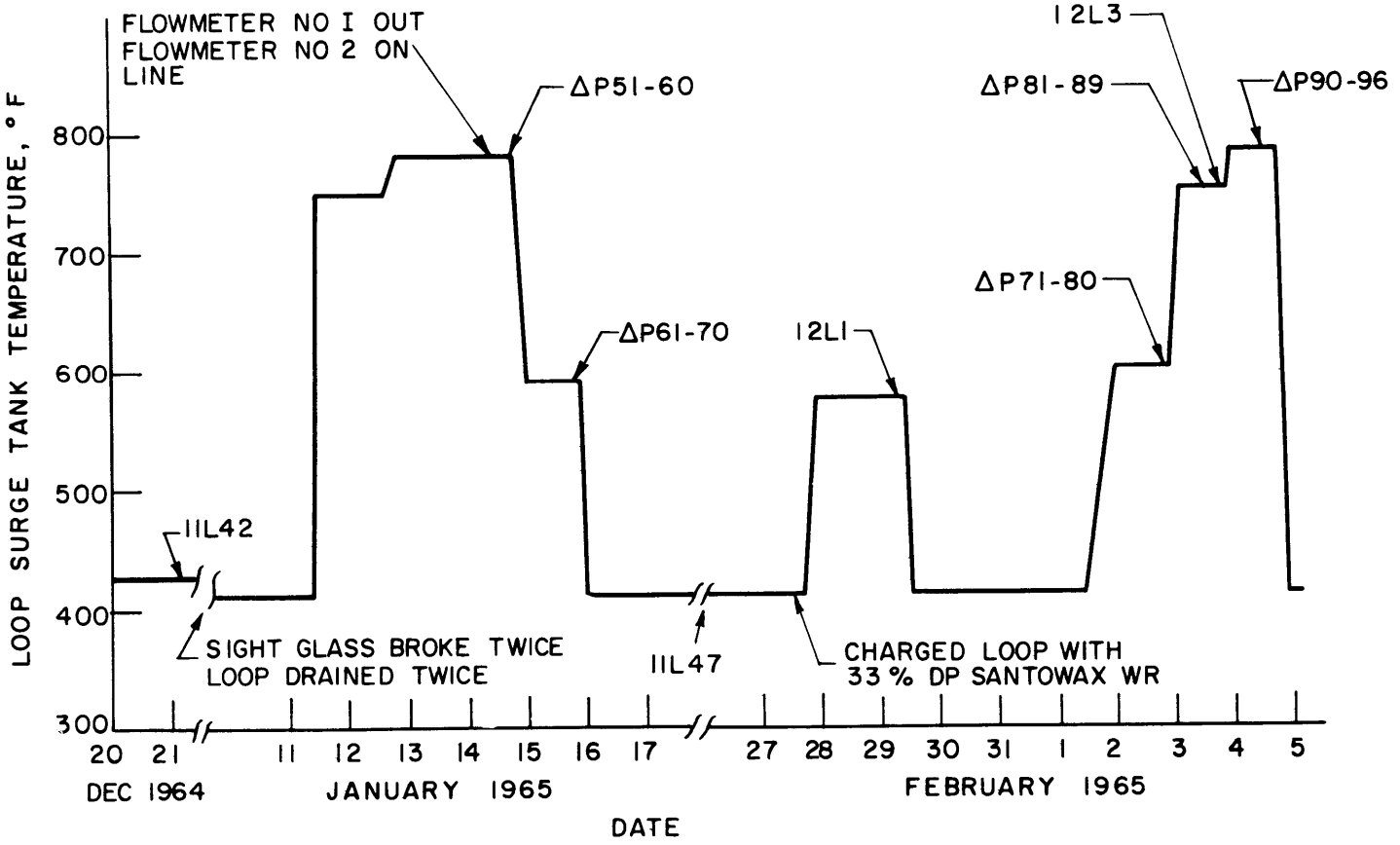

FIG. 28b HISTOGRAPH DURING FRICTION FACTOR AND HEAT TRANSFER RUNS

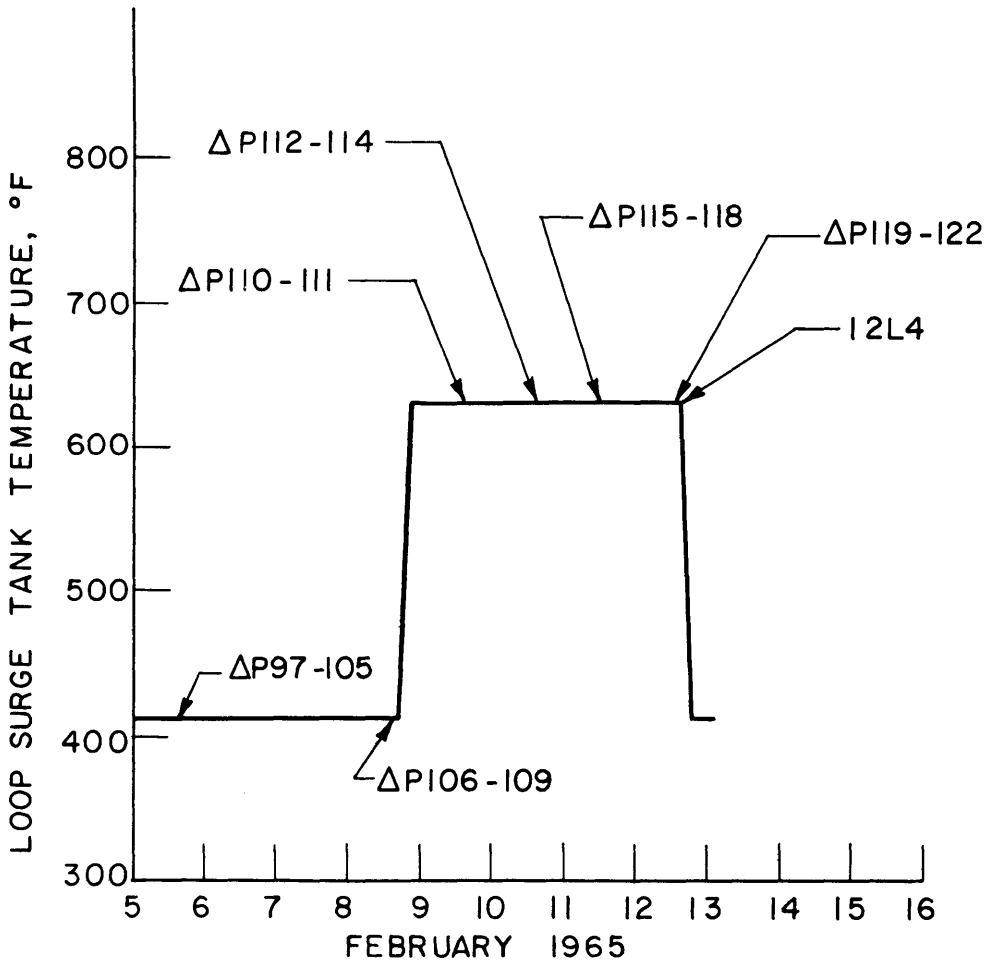

FIG. 28c HISTOGRAPH DURING FRICTION FACTOR AND HEAT TRANSFER RUNS

they were measured at high temperatures, it was also necessary to calibrate the leads that went from the instrument to the heater lugs (27). These corrected data are plotted on Figure 29.

The resistance of TH7 was also measured, while the oven was heated by the adiabatic oven, by AC voltage and current measurements. Small AC currents (approximately 30 amperes in each leg) were passed through the heater and the voltage differences (ΔE_3, ΔE_4, ΔE_5, ΔE_6) were used to calculate the resistance from

$$R = \Delta E/I$$

These values are also plotted against the test heater average temperature in Figure 29.

The equation that gives the best least square fit to all of the resistance data for Test Heater 7 is

$$R_{total} = 0.0491 + 0.0245 \left[\frac{T, {}^{\circ}F}{1,000} \right] \quad . \tag{24}$$

Equation (24) can be normalized and the resulting expression for the resistivity is

$$\rho_e = 2.42 \times 10^{-6} \ (1 + 5.0 \times 10^{-4} \ T) \tag{25}$$

where ρ_e is the electric resistivity in ohm-ft. and T is the average wall temperature in $^{\circ}F$.

This calibration compares quite well with the calibration reported for TH5 (2) which is

$$\rho_e = 2.42 \times 10^{-6} \ (1 + 4.61 \times 10^{-4} \ T) \tag{26}$$

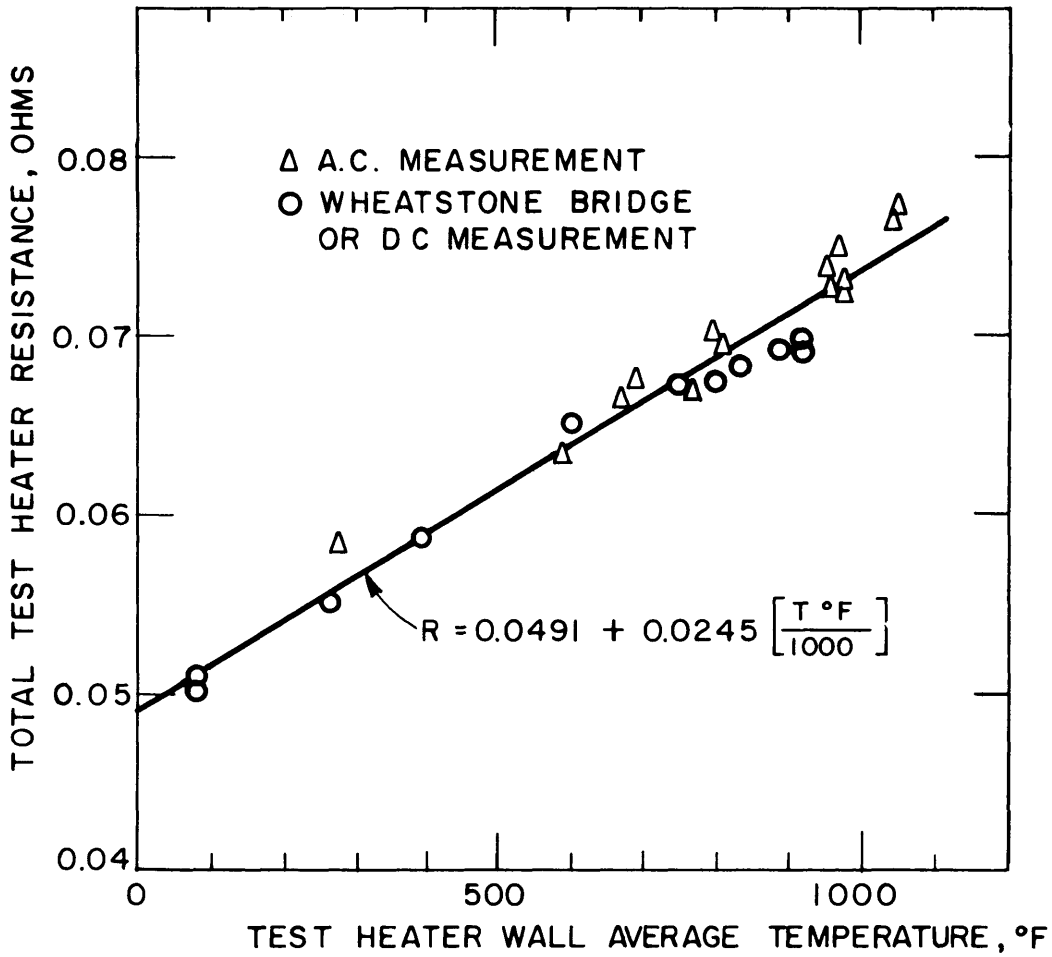

FIG. 29 TEST HEATER 7 TOTAL RESISTANCE

Also, both of these measurements made at MIT agree well with those of Bergeles, et. al. (24), who measured the resistivity of small 304SS tubes. They reported for 16 gage tubes

$$\rho_e = 2.53 \times 10^{-6} (1 + 4.61 \times 10^{-4} T) \quad . \qquad (27)$$

Reference (23) reports the resistivity of 304SS as

$$\rho_e = 2.31 \times 10^{-6} (1 + 5.4 \times 10^{-4} T) \quad . \qquad (28)$$

In summary, all of the resistance data noted above agree quite well.

7.3 Calibration of Foxboro DP Cell

The Foxboro differential pressure cell has an adjustable range and hence it must be calibrated whenever this adjustment is changed.

For calibration the cell must be disconnected from the source of pressure drop, be completely drained of liquid, and compared with a reliable standard. When the DP cell was calibrated in the laboratory, a column of mercury was used as this standard. When the cell was calibrated at the loop console, a secondary calibrated test gage (range 0 to 15 psig) was used. Details of the Calibration Procedure can be found in References (18) and (27).

Because the DP cell must also be heated for coolants with high melting points, a series of calibrations were made to test the reproducibility of the cell

and the influence of temperature (27). The results of these tests indicate that the cell should be calibrated at the approximate temperature it will be used at but that large deviations ($\pm 50^{\circ}F$) from this calibration temperature will not influence the calibration. It was found that as long as the cell was rezeroed at each temperature level, that raising the temperature of the cell body from room temperature to $325^{\circ}F$ changed the calibration by only 1%.

The results of the calibrations used for data reduction are presented in Figure 30.

7.4 Friction Factor of Distilled Water Measured With Test Heater 7

Before Test Heater 7 and the DP cell were installed at the organic loop console, friction factor measurements were made using distilled water as the test liquid. The principal reason for these tests was to determine if the pressure taps would measure the true static pressure drop across the test section. Care was taken to remove any burrs from the inside of the tube after the pressure tap holes had been drilled (Section 7.8) but since the tube ID was only 0.211 inches, it was impossible to check the holes visually for burrs.

The results of these measurements indicate that pressure taps 2 and 3 do measure the actual static pressure drop. Erratic results were obtained from pressure tap 1 and this is attributed to an entrance effect because tap 1

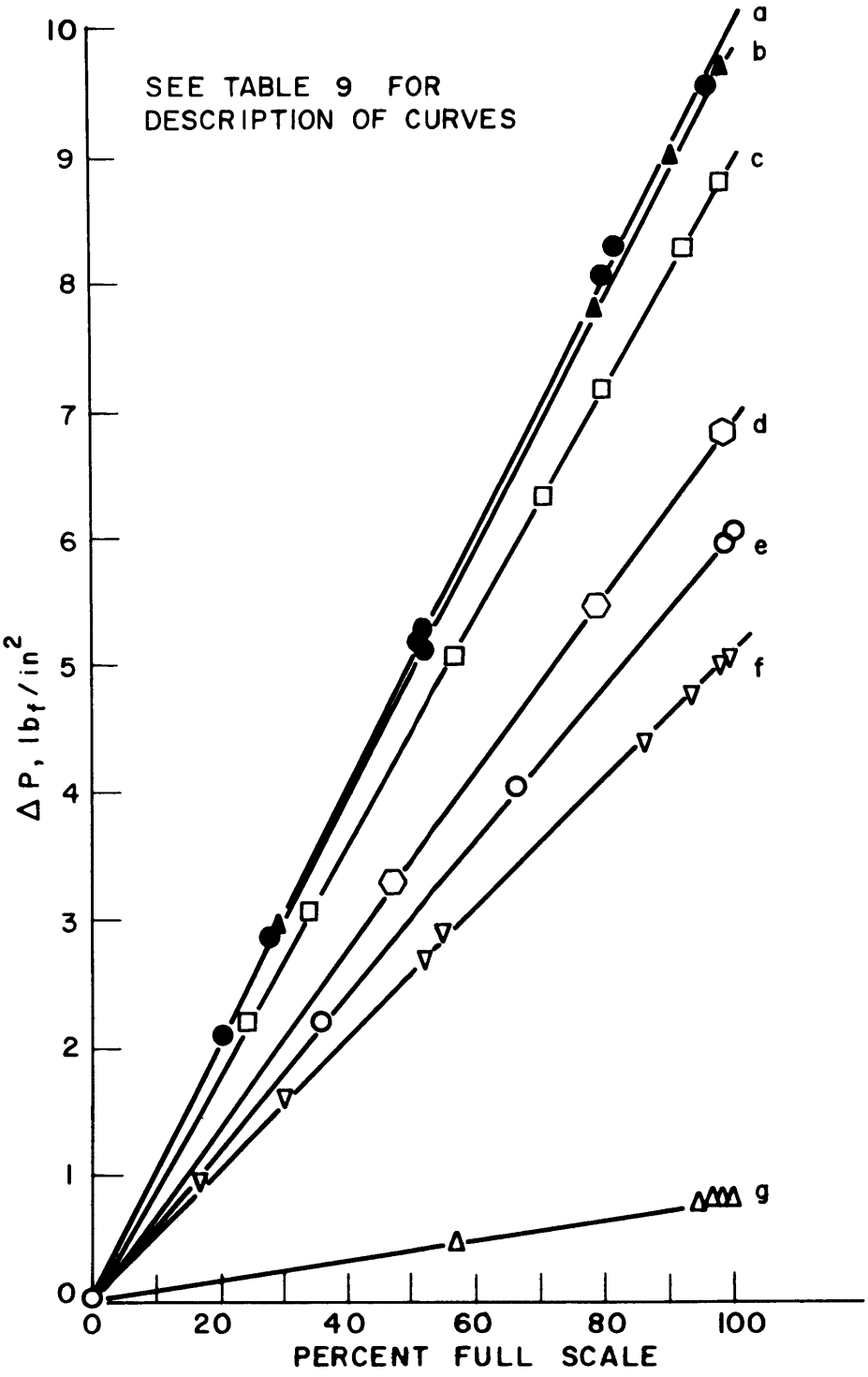

FIG. 30 CALIBRATION CURVES FOR DP CELL

TABLE 9

NOMENCLATURE FOR FIGURE 30
(CALIBRATION OF DP CELL)

Curve	Symbol	Temperature of DP Cell T_{body}, °F TC No. 228	Temperature of DP Cell T_{cell}, °F TC No. 227	Use for Run Number	Full Scale lb_f/in^2
				Santowax WR	
a	●	225	145	1-70	10.00
b	▲	193	—	71-122	9.85
				Water	
c	□	80	80	1-18	8.95
d	⬡	80	80	50-54	6.93
e	○	80	80	21-49	6.02
f	▽	80	80	19-20	5.05
g	△	80	80	55-61	0.80

is very close to the test heater inlet. On the basis of these results all of the data reported for both water and Santowax WR were taken with pressure taps 2 and 3.

The results of the water measurements are presented in Figure 31 and values of all of the actual data are tabulated in Tables 10 and 11. Figure 31 shows that all of the data can be correlated with the equation

$$f = 0.175\ Re_B^{-0.2} \tag{15}$$

which is only 5% lower than the correlation usually quoted for smooth tubes (7).

7.5 Methods of Data Reduction

7.5.1 Heat Transfer Data

The techniques used in this report for determining heat transfer coefficients are, with minor modifications, the same as those reported by Morgan and Mason (2) and Sawyer and Mason (3).

The heat transfer coefficient determined was the local coefficient from the test heater inside wall to organic coolant, defined by

$$U \equiv \frac{dQ_{in}}{dA(T_{Wi} - T_B)} \tag{29}$$

Morgan and Mason (2) showed that except near the electrodes of the test heater, the temperature difference is constant along the test heater length and that dQ_{in}

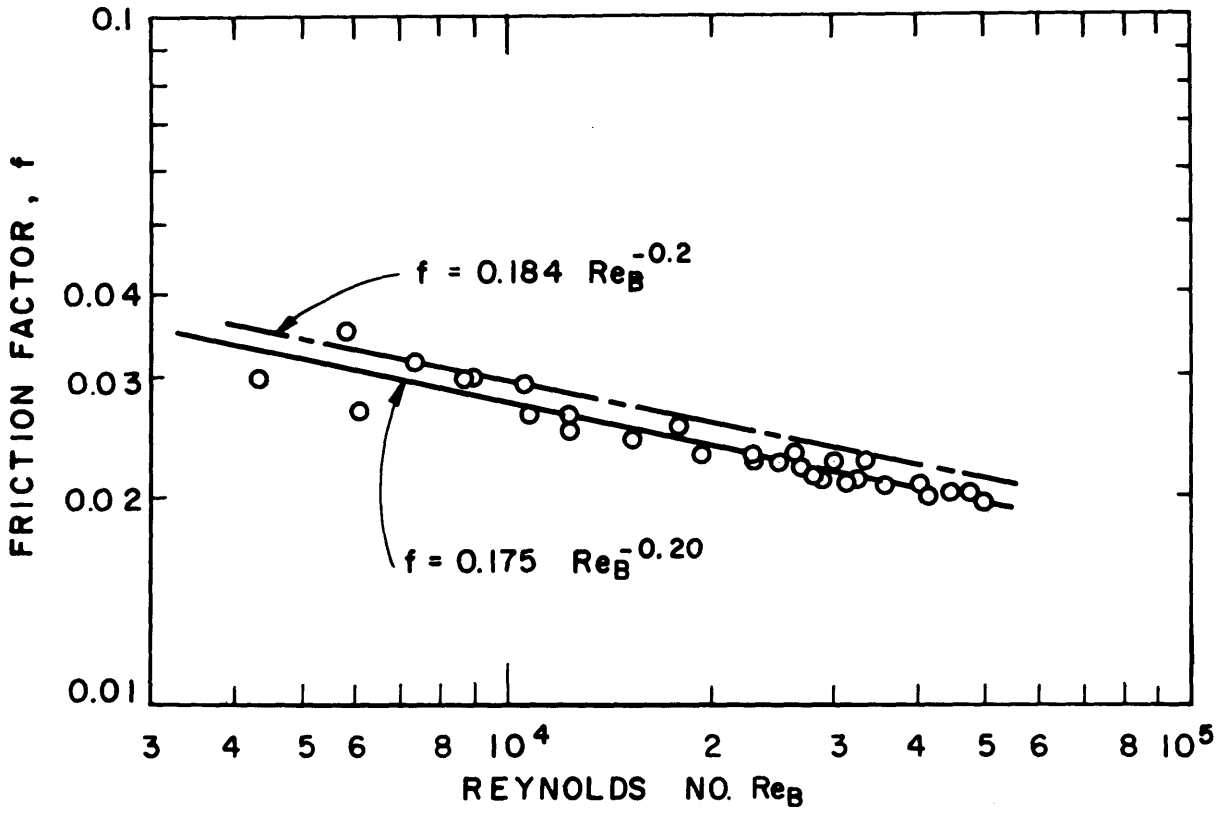

FIG. 31 FRICTION FACTOR FOR TEST HEATER 7 MEASURED WITH WATER

TABLE 10

RAW FRICTION FACTOR DATA FOR DISTILLED WATER

Run No.	Calibration Curve From Figure 30	% Full Scale D.P. Cell	Inlet Thermocouple Millivolts	Outlet Thermocouple Millivolts	Mass Water Collected Grams	Collection Time in Seconds
1	c	50.0	0.874	0.874	3159	30
5	c	49.0	0.977	0.977	3780	35
7	c	38.5	1.320	1.320	3720	40
10	c	49.5	1.328	1.328	3225	30
11	c	30.3	1.328	1.328	2490	30
14	c	23.1	1.328	1.328	3225	45
16	c	15.3	1.328	1.328	2310	50
18	c	7.6	1.328	1.328	2275	60
23	e	71.5	1.390	1.390	3219	30
24	e	61.0	1.402	1.402	2957	30
27	e	53.0	1.394	1.394	3235	35
28	e	44.8	1.394	1.394	3372	40
31	e	37.8	1.385	1.385	3020	40
32	e	30.5	1.385	1.385	3085	45
35	e	22.8	1.398	1.398	3468	60
36	e	15.3	1.398	1.398	2767	60
39	e	10.1	1.398	1.398	3330	90
40	e	6.5	1.398	1.398	2465	90
43	e	4.6	1.398	1.398	2665	120
44	e	3.2	1.400	1.400	1052	60
48	e	81.0	1.542	1.542	3493	30
50	d	70.0	1.554	1.554	3442	30
52	d	92.5	1.558	1.558	3345	25
53	d	91.5	1.596	1.600	3373	25
54	d	77.4	1.584	1.584	3690	30
55	g	96.0	1.103	1.097	2440	60
56	g	97.5	1.102	1.093	2325	60
57	g	61.5	1.105	1.105	1820	60
58	g	15.0	1.109	1.109	1810	120
61	g	25±4	1.148	1.148	2470	120

TABLE 11

REDUCED FRICTION FACTOR DATA FOR DISTILLED WATER*
L/D = 123.5

Run No.	ΔP lb_f/in^2	Water Average Temp. ^oF	Water Flow Rate lb_m/hr	Mean Velocity $ft/hr \times 10^{-4}$	Reynolds No. $Re \times 10^{-4}$	Friction Factor $f \times 10^2$
1	4.48	71.0	835	5.54	2.64	2.29
5	4.39	75.0	857	5.69	2.85	2.13
7	3.43	92.0	738	4.90	3.00	2.25
10	4.39	92.0	826	5.48	3.36	2.29
11	2.71	92.0	660	4.38	2.69	2.22
14	2.06	92.0	568	3.77	2.30	2.28
16	1.36	92.0	439	2.91	1.78	2.52
18	0.67	92.0	302	2.01	1.23	2.62
23	4.27	95.0	851	5.67	3.58	2.09
24	3.64	95.0	782	5.20	3.28	2.12
27	3.18	95.0	734	4.88	3.08	2.10
28	2.68	95.0	668	4.45	2.81	2.13
31	2.26	95.0	599	3.98	2.51	2.24
32	1.84	95.0	545	3.63	2.29	2.20
35	1.36	95.0	458	3.05	1.93	2.29
36	0.92	95.0	366	2.44	1.54	2.42
39	0.60	95.0	293	1.95	1.23	2.48
40	0.39	95.0	217	1.45	0.91	2.94
43	0.28	95.0	176	1.17	0.74	3.17
44	0.19	95.0	139	0.93	0.59	3.49
48	4.84	101.8	921	6.16	4.13	2.01
50	4.85	101.8	910	6.08	4.08	2.07
52	6.40	101.8	1062	7.10	4.77	2.00
53	6.33	103.7	1069	7.13	4.94	1.96
54	5.35	103.7	976	6.50	4.50	2.00
55	0.77	81.7	322	2.14	1.18	2.63
56	0.78	81.7	307	2.05	1.12	2.90
57	0.49	81.7	241	1.60	0.88	2.98
58	0.12	81.7	120	0.80	0.44	2.97
61	0.20	84.0	163	1.09	0.61	2.67

*Physical Properties for water were taken from McAdams (7).

and dA can also be considered constant. Thus U, was calculated from

$$U = \frac{Q_{in}}{A(T_{Wi} - T_B)} \tag{30}$$

For each section of the test heater, a smoothed curve was drawn through the corrected outside wall temperature and then the average outside wall temperature was calculated. For the determination of U, the average inside wall temperature was calculated from the theoretical relation for a tube with a uniformly distributed heat source and adiabatic conditions at the outside wall (2) (3)

$$T_{Wi} = T_{Wo} - \frac{1}{k_s L}\left[\frac{Q}{2\pi\left[1-\left(\frac{r_i}{r_o}\right)^2\right]}\left[\left(\frac{r_i}{r_o}\right)^2 - 1 - 2\ln\frac{r_i}{r_o}\right] + \frac{Q_{loss}}{\pi}\ln\frac{r_i}{r_o}\right] \tag{31}$$

where

T_{Wi} is the tube inside wall temperature.

T_{Wo} is the tube outside wall temperature.

k_s is the thermal conductivity at the test heater section evaluated at the average outside wall temperature, thermal conductivity data were taken from McAdams (7).

L is the total test heater length (24 inches for this experiment).

r_i is the inner radius of the test heater section.

r_o is the outer radius of the test heater section.

Q is the heat produced in the half section of the test heater (see below).

Q_{loss} is the heat lost in the half section of the test heater (see below).

The average bulk temperature of the coolant in each half section was calculated from

$$\overline{T_B} = T_{B_{in}} + \frac{Q_{up}}{Q_{up} + Q_{down}} \left[T_{B_{out}} - T_{B_{in}} \right] \tag{32}$$

$$\overline{T_{B_{up}}} = \frac{1}{2} \left[\overline{T_B} + T_{B_{in}} \right] \tag{33}$$

$$\overline{T_{B_{down}}} = \frac{1}{2} \left[\overline{T_B} + T_{B_{out}} \right] \tag{34}$$

where

$T_{B_{in}}$ is the inlet bulk temperature.

$T_{B_{out}}$ is the outlet bulk temperature.

Q_{up} is the heat transferred to the coolant in the upstream half of the test heater (see below).

Q_{down} is the heat transferred to the coolant in the downstream half of the test heater (see below).

$\overline{T_{B_{up}}}$ is the average bulk temperature in the upstream section of the test heater.

$\overline{T_{B_{down}}}$ is the average bulk temperature in the downstream section of the test heater.

so that, with the aid of Equations (31), (33) and (34), the desired temperature difference $(T_{W_{in}} - T_B)$ was calculated for each half of the test heaters from the measured temperature profile.

The heat transferred to the fluid for each half section of the test heater was calculated from

$$Q_{up} \text{ or } Q_{down} = \frac{\Delta E^2}{R} - Q_{loss} = Q - Q_{loss} \qquad (35)$$

where

ΔE is the measured voltage drop across the section.

R is the resistance of the test heater section evaluated at the mean outside wall temperature.

Q_{loss} is the heat loss in the test heater section evaluated at the mean outside wall temperature.

Test heater resistance and heat loss measurements as a function of temperature were reported by Morgan and Mason (2) for TH6. The test heater resistance for TH7 is reported in Section 7.2. The heat losses of TH7 were assumed equal to 0.1 of TH6 heat losses because no actual heat loss measurements were made on TH7. As a check on Equation (35), the heat input to the

coolant for each half section was also calculated from

$$Q_{up} = m\ c_p\ \Delta T_{B_{up}} \tag{36}$$

$$Q_{down} = m\ c_p\ \Delta T_{B_{down}} \tag{37}$$

These two values of heat input to the coolant generally agreed within $\sim 5\%$ for both Test Heater 6 and Test Heater 7, so the heat losses used for TH7 are assumed to be reasonable.

Knowing the temperature difference $(T_{W_{in}} - T_B)$, the heat input to the coolant, and the geometry of the test heater, a heat transfer coefficient for each half of the test heater was calculated from

$$U = \left[\frac{Q - Q_{loss}}{A}\right]\left[\frac{1}{T_{Wi} - T_B}\right] \tag{38}$$

The film heat transfer coefficient is related to U, by Equation (17)

$$1/U = 1/h_f + 1/h_s \tag{17}$$

The film coefficient is equal to U only when there is no scale resistance, or when h_s is infinite. One method of determining the scale resistance is that proposed by Wilson (2) (3) (7) (34) (Appendix 7.9). This method is based on the fact that the film heat transfer coefficient is related to the fluid velocity by (2)

$$h_f = AV^b \quad (0.8 < b < 1.0) \tag{39}$$

where b is the exponent on the Reynolds Number for a

given heat transfer correlation and A is an arbitrary constant. Thus, by plotting 1/U versus $1/V^b$ and extrapolating to infinite velocity, the scale resistance is given as the intercept. The computer program MNHTR, described below, performs this analysis by fitting the set of data taken at different velocities on a given day to Equations (17) and (39) by the method of least squares. The program uses the value of b determined by the computer for the over-all correlation of the heat transfer data. (U is assumed equal to h_f for a first approximation in the correlation. Corrections may be applied in further iterations if required.) The results of these calculations indicate that there has been no measurable scale buildup on the inside surface of TH6 over a period of three years (3). Also, during the same period of time there has not been any measurable change in the measured coefficient, U, and therefore for all of the correlations reported here, U was set equal to h_f.

Typical Wilson plots are presented in Appendix 7.9 for the Santowax OMP data of Sawyer and Mason (3) and for Santowax WR data.

The heat transfer data were then correlated with the physical properties of the coolant by an equation of the type

$$Nu_B = a\ Re_B^b\ Pr_B^c \left[\frac{\mu_B}{\mu_W}\right]^d \quad . \tag{40}$$

All physical properties except μ_w were evaluated at the bulk fluid temperature. The heat transfer coefficient, U, and the fluid velocity, V, were measured at the loop, and the physical properties were determined from measurements made on samples from the loop. These data are reported in Section 7.6 as a function of percent degradation products in the coolant and temperature.

The computer program MNHTR was written by Sawyer (3) to perform the above data reduction as well as to find the best least square fit to Equation (40). The program provides the option of selecting the best value of each of the "constants" a, b, c or d individually or collectively.

In general, the program would be requested to find the best value for all four "constants" and then with the best rounded-off value for the Prandtl Number exponent and the viscosity ratio exponent it would be programmed to find the values of a and b that gave the "best least square" fit to Equation (40). The values for a, b, c and d, determined by these calucations, are presented in Table 12. Table 12 presents results from the data of Sawyer and Mason (3) as well as all of the Santowax WR data. A similar tabulation was made for Santowax OMP by Sawyer and Mason, where their reported values are slightly different ($\pm$0.01 on the values of b and c). Since the time of their report (3), more specific heat and thermal conductivity data were made available (30) and these more

TABLE 12

LEAST SQUARE ANALYSIS OF MIT TRANSFER DATA

USING THE CORRELATION $Nu_B = a\, Re_B^b\, Pr_B^c\, (\mu_B/\mu_W)^d$

MIT Irradiation Run No.	Coolant Santowax-	Temp. of Irradiation °F	Number of Data Points	Test Heater Used	Nominal Heat Flux BTU/hr-ft^2	a	b	c	d	RMS Deviation*	d = 0.14 a	d = 0.14 b	d = 0.14 c	RMS Deviation*
1	OMP	610	93	TH5	10^5 to 2×10^5	0.0034	0.97	0.45	0.007	2.1%	0.0029	0.98	0.46	2.2%
1	OMP	610	169	TH6	10^5	0.0036	0.95	0.46	0.230	3.2%	0.0052	0.92	0.45	3.3%
1	OMP	610	267 All Run 1 Data	TH5-TH6	10^5 to 2×10^5	0.0039	0.97	0.38	0.200	3.6%	0.0049	0.95	0.37	3.6%
2	OMP	750	102	TH6	1.3×10^5	0.0041	0.94	0.43	0.120	2.7%	0.0038	0.95	0.44	2.7%
3	WR	750	58	TH6	$.9 \times 10^5$ 1.6×10^5	0.0140	0.83	0.46	0.110	4.2%	0.0220	0.84	0.46	4.1%
5	WR	700	10	TH6	1.3×10^5	Not Reported					0.0065	0.80	0.96	1.5%
11	WR	610	16	TH6	1.3×10^5	Too Few Data Points					0.0740	0.84	-0.42	1.9%
12 & 13	WR	-	13	TH7	1.3×10^5	To Give Useful Results for d					0.0290	0.78	0.41	3.7%

*Root Mean Square Deviation of data from the given correlation.

recent values were used in the preparation of Table 12. While these new values are different, it should be noted that a difference of ± 0.01 on the value of b or c is not a significant change. The first tabulated values of a, b, c and d are for the case when all exponents are varied to find the best least square fit to Equation (40). Then the value of d was set at 0.14 and the remaining exponents, a, b and c are varied to determine the best fit. From the results of Table 12, it was concluded that including the viscosity ratio term in the correlation did not significantly improve the fit of the data.

Based on the above evaluation, all the data were correlated with the exponent d set equal to zero and these results are presented in Table 13. In Table 13, three correlations are presented; first, where a, b and c are varied to give the best least square fit, then when a and b are varied with $c = 0.4$ and finally, a is varied to find the best least square fit to the Dittus-Boelter type equation ($b = 0.8$ and $c = 0.4$).

A sample input for MNHTR, where Run 12 heat transfer data were used, is presented in Table 14. A complete description of this program is given by Sawyer and Mason (3), therefore, this input is given as a reference so that the program can be used with Test Heater 7. The output of MNHTR for Run 12 is presented in Table 15 for reference.

TABLE 13

LEAST SQUARE ANALYSIS OF MIT TRANSFER DATA

USING THE CORRELATION $Nu_B = a\, Re_B^b\, Pr_B^c$

MIT Irradiation Run No.	Coolant Santowax-	Temp. of Irradiation °F	Number of Data Points	Test Heater Used	Nominal Heat Flux BTU/hr-ft^2	a	b	c	RMS Deviation*	c = 0.4 a	c = 0.4 b	RMS Deviation*	b = 0.8, c = 0.4 a	RMS Deviation*
1	OMP	610	93	TH5	10^5 to 2×10^5	0.0040	0.960	0.440	2.3%	0.0054	0.940	2.3%	0.0243	5.6%
1	OMP	610	169	TH6	10^5	0.0086	0.880	0.440	3.7%	0.0103	0.870	3.7%	0.0213	4.5%
1	OMP	610	267 All Run 1 Data	TH5-TH6	10^5 to 2×10^5	0.0079	0.920	0.350	4.0%	0.0052	0.940	4.2%	0.0224	8.1%
2	OMP	750	102	TH6	1.3×10^5	0.0059	0.910	0.430	2.8%	0.0069	0.900	2.8%	0.0213	4.7%
2	OMP	750	50**	TH6	1.3×10^5	0.0082	0.860	0.511	3.2%	0.0157	0.830	3.5%	0.0210	4.0%
3	WR	750	58	TH6	$.9 \times 10^5$ to 1.6×10^5	0.2100	0.810	0.430	4.1%	0.0260	0.790	4.1%	0.0230	4.1%
5	WR	700	10	TH6	1.3×10^5	0.0100	0.768	0.942	1.6%	0.0330	0.770	1.5%	0.0230	1.8%
11	WR	610	16	TH6	1.3×10^5	0.1050	0.802	-0.380	1.9%	0.0320	0.770	2.0%	0.0232	2.1%
12 & 13	WR		13	TH7	1.3×10^5	0.4350	0.750	0.380	3.7%	0.0410	0.750	3.6%	0.0234	4.0%

*Root Mean Square Deviation of data from the given correlation.

**Steady State Data Only.

TABLE 14

SAMPLE INPUT TO HEAT TRANSFER PROGRAM, MNHTR

```
      CONSTANT DATA RUN NO.12, TH7
 1   2   2   2   3   1   2   2   2   1   2   1   2  17  12  10   1   1
 1   3   1   1
      GEOMETRY AND CONVERSION FACTORS  TH-7
0.211        100.0        0.00005      0.40856      312.86       146.78
0.727        100.0        1635.0       1.167073     0.0          8.5166667
0.00416667   0.0          0.023        0.8          0.4          0.0
0.023        0.8          0.4          0.0          0.023        0.8
0.40         0.0
      DENSITY=F(T,MWH) TABLE FOR RUN 12, GM/CC,
400.         0.984        0.984        800.0        0.812        0.812
0.001        11.1
      VISCOSITY=F(1.0/T+460,MWH) TABLE RUN 12, MU IN CP
0.60252E-3   -1.93        -1.93        0.79384E-3   -1.17        -1.17
1.16320E-3   0.30         0.30         0.001        11.1
      SPECIFIC HEAT=F(T,MWH) TABLE FOR RUN 12, OM2 ELBERG DATA
400.0        0.492        800.         0.615        0.0
      THERMAL CONDUCTIVITY=F(T,MWH) TABLE RUN 12, OM2 ELBERG DATA
400.0        3.02         3.02         800.0        2.52         2.52
0.001        11.1
      ELECTRIC RESISTANCE OF TH-7 AS F(T,MWH)
400.0        0.0295       0.0295       950.0        0.0365       0.0365
0.0
      HEAT LOSS AS A F(T,MWH) TABLE FOR TH-7, ASSUMED 0.1 OF TH-6
400.0        5.5          1200.0       33.1         0.0
      THERMOCOUPLE TEMPERATURE- VOLTAGE TABLE
400.0        8.31         450.0        9.43         500.0        10.57
550.0        11.71        600.0        12.86        650.0        14.02
700.0        15.18        750.0        16.35        800.0        17.53
850.0        18.70        900.0        19.89        950.0        21.07
1000.0       22.26        1050.0       23.44        1100.0       24.63
1150.0       25.81        1200.0       26.98
      TEST HEATER TABLE
-1.0         0.0
      THERMOCOUPLE CORRECTION TABLE FOR TH-7
0.0          0.           0.           0.           0.           0.
0.           0.           0.           0.           0.           0.
0.0          10.          10.          10.          10.          10.
10.          10.          10.          10.          10.          10.
10.          10.          11.          11.          11.          11.
11.          11.          11.          11.          11.          11.
11.          11.          11.          12.          12.          12.
12.          12.          12.          12.          12.          12.
12.          12.          12.          12.          13.          13.
13.          13.          13.          13.          13.          13.
13.          13.          13.          13.          13.          14.
14.          14.          14.          14.          14.          14.
14.          14.          14.          14.          14.          14.
15.          15.          15.          15.          15.          15.
15.          15.          15.          15.          15.          15.
15.          16.          16.          16.          16.          16.
16.          16.          16.          16.          16.          16.
16.          16.          17.          17.          17.          17.
```

TABLE 14 (Cont'd)

SAMPLE INPUT TO HEAT TRANSFER PROGRAM, MNHTR

```
17.          17.          17.          17.          17.          17.
17.          17.          17.          30.          30.          30.
30.          30.          30.          30.          30.          30.
30.          30.          30.          30.
      THERMOCOUPLE DISTANCES TABLE
0.0          24.0         3.0          4.5          6.0          7.5
9.0          15.0         16.5         18.0         19.5         21.0
      SLOPE OF G CALIBRATION CURVE TABLE
1.051        0.0
      INTERCEPT OF G CALIBRATION CURVE TABLE
0.696        0.0
            95 PER CENT CONFIDENCE LIMIT TABLE
12.706       4.303        3.182        2.776        2.571        2.447
2.365        2.306        2.262        2.228        2.201        2.179
2.160        2.145        2.131        2.120        2.110        2.101
2.093        2.086        2.080        2.074        2.069        2.064
2.060        2.056        2.052        2.048        2.045        2.042
1.99996
                         RSCALE TABLE
 1
0.           0.
1 RUN 12-LOOP OUT OF PILE-MNH (NOT ACTUAL-ONLY USED FOR PROPERTIES AS F(TIME)
                         CONTROL TABLE
 7   1   0   1   0   0   1   1   0   1   1   1   1   1   1   1   0   1
1 .          2.450        8.23         8.07         13.41        13.90        12-111
15.25        15.394       15.495       15.58        15.62        15.51
15.52        15.50        15.46        15.40
10.          1.89         8.30         8.12         13.693       14.325       12-115
15.88        16.04        16.16        16.22        16.28        16.17
16.19        16.14        16.13        16.08
10.          1.59         8.30         8.11         12.928       13.672       12-116
15.58        15.74        15.86        15.96        16.00        15.89
15.91        15.88        15.86        15.81
10.          1.19         8.22         8.06         12.936       13.882       12-118
16.36        16.524       16.67        16.82        16.86        16.752
16.78        16.72        16.66        16.486
11.          2.46         8.20         8.00         13.392       13.88        12-120
15.31        15.45        15.55        15.628       15.67        15.55
15.56        15.54        15.50        15.44
11.          1.60         8.22         8.03         13.013       13.747       12-121
15.56        15.72        15.84        15.91        15.98        15.88
15.91        15.88        15.83        15.83
11.          0.82         8.25         8.08         12.916       14.185       12-122
16.96        17.17        17.33        17.42        17.50        17.42
17.40        17.47        17.48        17.45
```

TABLE 15

SAMPLE OUTPUT FROM HEAT TRANSFER PROGRAM, MNHTR
RUN 12

```
 RUN 12,LCOP CUT OF PILE,MWH NOT ACTUAL,ONLY USED FOR PROPERTIES AS F(TIME)
THE DATE IS  JULY 01, 1965.
THE TIME IS 1839.0
                                BATCH NO.= 1

                          TEMPERATURE PROFILES FOR ALL RUNS
12-111 623.7 644.8 703.0 709.1 713.5 717.1 718.8 714.1 714.5 713.7 712.0 709.4

12-115 635.9 663.1 729.9 736.8 741.9 744.4 747.0 742.3 743.2 741.0 740.6 738.5

12-116 602.9 635.0 717.1 723.9 729.1 733.3 735.0 730.3 731.2 729.9 729.1 726.9

12-118 603.3 644.1 750.4 757.4 763.6 769.9 771.6 767.0 768.2 765.7 763.1 755.8

12-120 622.9 644.0 705.6 711.5 715.8 719.1 720.9 715.8 716.2 715.4 713.7 711.1

12-121 606.6 638.2 716.2 723.1 728.2 731.2 734.2 729.9 731.2 729.9 727.8 727.8

12-122 602.4 657.1 775.8 784.7 791.5 795.3 798.7 795.3 798.3 797.5 797.9 796.6
```

DATA FOR LEFT HALF HEATER

RUN	SLOPE	S.D.(SLOPE)	INTERCEPT	S.D.(INTCP)	CORR. COEFF
12-111	2.63819E 00	3.10678E-01	6.96470E 02	1.97714E 00	9.79846E-01
12-115	2.79203E 00	3.73512E-01	7.23248E 02	2.37701E 00	9.74176E-01
12-116	3.01994E 00	3.67400E-01	7.09573E 02	2.33812E 00	9.78503E-01
12-118	3.66102E 00	3.80287E-01	7.40610E 02	2.42013E 00	9.84194E-01
12-120	2.55839E 00	3.04504E-01	6.99248E 02	1.93785E 00	9.79405E-01
12-121	2.93447E 00	3.27896E-01	7.08974E 02	2.08672E 00	9.81787E-01
12-122	3.75705E 00	4.66577E-01	7.66695E 02	2.96928E 00	9.77624E-01

RUN	VELOCITY	Q	QLOST	QNET	Q HEAT
12-111	2.36848E 01	2.02340E 03	1.62743E 01	2.00713E 03	2.03207E 03
12-115	1.82838E 01	2.03652E 03	1.72300E 01	2.01929E 03	2.02974E 03
12-116	1.53903E 01	2.04600E 03	1.68054E 01	2.02919E 03	2.01004E 03
12-118	1.15324E 01	1.98063E 03	1.80089E 01	1.96262E 03	1.90873E 03
12-120	2.37813E 01	2.00693E 03	1.63536E 01	1.99057E 03	2.04185E 03
12-121	1.54868E 01	2.00759E 03	1.67671E 01	1.99082E 03	1.99677E 03
12-122	7.96380E 00	1.97546E 03	1.89287E 01	1.95654E 03	1.77272E 03

RUN	Q/A	TWO	TWI	TBULK	H
12-111	1.24003E 05	7.12299E 02	7.03732E 02	6.29092E 02	1.66135E 03
12-115	1.24754E 05	7.40000E 02	7.31463E 02	6.42868E 02	1.40814E 03
12-116	1.25366E 05	7.27692E 02	7.19077E 02	6.11138E 02	1.16145E 03
12-118	1.21253E 05	7.62576E 02	7.54340E 02	6.13675E 02	8.61997E 02
12-120	1.22980E 05	7.14598E 02	7.06108E 02	6.28320E 02	1.58098E 03
12-121	1.22995E 05	7.26581E 02	7.18124E 02	6.14695E 02	1.18917E 03
12-122	1.20877E 05	7.89237E 02	7.81100E 02	6.16397E 02	7.33910E 02

TABLE 15 (Cont'd)

SAMPLE OUTPUT FROM HEAT TRANSFER PROGRAM, MNHTR
RUN 12

DATA FOR RIGHT HALF HEATER

RUN	SLOPE	S.D.(SLOPE)	INTERCEPT	S.D.(INTCP)	CORR. COEFF
12-111	-7.97708E-01	1.24129E-01	7.27094E 02	2.24978E 00	9.70208E-01
12-115	-6.83785E-01	1.54273E-01	7.53419E 02	2.79607E 00	9.36018E-01
12-116	-5.98299E-01	1.76920E-01	7.40257E 02	3.20666E 00	8.94741E-01
12-118	-1.94184E 00	5.60916E-01	7.97119E 02	1.01664E 01	8.85621E-01
12-120	-7.97708E-01	2.06905E-01	7.28803E 02	3.75006E 00	9.14988E-01
12-121	-5.12812E-01	1.60678E-01	7.38547E 02	2.91227E 00	8.97981E-01
12-122	1.41215E-01	2.83418E-01	7.94577E 02	5.13683E 00	1.40542E-01

RUN	VELOCITY	Q	QLOST	QNET	Q HEAT
12-111	2.36849E 01	1.94517E 03	1.62894E 01	1.92888E 03	1.95405E 03
12-115	1.82838E 01	1.94833E 03	1.72683E 01	1.93107E 03	1.94239E 03
12-116	1.53903E 01	1.95207E 03	1.68673E 01	1.93520E 03	1.91898E 03
12-118	1.15324E 01	1.90329E 03	1.80568E 01	1.88523E 03	1.83585E 03
12-120	2.37813E 01	1.91033E 03	1.63483E 01	1.89398E 03	1.94397E 03
12-121	1.54868E 01	1.91387E 03	1.68614E 01	1.89721E 03	1.90462E 03
12-122	7.96330E 00	1.88939E 03	1.92006E 01	1.87019E 03	1.69729E 03

RUN	Q/A	TWO	TWI	TBULK	H
12-111	1.19169E 05	7.12736E 02	7.04501E 02	6.39652E 02	1.83765E 03
12-115	1.19304E 05	7.41111E 02	7.32947E 02	6.56488E 02	1.56037E 03
12-116	1.19559E 05	7.29487E 02	7.21273E 02	6.27173E 02	1.27055E 03
12-118	1.16472E 05	7.63966E 02	7.56056E 02	6.34263E 02	9.54743E 02
12-120	1.17013E 05	7.14445E 02	7.06362E 02	6.38838E 02	1.73289E 03
12-121	1.17200E 05	7.29317E 02	7.21263E 02	6.30514E 02	1.29148E 03
12-122	1.15542E 05	7.97119E 02	7.89357E 02	6.43746E 02	7.93500E 02

MEAN PROPERTIES OF THE HEATER SECTION

RUN	Q ELECTRIC	Q THERMAL	ERROR %/Q	MEAN H	BULK T
12-111	3.93601E 03	3.98620E 03	-1.27496E 00	1.66135E 03	6.34477E 02
12-115	3.95036E 03	3.97224E 03	-5.53886E-01	1.40814E 03	6.49830E 02
12-116	3.96446E 03	3.92919E 03	8.88103E-01	1.16145E 03	6.19346E 02
12-118	3.84785E 03	3.74478E 03	2.67864E 00	8.61997E 02	6.24074E 02
12-120	3.88456E 03	3.98591E 03	-2.60924E 00	1.58098E 03	6.33710E 02
12-121	3.88783E 03	3.90155E 03	-3.52810E-01	1.18917E 03	6.22795E 02
12-122	3.82672E 03	3.47031E 03	9.31373E 00	7.33910E 02	6.30380E 02

RUN	DENSITY	MU	MUW	CP	K
12-111	8.83175E-01	5.00043E-01	4.02287E-01	5.64102E-01	2.72690E 00
12-115	8.76573E-01	4.75512E-01	3.71154E-01	5.68823E-01	2.70771E 00
12-116	8.89681E-01	5.26195E-01	3.84001E-01	5.59449E-01	2.74582E 00
12-118	8.87648E-01	5.17801E-01	3.48436E-01	5.60903E-01	2.73991E 00
12-120	8.83505E-01	5.01321E-01	3.99796E-01	5.63866E-01	2.72786E 00
12-121	8.88198E-01	5.20050E-01	3.84530E-01	5.60510E-01	2.74151E 00
12-122	8.84937E-01	5.06922E-01	3.21974E-01	5.62842E-01	2.73292E 00

TABLE 15 (Cont'd)

SAMPLE OUTPUT FROM HEAT TRANSFER PROGRAM, MNHTR
RUN 12

RUN	NUSSELT NO.	PRANDTL NO.	MU/MUW
12-111	4.42922E 02	1.03442E 01	1.24300E 00
12-115	3.78C75E 02	9.98931E 00	1.28117E 00
12-116	3.07514E 02	1.07210E 01	1.37030E 00
12-118	2.29720E 02	1.06002E 01	1.48607E 00
12-120	4.21345E 02	1.03626E 01	1.25394E 00
12-121	3.15348E 02	1.06326E 01	1.35243E 00
12-122	1.95296E 02	1.04434E 01	1.57442E 00

RUNS	WILSON SLOPE	INTERCEPT	S.D.(SLOPE)	S.D.(INTCP)	CORR. COEFF
12-111-12-118	9.24165E-03	-1.56965E-04	7.48479E-04	8.19599E-05	9.93505E-01
12-120-12-122	6.61172E-03	1.09603E-04	4.96880E-05	6.69110E-06	9.99972E-01

RUN	1.0/H	1.0/V**B	REYNOLDS NO	CORRELATION	CONF. LEVEL
12-111	6.01918E-04	7.90096E-02	6.83955E 04	1.7396CE 02	.00000E 00
12-115	7.10157E-04	9.72363E-02	5.51074E 04	1.50579E 02	.00000E 00
12-116	8.60991E-04	1.11643E-01	4.25454E 04	1.19261E 02	.00000E 00
12-118	1.16010E-03	1.40716E-01	3.23233E 04	8.89567E 01	.00000E 00
12-120	6.32519E-04	7.87525E-02	6.85246E 04	1.65368E 02	.00000E 00
12-121	8.40920E-04	1.11085E-01	4.32457E 04	1.22500E 02	.00000E 00
12-122	1.36257E-03	1.89367E-01	2.27305E 04	7.64109E 01	.00000E 00

NU= .023C0$ .00C0E 00*(RE** .80200$ .0000E 001*(PR** .40CC0$ .00C0E C0)*

(MU/MUW** .CCCCE 0C$ .C000E 00) RMS DEV.= 4.538 0/0 CORRELATION COEF= .9890

RUNS	WILSON SLOPE	INTERCEPT	S.D.(SLOPE)	S.D.(INTCP)	CORR. COEFF
12-111-12-118	9.21359E-03	-1.59409E-04	7.47761E-04	8.23246E-05	9.93478E-01
12-120-12-122	6.59504E-03	1.07545E-04	5.09114E-05	6.88809E-06	9.99970E-01

RUN	1.0/H	1.0/V**B	REYNOLDS NO	CORRELATION	CONF. LEVEL
12-111	6.01918E-04	7.95103E-02	6.83955E 04	1.71228E 02	.00000E 00
12-115	7.10157E-04	9.78020E-02	5.51074E 04	1.47889E 02	.00000E 00
12-116	8.60991E-04	1.12254E-01	4.25454E 04	1.16363E 02	.00000E 00
12-118	1.16010E-03	1.41405E-01	3.23233E 04	8.64295E 01	.00000E 00
12-120	6.32519E-04	7.92523E-02	6.85246E 04	1.62667E 02	.00000E 00
12-121	8.40920E-04	1.11694E-01	4.32457E 04	1.19838E 02	.00000E 00
12-122	1.36257E-03	1.90153E-01	2.27305E 04	7.39288E 01	.00000E 00

NU= .023C0$ .0000E 00*(RE** .80000$ .0000E 001*(PR** .40000$ .0000E 00)*

(MU/MUW** 7.2756E-02$ .0000E 00) RMS DEV.= 4.431 0/0 CORRELATION COEF= .9895

RUNS	WILSON SLOPE	INTERCEPT	S.D.(SLOPE)	S.D.(INTCP)	CORR. COEFF
12-111-12-118	9.21359E-03	-1.59409E-04	7.47761E-04	8.23246E-05	9.93478E-01
12-120-12-122	6.59504E-03	1.07545E-04	5.09114E-05	6.88809E-06	9.99970E-01

RUN	1.0/H	1.0/V**B	REYNOLDS NO	CORRELATION	CONF. LEVEL
12-111	6.01918E-04	7.95103E-02	6.83955E 04	1.73960E 02	.00000E 00
12-115	7.10157E-04	9.78020E-02	5.51074E 04	1.50579E 02	.00000E 00
12-116	8.60991E-04	1.12254E-01	4.25454E 04	1.19261E 02	.00000E 00
12-118	1.16010E-03	1.41405E-01	3.23233E 04	8.89567E 01	.00000E 00
12-120	6.32519E-04	7.92523E-02	6.85246E 04	1.65368E 02	.00000E 00
12-121	8.40920E-04	1.11694E-01	4.32457E 04	1.22500E 02	.00000E 00
12-122	1.36257E-03	1.90153E-01	2.27305E 04	7.64109E 01	.00000E 00

NU= .02351$ .0000E 00*(RE** .80000$ .0000E 001*(PR** .40000$ .0000E 00)*

(MU/MUW** .0000E 00$ .0000E 00) RMS DEV.= 4.512 0/0 CORRELATION COEF= .9891

7.5.2 Friction Factor Data

The pressure drop along a finite length of tube, under steady flow conditions, can be written (7)

$$\Delta P_{measured} = \Delta P_{acc} + \Delta P_f + \Delta P_H \quad . \qquad (41)$$

ΔP_{acc} is the head loss due to the acceleration of the fluid when there are density changes. For small changes in density this loss can be written as

$$\Delta P_{acc} = \frac{G^2}{g_o} \left[\frac{1}{\rho_{in}} - \frac{1}{\rho_{out}} \right] \quad .$$

ΔP_f is the friction head loss and ΔP_H is the elevation head loss.

For isothermal conditions, ΔP_{acc} is zero, and for the non-isothermal conditions considered here the term was found to be negligible.

Since the test section used here (TH7) was horizontal, ΔP_H is also zero. Therefore, $\Delta P_{measured}$ was equal to ΔP_f.

The friction factor, f, was calculated from

$$f = \frac{\Delta P_{measured}}{\frac{1}{2g_o} \rho_B V_m^2 \frac{L}{D}} \quad . \qquad (42)$$

These data were then correlated by plotting against the bulk Reynolds Number, Re_B

$$Re_B = \frac{\rho_B V_m D}{\mu_B}$$

where the physical properties used are reported in Appendix 7.6.

For non-isothermal friction factor data, other investigators (7) (12) (35) (36) recommend plotting $f(\mu_B/\mu_W)^{.14}$ against Re_B or the friction factor f against the film Reynolds Number, Re_f. For the data taken on TH7, (μ_B/μ_W) was generally less than 1.3 so these suggested correlations did not significantly change the scatter in the data.

In conclusion, since there was no significant difference between the friction factor data taken isothermally and that taken under non-isothermal conditions, all the data were plotted as a function of the bulk Reynolds Number, Re_B.

7.6 Physical Properties Data

The values for the physical properties, density, viscosity, specific heat and thermal conductivity, used for the reduction of the Santowax WR heat transfer and friction factor data are reported in this section. The density and the viscosity were measured at MIT, and for the specific heat and the thermal conductivity, the OM_2 values reported by Elberg (20) were used.

Since the physical properties are a function of the amount of degradation products (% DP) present, it is necessary to evaluate these properties as a function of the time that the coolant has been circulating in the reactor core. A convenient variable to use is the number of megawatt hours (MWHr) that the coolant has been irradiated where

MWHr ≡ Megawatts of Reactor Power x Hours of Operation. In general, two cases are encountered, a transient phase where the properties are continuously changing, and a steady state phase where the coolant properties are kept constant by a feed and bleed of the irradiated coolant. It is assumed that the physical properties do not change when the reactor is shut down or when the loop is circulating out of pile.

The properties used for Irradiation Runs 3, 5, 11 and 13, and for the period of time when the loop was out of pile (the last part of Run 11 and Run 12) are presented in Table 16. For the period when the loop was in-pile the properties are presented as a function of MWHr. For properties at values of MWHr not given in Table 16, linear interpolation is used. For the period of time that the loop was out of pile, the properties are given as a function of the % DP (at 12, 17 and 33%).

During this period it was assumed that pyrolysis of the coolant was negligible and, therefore, the properties did not change as a function of time. The changes in % DP noted are due to the actual addition of High Boilers (HB) to the coolant.

The mixed units presented in this table are those required by the computer program MNHTR.

At a given MWHr (or % DP) the density, specific heat and thermal conductivity are linear functions of

TABLE 16

PHYSICAL PROPERTIES USED FOR IRRADIATED SANTOWAX WR

Run 3

MWHr	Viscosity, μ Centipoise			Density, ρ Grams/cc		Specific Heat, c_p BTU/lb_m-^oF		Thermal Conductivity, k Cal/cm-sec-^oC x 10^4		Degradation Products % DP
	400°F	800°F	1200°F*	400°F	800°F	400°F	800°F	400°F	800°F	
0	0.879	.192	.0878	.9717	.7836	.50	.61	2.90	2.35	5%
255	1.045	.214	.0950	.9828	.7957	.50	.61	2.95	2.50	19%
363	1.100	.217	.0995	.9747	.7918	.50	.61	2.95	2.50	22%
475	1.165	.254	.1155	.9787	.7976	.50	.61	2.98	2.55	28%
622	1.110	.240	.1090	.9812	.8004	.50	.61	3.03	2.60	34%
623	1.033	.230	.1065	.9731	.7940	.50	.61	2.98	2.50	26%
742	1.182	.268	.1240	.9810	.8010	.50	.61	3.00	2.55	32%
1080	1.464	.318	.1450	.9894	.8156	.50	.61	3.05	2.70	44%
1500	2.030	.420	.1870	1.0014	.8333	.50	.61	3.11	2.85	51%
1630	2.400	.430	.1760	1.1600	.8360	.50	.61	3.13	2.90	56%
1800	1.700	.350	.1500	1.0000	.8220	.50	.61	3.05	2.75	45%
3056	1.700	.350	.1500	1.0000	.8220	.50	.61	3.05	2.75	45%

*Extrapolated Value.

TABLE 16 (Cont'd)

PHYSICAL PROPERTIES USED FOR IRRADIATED SANTOWAX WR

MWHr	Viscosity, μ Centipoise 400°F	800°F	1200°F*	Density, ρ Grams/cc 400°F	800°F	Specific Heat, c_p BTU/lb$_m$-°F 400°F	800°F	Thermal Conductivity, k Cal/cm-sec-°C x 10^4 400°F	800°F	Degradation Products % DP
Run 5										
500 to 1100	1.600	.341	.1430	.9850	.8200	.50	.61	3.38	2.88	45%
Run 11										
330 to 723	0.930	.206	.0910	.9700	.7820	.50	.61	3.10	2.50	15%
Loop Out of Pile	0.930	.200	.0900	.9700	.7750	.50	.61	3.10	2.50	12%
	1.050	.215	.1000	.9800	.8000	.50	.61	3.10	2.50	17%
Run 12										
Loop Out of Pile	1.350	.310	.1450	.9840	.8120	.50	.61	3.02	2.52	33%
Run 13**										
249-251	.830	.194	.0870	.9520	.7590	.50	.61	2.92	2.40	9%

*Extrapolated Value.

**For Run 13 Used Physical Properties of OM_2 (20) at 10% DP.

temperature, so linear interpolation may be used for intermediate values of temperature. For interpolation of the viscosity data, use the fact that

$$\log_e \mu = \frac{A}{{}^{o}F_{abs}}$$

where A is a constant. In addition, for the period of time when the organic coolant was not circulating in-pile, and when most of the TH7 heat transfer and friction factor data were taken, the physical properties of each sample taken are presented in Figures 32, 33, 34 and 35. For data reduction, the properties of the sample taken nearest to the time the data were taken were used (see the Histograph for this period, Figure 28).

These samples, taken for physical properties measurements, were also analyzed for composition and amount of degradation products (% DP) by gas chromatography. The results of these analyses are presented in Table 17.

For the preliminary heat transfer results reported for MIT Irradiation Run 13, all physical properties were taken from Elberg (20) at 10% DP.

7.7 Tabulated Heat Transfer and Friction Factor Data for Santowax WR

These data presented in Tables 18 to 24 were presented graphically in Section 5 and the recommended correlations were given in Section 6.

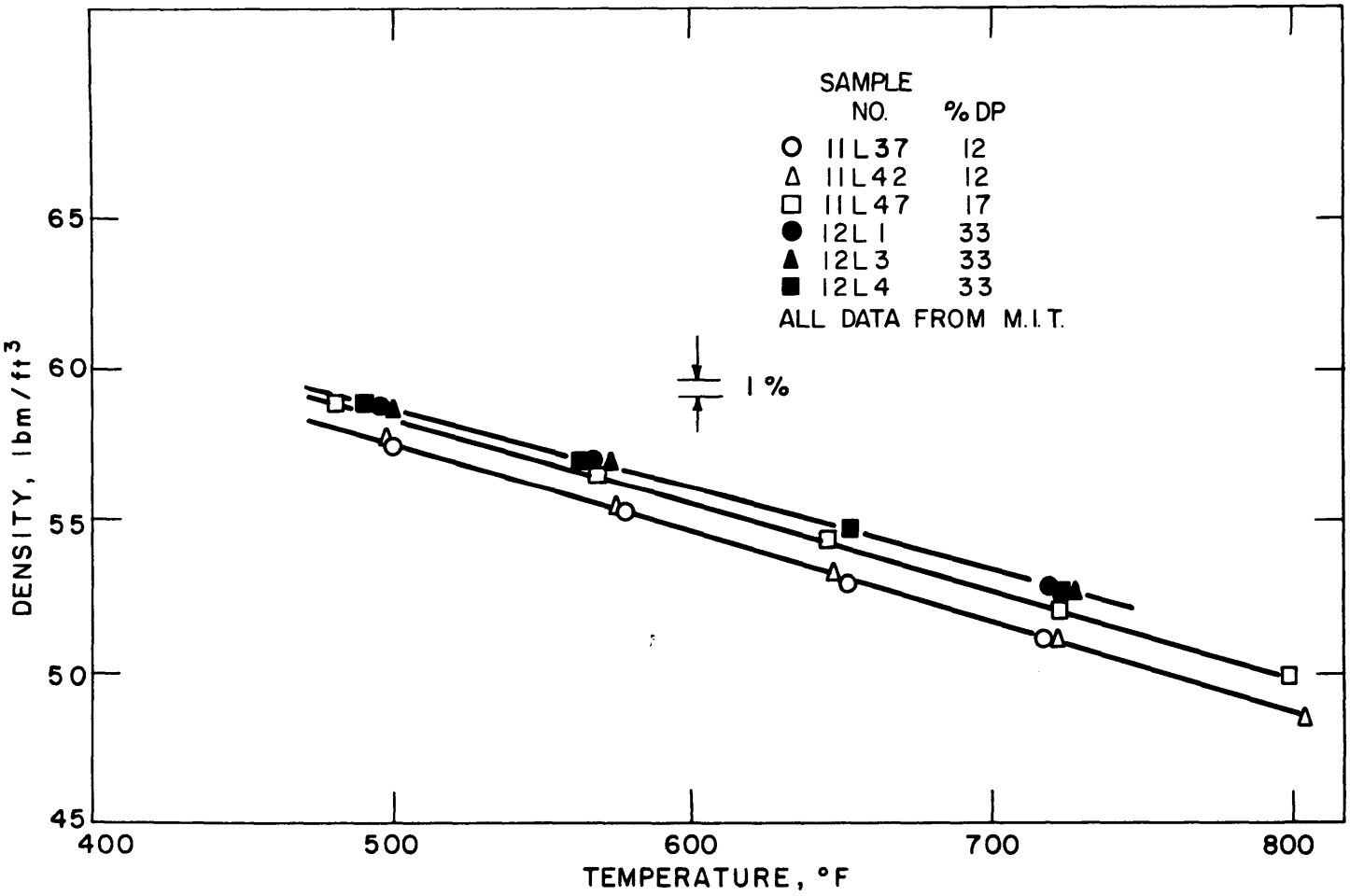

FIG. 32 DENSITY OF SANTOWAX WR

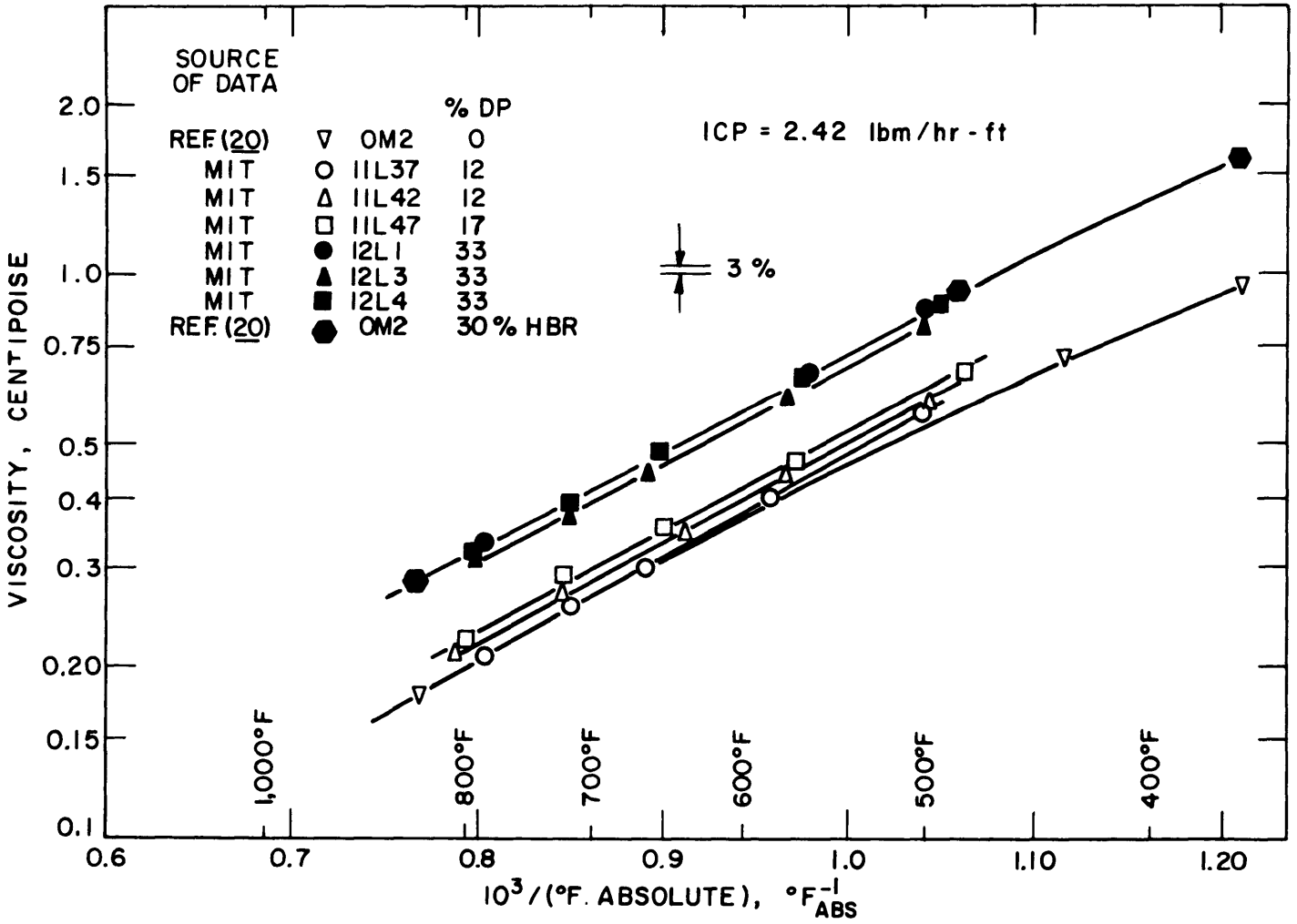

FIG. 33 VISCOSITY OF SANTOWAX WR

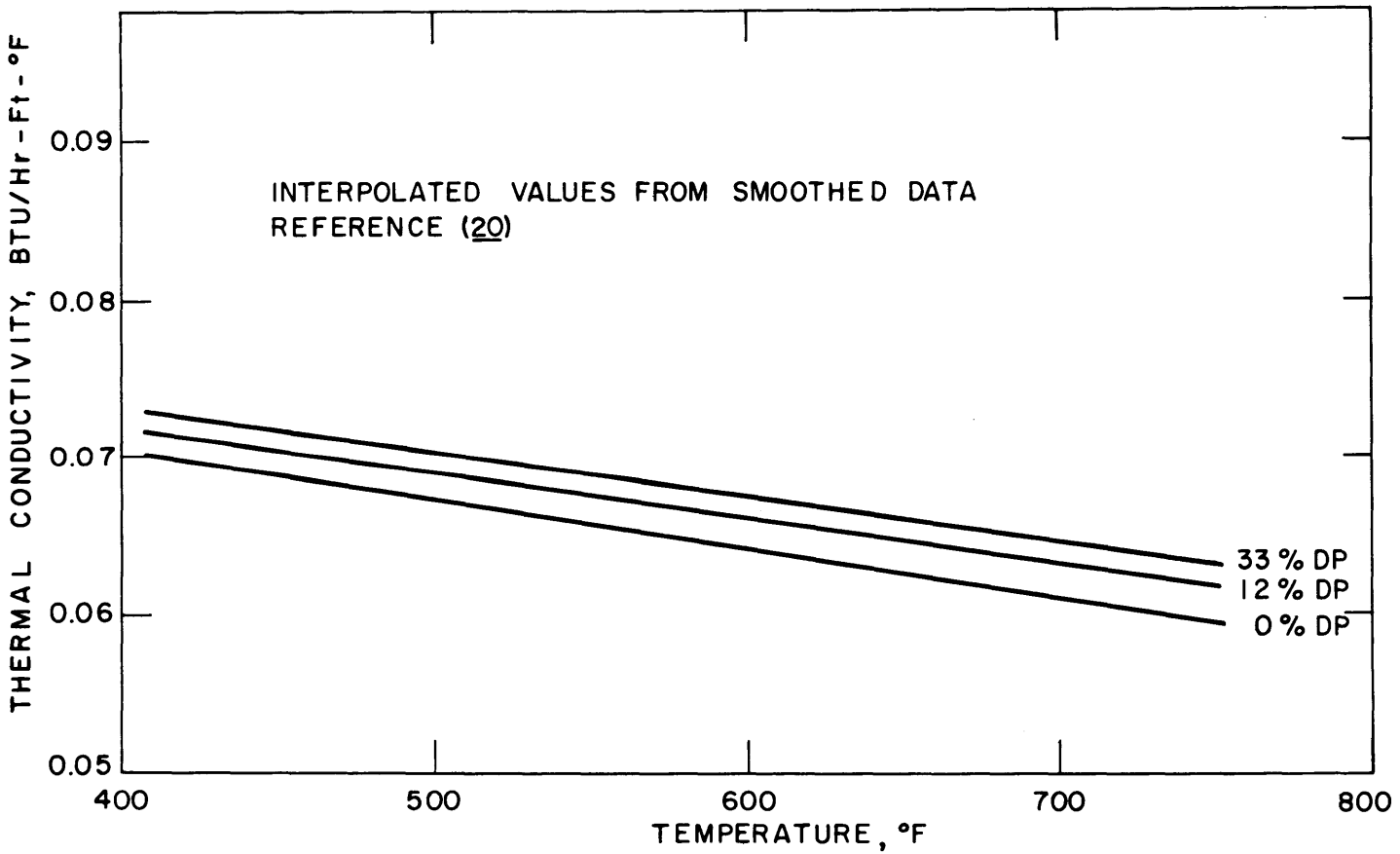

FIG. 34 THERMAL CONDUCTIVITY OF OM2 COOLANT

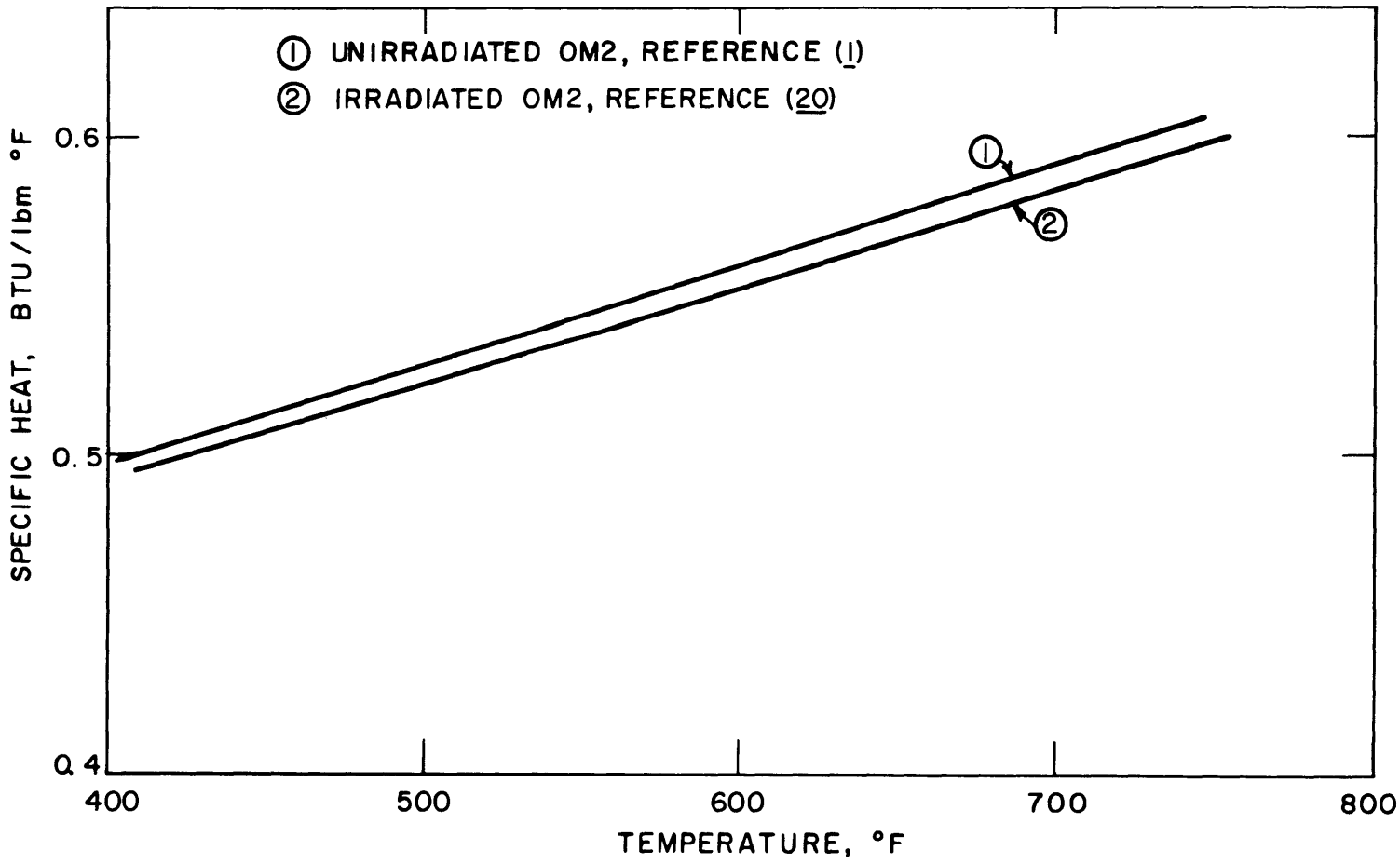

FIG. 35 SPECIFIC HEAT OF OM2 COOLANT

TABLE 17

COMPOSITION OF COOLANT SAMPLES
FROM RUN 11 AND RUN 12
USED FOR PHYSICAL PROPERTIES
(BY GAS CHROMATOGRAPHY)

Sample No.	Ortho %	Meta %	Para %	Biphenyl %	Percent Degradation Products % DP
11L-37	22.5	60.6	4.6	~2	12
11L-42	23.5	60.5	4.6	~2	12
11L-47	22.0	56.9	4.1	~2	17
Charge Material Run 12*	13.8	37.0	2.6	~4	47
12L-1	16.6	47.1	3.4	~3	33
12L-3	15.9	47.6	3.6	~4	33
12L-4	15.5	47.6	3.3	~4	33

*Charge material was 38% HB by distillation.

TABLE 18

HEAT TRANSFER DATA FROM TEST HEATER 6
750°F IRRADIATION OF SANTOWAX WR
RUN 3

Nominal Heat Flux, Q/A = 160,000 BTU/hr-ft^2

RUN	REACTOR MWH	VELOCITY FT/SEC	FT COEF, U BTU/HR/FT**2 /DEG. F	NUSSELT NO.	REYNOLDS NO.	PRANDTL NO.	MU/MUW
3-05	24	21.7	1961	579	125380	5.54	1.24
3-04	24	17.1	1583	467	98333	5.57	1.31
3-03	24	14.6	1489	440	84532	5.53	1.33
3-02	24	12.4	1186	348	70007	5.63	1.42
3-01	24	10.5	1024	299	58534	5.68	1.47
3-10	166	21.3	1827	515	116690	5.61	1.28
3-09	166	17.0	1499	422	92874	5.62	1.33
3-08	166	14.8	1350	379	80230	5.66	1.38
3-07	166	12.5	1163	326	67253	5.69	1.44
3-06	166	10.7	1006	281	56779	5.75	1.49
3-11	736	20.4	1755	462	88568	6.68	1.23
3-12	736	18.6	1607	423	80654	6.69	1.26
3-13	736	16.7	1473	388	72539	6.68	1.28
3-14	736	14.3	1294	341	62353	6.66	1.32
3-15	736	12.6	1152	303	54643	6.68	1.37
3-16	795	20.0	1493	390	84128	6.86	1.25
3-17	795	18.2	1490	389	76417	6.87	1.26
3-18	795	16.3	1349	352	68310	6.88	1.30
3-19	795	14.5	1219	318	60501	6.90	1.33
3-20	795	12.3	1072	280	51534	6.88	1.38
3-21	933	21.2	1670	427	83395	7.24	1.24
3-22	933	19.1	1528	391	75417	7.22	1.27
3-23	933	17.1	1394	357	67712	7.20	1.30
3-24	933	15.1	1246	319	59286	7.25	1.34
3-25	933	13.1	1111	284	51191	7.28	1.38
3-26	1588	17.2	1482	347	48181	9.75	1.30
3-27	1588	16.5	1354	317	46238	9.75	1.33
3-28	1588	15.1	1280	300	42371	9.73	1.35
3-29	1588	13.6	1159	272	38114	9.74	1.39
3-30	1588	12.5	1064	249	34922	9.77	1.43
3-31	1836	20.6	1608	382	69213	8.00	1.29
3-32	1836	17.9	1431	340	59923	8.03	1.33
3-33	1836	15.9	1312	312	53247	8.02	1.37
3-34	1836	13.8	1157	275	46172	8.03	1.42
3-35	1836	12.1	1038	247	40456	8.03	1.46
3-40	2250	20.1	1540	366	67379	8.02	1.29
3-39	2250	17.6	1392	331	58804	8.04	1.32
3-38	2250	15.4	1250	297	51598	8.04	1.37
3-37	2250	13.7	1111	264	45855	8.05	1.41
3-36	2250	11.6	1027	244	38596	8.06	1.46
3-51	2630	20.1	1551	368	66350	8.13	1.31
3-52	2630	18.1	1429	339	59571	8.15	1.34
3-53	2630	16.1	1305	310	53037	8.14	1.38
3-54	2630	14.1	1171	278	46612	8.11	1.42
3-55	2630	12.1	1033	245	39854	8.13	1.48
3-56	3055	17.6	1433	340	58327	8.10	1.35
3-57	3055	14.7	1245	295	48667	8.10	1.40
3-58	3055	11.1	1072	254	36711	8.10	1.49

TABLE 18 (Cont'd)

HEAT TRANSFER DATA FROM TEST HEATER 6
750°F IRRADIATION OF SANTOWAX WR
RUN 3
Nominal Heat Flux, Q/A = 90,000 BTU/hr-ft^2

RUN	REACTOR MWH	VELOCITY FT/SEC	FT COEF, U BTU/HR/FT**2 /DEG. F	NUSSELT NO.	REYNOLDS NO.	PRANDTL NO.	MU/MUW
3-41	2266	19.3	1285	292	43694	11.39	1.24
3-42	2266	17.1	1162	264	38783	11.37	1.26
3-43	2266	15.1	1060	241	34115	11.41	1.29
3-44	2266	12.2	898	204	27617	11.38	1.35
3-45	2266	9.1	715	163	2C598	11.37	1.45
3-46	2266	18.1	115C	255	3C728	14.78	1.34
3-47	2266	16.1	1047	232	27109	14.89	1.38
3-48	2266	14.1	946	21[illegible]	23906	14.79	1.42
3-49	2266	12.1	841	186	20618	14.72	1.48
3-5C	2266	9.1	658	146	15644	14.58	1.61

TABLE 19

HEAT TRANSFER DATA FROM TEST HEATER 6
700°F IRRADIATION OF SANTOWAX WR
RUN 5

Nominal Heat Flux, Q/A = 130,000 BTU/hr-ft^2

Run	Reactor MWHr	Velocity ft/sec	Measured h BTU/ht-ft^2-°F	Nusselt No. Nu	Reynolds No. Re	Prandtl No. Pr	Viscosity Ratio μ/μ_W
1	510	19.6	1545	366	59240	8.8	1.29
2	510	16.1	1312	311	48780	8.8	1.33
3	510	14.1	1186	282	42500	8.8	1.37
4	510	12.1	1018	242	36620	8.8	1.44
5	510	7.7	740	176	23220	8.8	1.59
11	1065	19.7	1543	367	60240	8.8	1.28
12	1065	16.0	1302	309	48760	8.8	1.34
13	1065	14.1	1179	280	42520	8.8	1.38
14	1065	12.1	1054	250	36560	8.8	1.42
15	1065	7.6	750	178	22920	8.8	1.60

TABLE 20

HEAT TRANSFER DATA FROM TEST HEATER 6
610°F IRRADIATION OF SANTOWAX WR,
RUN 11
Nominal Heat Flux, Q/A = 130,000 BTU/hr-ft^2

Run	Reactor MWHr	Velocity ft/sec	Measured h BTU/hr-ft^2-°F	Nusselt No. Nu	Reynolds No. Re	Prandtl No. Pr	Viscosity Ratio μ/μ_W
1	338	17.2	1419	363	65770	7.31	1.33
2	338	15.1	1279	328	58340	7.24	1.39
3	338	12.2	1077	277	48040	7.13	1.43
4	338	7.6	733	189	30550	7.10	1.63
5	700	16.1	1379	354	62480	7.22	1.35
9	700	14.6	1261	325	57480	7.13	1.38
6	700	14.1	1260	324	55400	7.14	1.38
10	700	12.6	1139	294	50120	7.07	1.42
7	700	11.6	1096	283	46260	7.05	1.43
8	700	7.9	814	211	32200	6.91	1.58
11	722	17.0	1389	358	67260	7.10	1.33
12	722	15.7	1316	339	61700	7.14	1.35
13	722	14.2	1233	317	55820	7.14	1.38
14	722	12.8	1129	291	50710	7.10	1.42
15	722	11.1	1031	266	44170	7.06	1.45
16	722	8.0	798	207	32310	7.00	1.58

TABLE 21

HEAT TRANSFER DATA FROM TEST HEATER 7 DURING RUN 12, LOOP RUN OUT OF PILE

Nominal Heat Flux, Q/A = 120,000 BTU/hr-ft^2

Run	Velocity ft/sec	Measured h BTU/hr-ft^2-^{o}F	Nusselt No. Nu	Reynolds No. Re	Prandtl No. Pr	Viscosity Ratio μ/μ_W
111	23.7	1661	443	68400	10.3	1.24
115	18.3	1408	378	55110	10.0	1.28
116	15.4	1161	307	42540	10.7	1.37
118	11.5	862	229	32320	10.6	1.48
120	23.7	1581	421	68520	10.4	1.25
121	15.5	1189	315	43250	10.6	1.35
122	7.9	734	195	22730	10.4	1.57

TABLE 22

HEAT TRANSFER DATA FROM TEST HEATER 7
572°F IRRADIATION OF SANTOWAX WR,
RUN NO. 13

Nominal Heat Flux, Q/A = 120,000 BTU/hr-ft^2
Reference (20) used for physical properties data.

Run	Reactor MWHr	Velocity ft/sec	Measured h BTU/hr-ft^2-°F	Nusselt No. Nu	Reynolds No. Re	Prandtl No. Pr	Viscosity Ratio μ/μ_W
1	250	21.8	1680	459	86580	7.33	1.25
2	250	21.9	1650	450	87030	7.33	1.25
3	250	18.3	1387	375	71400	7.42	1.31
4	250	13.7	1166	317	54030	7.38	1.37
5	250	11.4	1014	276	44900	7.38	1.43
6	250	8.2	807	220	32000	7.40	1.56

TABLE 23

SUMMARY OF FRICTION FACTOR DATA
FOR IRRADIATED SANTOWAX WR

Runs No.	Nominal Bulk Temperature ^{o}F	Percent DP	Nominal Prandtl No.	Nominal Heat Flux BTU/hr-ft^2 x 10^{-3}	Sample No. For Analysis
1 - 5	590	12	6.9	130	11L37
6 - 7	590	12	7.0	65	11L37
8 - 28	590	12	7.8	0	11L37
29 - 45	435	12	13.5	0	11L42
46 - 50	750	12	5.7	65	11L42
51 - 60	785	17	5.6	75	11L47
61 - 70	585	17	8.7	0	11L47
71 - 80	600	33	11.3	0	12L1
81 - 89	755	33	8.1	75	12L3
90 - 96	785	33	7.7	75	12L4
97 - 109	425	33	19.5	0	12L4
110 - 122	625	33	10.1	100	12L4

TABLE 24

FRICTION FACTOR DATA FOR IRRADIATED SANTOWAX WR
L/D = 123.5, Heat Flux = 0

Run No.	Average Temp. ^{o}F	Flow Rate gpm	ΔP lb_f/in^2	V_m ft/hr x 10^{-4}	Reynolds No. Re x 10^{-4}	Friction Factor, f
8	593	2.35	7.12	8.24	8.53	.0186
9	591	2.34	7.15	8.20	8.39	.0190
12	591	2.34	7.05	8.20	8.39	.0187
14	591	2.34	7.05	8.20	8.39	.0187
15	590	2.08	5.80	7.28	7.44	.0194
16	590	2.08	5.80	7.28	7.45	.0194
17	590	1.78	4.43	6.23	6.37	.0203
13	590	1.77	4.43	6.20	6.33	.0205
19	593	1.41	2.98	4.93	5.10	.0218
20	594	1.41	2.98	4.93	5.16	.0218
21	591	1.18	2.15	4.13	4.23	.0224
22	591	1.18	2.15	4.13	4.23	.0224
23	595	0.82	1.18	2.87	3.00	.0255
24	590	0.60	0.82	2.10	2.15	.0330
25	590	0.58	0.78	2.03	2.08	.0336
26	590	0.55	0.74	1.93	1.97	.0355
27	590	0.28	0.20	0.98	1.00	.0370
28	589	2.35	7.05	8.23	8.41	.0185
29	431	1.67	4.60	5.85	3.25	.0220
30	435	1.66	4.64	5.81	3.14	.0225
31	435	1.66	4.64	5.81	3.14	.0225
32	433	1.49	3.83	5.22	2.86	.0231
33	434	1.48	3.70	5.18	2.82	.0226
34	434	0.85	1.50	2.98	1.62	.0278
35	434	0.82	1.44	2.85	1.55	.0290
36	434	1.85	5.50	6.48	3.53	.0215
37	434	1.75	5.00	6.13	3.34	.0219
38	431	1.71	4.75	5.99	3.32	.0218
39	432	1.38	3.13	4.31	2.65	.0220
40	433	1.40	3.21	4.90	2.68	.0220
41	433	1.42	3.35	4.97	2.72	.0222
42	434	1.08	2.10	3.78	2.06	.0240
43	435	0.78	1.24	2.73	1.47	.0273

TABLE 24 (Cont'd)

FRICTION FACTOR DATA FOR IRRADIATED SANTOWAX WR
L/D = 123.5, Heat Flux = 0

Run No.	Average Temp. ^{o}F	Flow Rate gpm	ΔP lb_f/in^2	V_m ft/hr x 10^{-4}	Reynolds No. Re x 10^{-4}	Friction Factor, f
44	436	0.52	0.62	1.82	0.98	.0307
45	436	0.53	0.61	1.86	1.00	.0289
61	587	2.40	7.25	8.40	7.95	.0180
62	589	2.18	6.20	7.63	7.22	.0186
63	589	1.83	4.72	6.40	6.05	.0201
64	590	1.51	3.38	5.28	5.00	.0212
65	591	1.28	2.49	4.48	4.24	.0212
66	590	0.90	1.50	3.15	2.98	.0265
67	590	0.68	0.95	2.38	2.25	.0293
68	590	0.50	0.60	1.75	1.66	.0343
69	591	2.00	5.38	7.00	6.60	.0192
70	590	2.40	7.10	8.40	7.95	.0176
71	600	2.35	6.75	8.23	5.89	.0174
72	604	2.37	6.60	8.30	6.03	.0167
73	604	2.12	5.45	7.42	5.40	.0173
74	605	1.88	4.43	6.58	4.78	.0178
75	605	1.59	3.37	5.56	4.04	.0190
76	606	1.27	2.36	4.44	3.23	.0208
77	606	0.88	1.43	3.08	2.24	.0263
78	605	0.47	0.59	1.65	1.20	.0381
79	607	1.71	3.74	5.99	4.36	.0182
80	609	2.39	6.50	8.37	6.18	.0162
97	434	2.31	9.25	8.10	3.11	.0227
98	434	2.08	7.78	7.28	2.78	.0236
99	436	1.82	6.25	6.37	2.44	.0248
100	439	1.50	4.48	5.25	2.03	.0262
101	439	1.19	3.07	4.17	1.61	.0284
102	440	0.90	1.98	3.14	1.22	.0323
103	440	0.70	1.38	2.45	0.95	.0370
104	443	0.47	0.77	1.65	0.67	.0455
105	439	2.33	9.25	8.15	3.15	.0224
106	444	1.55	4.62	5.43	2.15	.0252
107	444	1.89	6.38	6.60	2.62	.0236
108	442	1.10	2.71	3.85	1.52	.0294
109	430	2.32	9.17	8.13	2.97	.0224

TABLE 24 (Cont'd)

FRICTION FACTOR DATA FOR IRRADIATED SANTOWAX WR
L/D = 123.5, Heat Flux As Noted

Run No.	Average Temp. ^{o}F	Flow Rate gpm	ΔP lb_f/in^2	V_m $ft/hr \times 10^{-4}$	Reynolds No. $Re \times 10^{-4}$	Friction Factor, f	Nominal Heat Flux $BTU/hr\text{-}ft^2$
1	631	1.95	4.82	6.83	8.05	.0188	130,000
4	637	1.15	1.80	4.03	4.76	.0202	130,000
6	622	2.32	6.95	8.12	9.21	.0192	65,000
46	758	2.42	6.05	8.47	12.70	.0164	65,000
47	752	1.84	3.68	6.44	9.70	.0172	65,000
48	755	1.11	1.43	3.88	5.84	.0185	65,000
49	750	0.85	0.80	2.98	4.50	.0182	65,000
50	752	2.43	6.05	8.50	12.80	.0163	65,000
51	790	2.50	6.05	8.75	13.50	.0157	75,000
53	790	2.29	5.22	8.02	12.40	.0161	75,000
54	792	2.08	4.38	7.28	11.20	.0164	75,000
55	793	1.72	3.10	6.02	9.40	.0172	75,000
56	793	1.43	2.22	5.00	7.80	.0178	75,000
57	793	1.14	1.50	3.99	6.24	.0189	75,000
58	793	0.85	0.89	2.98	4.65	.0202	75,000
59	793	1.55	2.50	5.43	8.47	.0170	75,000
60	794	2.15	4.65	7.53	11.70	.0165	75,000
60A	793	2.50	6.02	8.75	13.70	.0158	75,000
81	755	2.49	5.71	8.72	10.00	.0141	75,000
82	755	2.27	4.90	7.95	9.08	.0146	75,000
83	755	1.88	3.57	6.58	7.50	.0155	75,000
84	755	1.49	2.41	5.22	5.96	.0167	75,000
85	755	1.10	1.50	3.85	4.40	.0190	75,000
86	756	0.88	1.08	3.08	3.52	.0213	75,000
87	755	2.49	5.71	8.72	9.96	.0141	75,000
88	753	2.49	5.73	8.72	9.96	.0142	75,000
89	754	1.10	1.56	3.85	4.40	.0198	75,000
90	786	2.50	5.55	8.75	10.00	.0139	75,000
91	786	2.20	4.48	7.70	8.80	.0145	75,000
92	786	1.90	3.55	6.65	7.60	.0153	75,000
93	786	1.59	2.58	5.57	6.36	.0159	75,000
94	786	1.18	1.60	4.13	4.71	.0179	75,000

TABLE 24 (Cont'd)

FRICTION FACTOR DATA FOR IRRADIATED SANTOWAX WR
L/D = 123.5, Heat Flux As Noted

Run No.	Average Temp. ^{o}F	Flow Rate gpm	ΔP lb_f/in^2	V_m ft/hr x 10^{-4}	Reynolds No. Re x 10^{-4}	Friction Factor, f	Nominal Heat Flux BTU/hr-ft^2
95	788	0.88	1.03	3.08	3.52	.0207	75,000
96	786	2.52	5.60	8.82	10.10	.0138	75,000
110	634	2.45	7.53	8.58	6.90	.0180	110,000
111	634	2.45	7.63	8.58	6.90	.0182	110,000
112	634	2.43	7.58	8.50	6.80	.0185	110,000
113	638	2.19	6.25	7.67	6.10	.0189	110,000
115	640	1.89	4.73	6.62	5.30	.0190	110,000
116	619	1.59	3.60	5.57	4.23	.0204	110,000
118	624	1.20	2.27	4.20	3.20	.0227	110,000
119	619	2.44	7.78	8.54	6.50	.0187	110,000
120	634	2.46	7.68	8.61	6.90	.0183	110,000
121	624	1.60	3.70	5.60	4.26	.0207	110,000
122	628	0.82	1.30	2.87	2.20	.0278	110,000

7.8 Construction of Test Heater 7

The print used for the construction of Test Heater 7 is presented in Figure 36, and the procedure followed is shown in Table 25.

The major problem encountered was drilling the small holes (Number 80 drill, 0.013 inches diameter) at the bottom of the 6" deep pressure taps. Many drills were broken while drilling the holes but by finally making a small drill arbor and feeding the drill by hand, the holes were successfully made.

After drilling, the inside of the tube was cleaned with fine steel wool to remove any burrs at the pressure taps. This procedure was satisfactory since all of the pressure drop data, measured between pressure taps 2 and 3, correlate quite well.

The measurements of TH7 outside diameter along the tube length, and the inside diameter at the ends are presented in Table 26.

7.9 Wilson Plots of MIT Organic Coolant Heat Transfer Data

Wilson (7) (34) was the first to suggest a graphical technique of plotting heat transfer data in order to determine individual coefficients. This technique is based on the fact that the over-all coefficient (U) is equal to the sum of the over-all resistances to heat flow. For the case of interest here, the over-all coefficient can be written as

NOTES - SEE ASSEMBLY PROCEDURE, TABLE 25

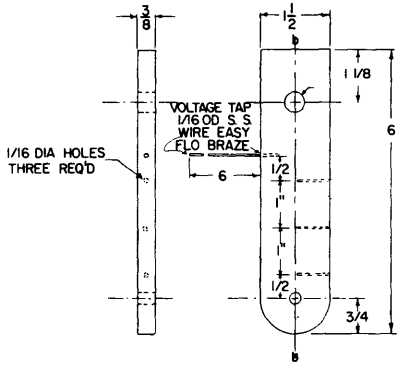

DETAIL A
COPPER CONNECTORS 3 REQUIRED SEE NOTE 2

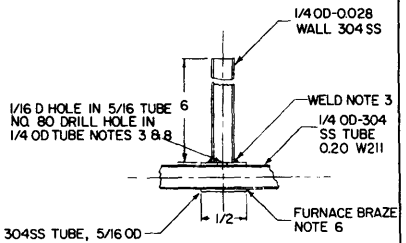

DETAIL B
PRESSURE TAP DETAIL 3 REQ'D

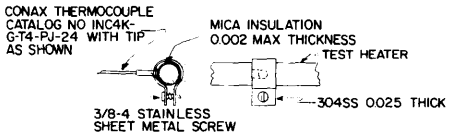

SECTION CC
THERMOCOUPLE DETAIL
DOUBLE SCALE

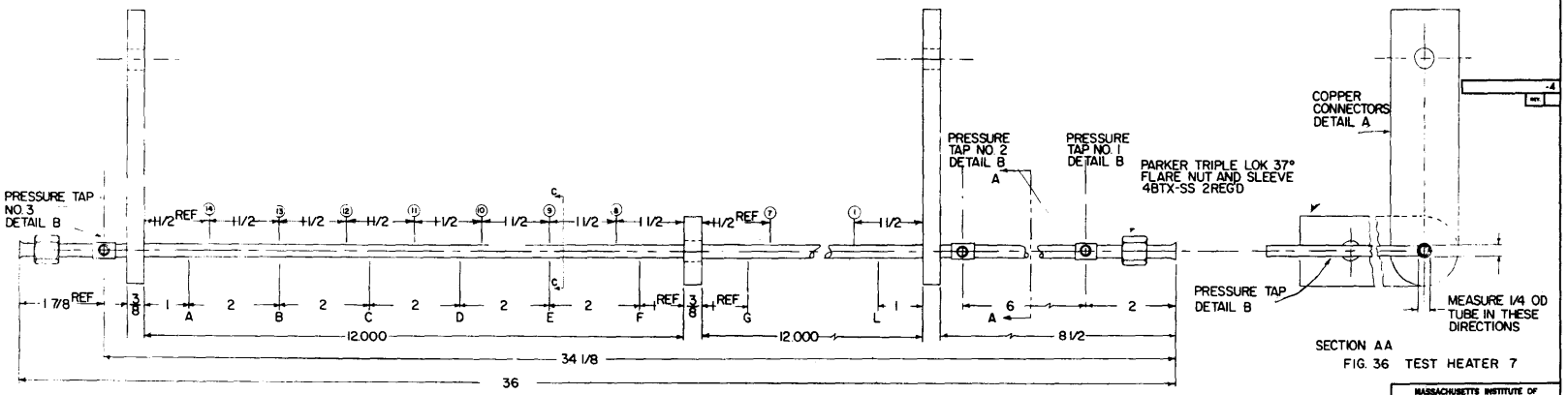

SECTION AA

FIG. 36 TEST HEATER 7

1	AS BUILT	AHS 4/1/65	
REV.	DESCRIPTION	BY DATE	

MASSACHUSETTS INSTITUTE OF TECHNOLOGY REACTOR			
ORGANIC LOOP TEST HEATER			
304SS,Ch	1	FULL	TEST HEATER NO. 7
MATERIAL	QUANTITY	SCALE	
2/27/64	AHS		OGL-5 -4
DATE	DRAWN BY	APPROVED	DRAWING NUMBER REV.

TABLE 25

NOTES FOR FIGURE 36, TEST HEATER 7

1. Select tube 0.250, 0.020 wall with deviation along length of tube $\pm$0.0005. Measure tube OD at locations A though L in two directions, as shown in Section AA. Measure tube ID at ends. Tabulate measurements.
2. Use O_2 free copper for lugs. Nickel plate lugs with minimum of 0.0002 plate.
3. Drill 1/16 OD hole in 5/16 OD tube. Weld 1/4 tube to 5/16 tube. Ream out 5/16 tube to the 3 ft. x 1/4 OD tube's actual OD plus 0.004 on the diameter. Helium leak check pressure tap assembly.
4. Assemble 3 pressure taps and 3 plated lugs on 1/4 tube.
5. Assemble 4BTXSS on tube flare tube ends.
6. Furnace braze 3 lugs and 3 pressure taps to 1/4 OD tube Handy Harman Lithobraze BT flow temperature 1435°F.
7. Drill holes in 1/4 OD tube down through pressure taps with no. 80 drill.
8. Remove burrs from inside drilled hole. Imperative that there be no burrs or indentations inside of the 1/4" tube.
9. Braze voltage taps to 3 lugs. Use Easy-Flo-45.
10. Helium leak check test heater assembly, maximum leak rate 10^{-9} cc/sec.

TABLE 26

MEASUREMENTS OF THE DIAMETER OF TEST HEATER 7

Location of Measurement See Figure 36	Outside Diameter 0°	Outside Diameter 90°
A	.2500	.2500
B	.2497	.2498
C	.2500	.2500
D	.2500	.2500
E	.2502	.2500
F	.2500	.2501
G	.2500	.2500
L	.2498	.2498
	Inside Diameter at Ends	
A	.2104	.2106
L	.2105	.2112

$$1/U = 1/h_f + 1/h_s \tag{17}$$

For turbulent flow of a fluid, during a period of time when the physical properties are constant, the film coefficient can be expressed

$$h_f = AV^b \tag{39}$$

where

A is an arbitrary constant,

V is the coolant velocity and

b is the exponent on the correlation for forced convection heat transfer, normally taken as 0.8.

Combining Equations (17) and (39), the expression for the over-all coefficient is

$$1/U = 1/h_s + A/V^b \tag{43}$$

Therefore, a plot of 1/U against $1/V^b$, when it is extrapolated back to infinite velocity, gives the value of $1/h_s$ as the intercept with the 1/U axis.

The computer program, MNHTR, performs this analysis by fitting the set of data taken at different velocities on a given day to Equation (43), by the method of least squares (3).

The values of the intercepts ($1/h_s$), for all of the Santowax OMP where b was set equal to 0.9, varied between -1 to +1 x 10^{-4} hr-ft^2-^{o}F/BTU. Considering a possible uncertainty of $\pm$10% in the measurement of U and the necessary extrapolations to obtain the intercepts, the

Wilson plot results indicate little or no scale buildup at all for the entire periods of irradiation. Using Reynolds Number powers of 0.8 and 0.9 served only to shift the range of intercepts on the Wilson plots down or up respectively, with about the same spread in the intercepts. Thus, it was concluded that within the accuracy of this technique, no appreciable fouling of the test heaters used was observed.

Typical Wilson plots for both Santowax OMP and Santowax WR data are presented in Figures 37 to 42. Each group of data is plotted twice, first with $1/V^{0.8}$, and then with $1/V^{0.9}$ as the abscissa.

Wilson plots can also be used as an aid in determining the best exponent for the Reynolds Number. Keeping in mind the uncertainty in U of $\pm 10\%$, and the fact that these data are extrapolated back to zero, the following generalizations can be made:

a. The Santowax OMP data intercepts the 1/U axis closer to zero when b = 0.9 is used rather than b = 0.8. However, also notice that the value of b = 0.8 reduces the scatter in the value of the intercept (or $1/h_s$). This may indicate that the corrections applied for heat losses and/or temperature measurements (Appendix 7.5.1) to the TH6 data may be incorrect and that the 1/U axis should be in effect moved down approximately one division.

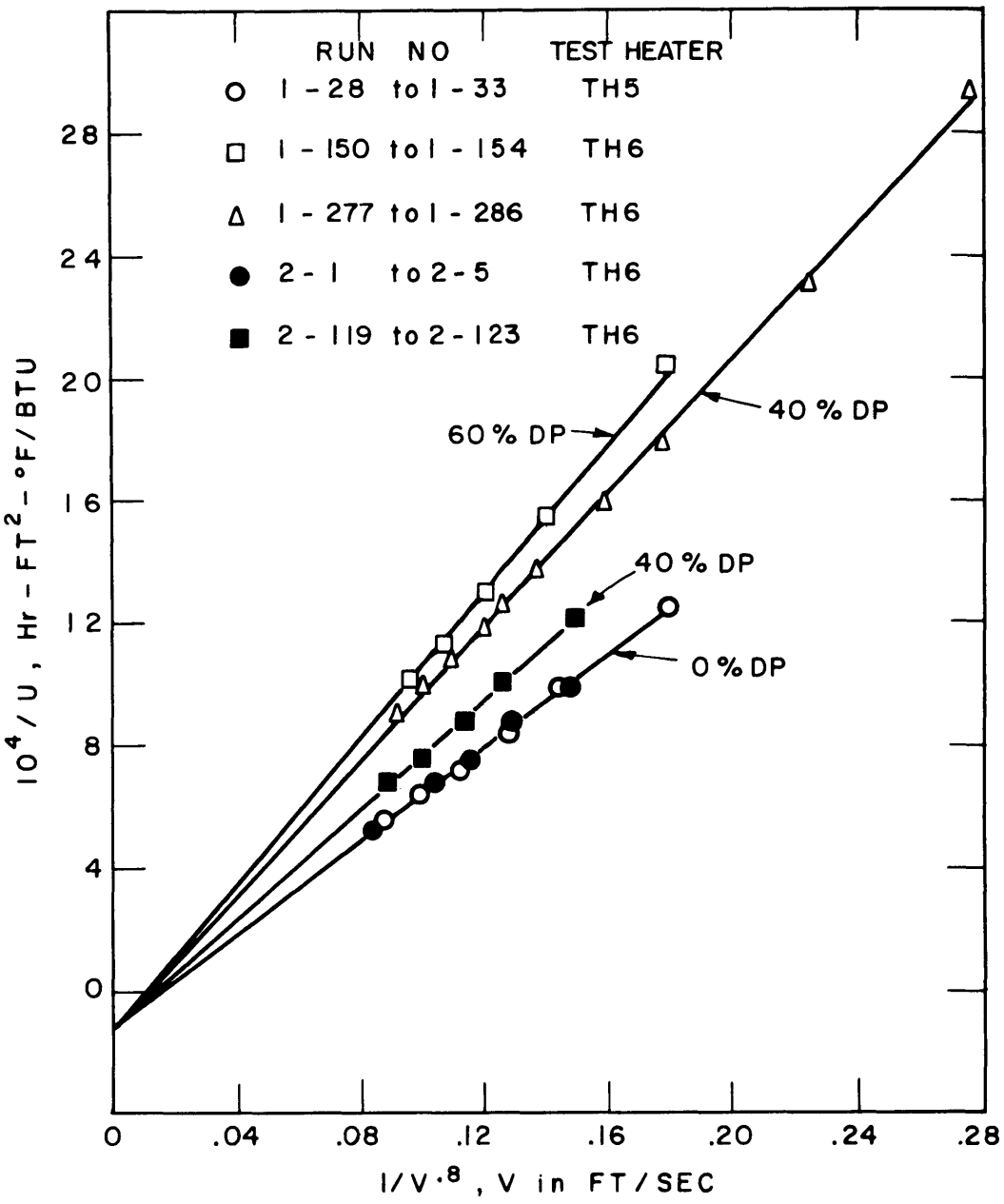

FIG. 37 TYPICAL WILSON PLOTS OF SANTOWAX OMP, SAWYER AND MASON (3) DATA

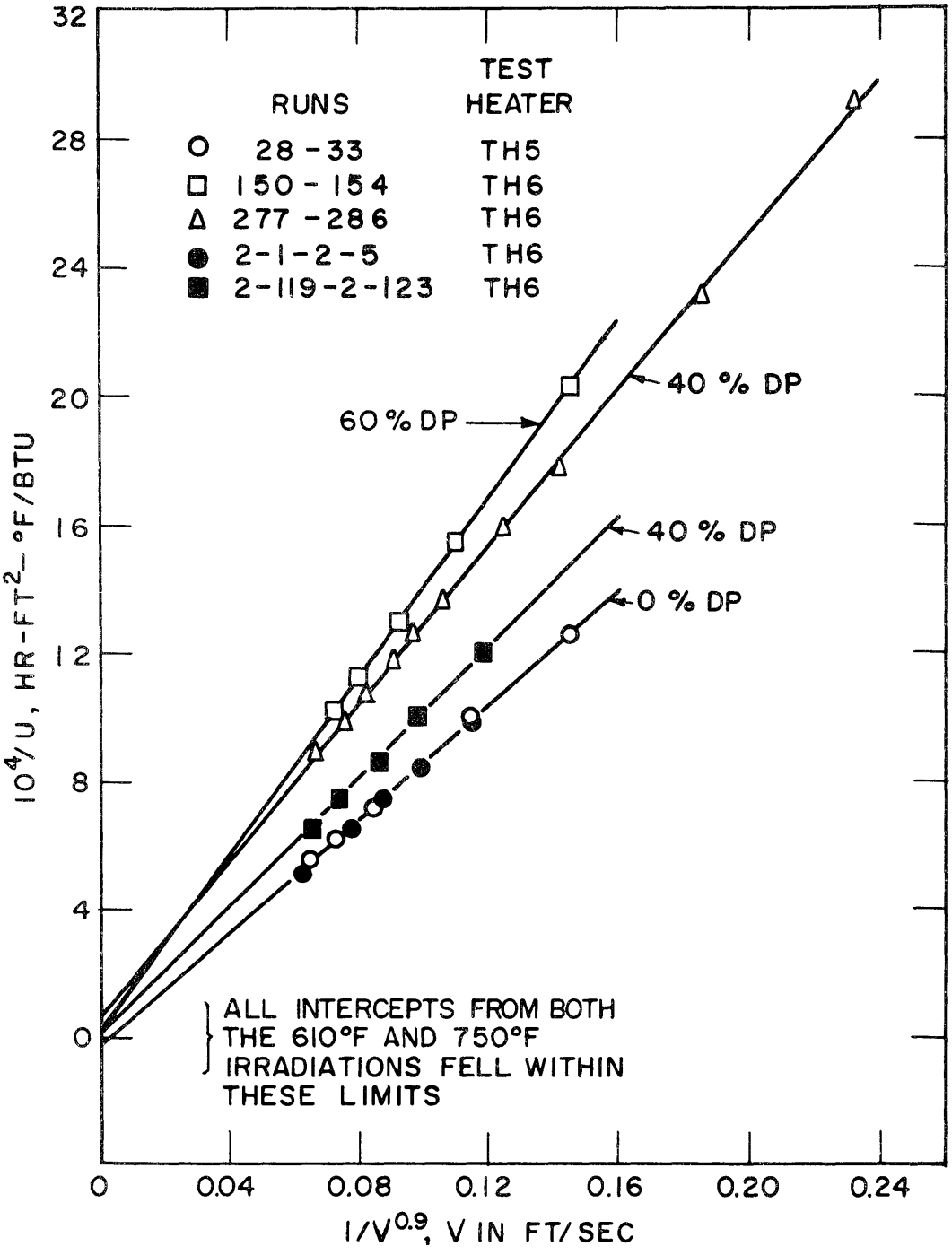

FIG. 38 TYPICAL WILSON PLOTS OF SANTOWAX OMP, SAWYER AND MASON (3) DATA

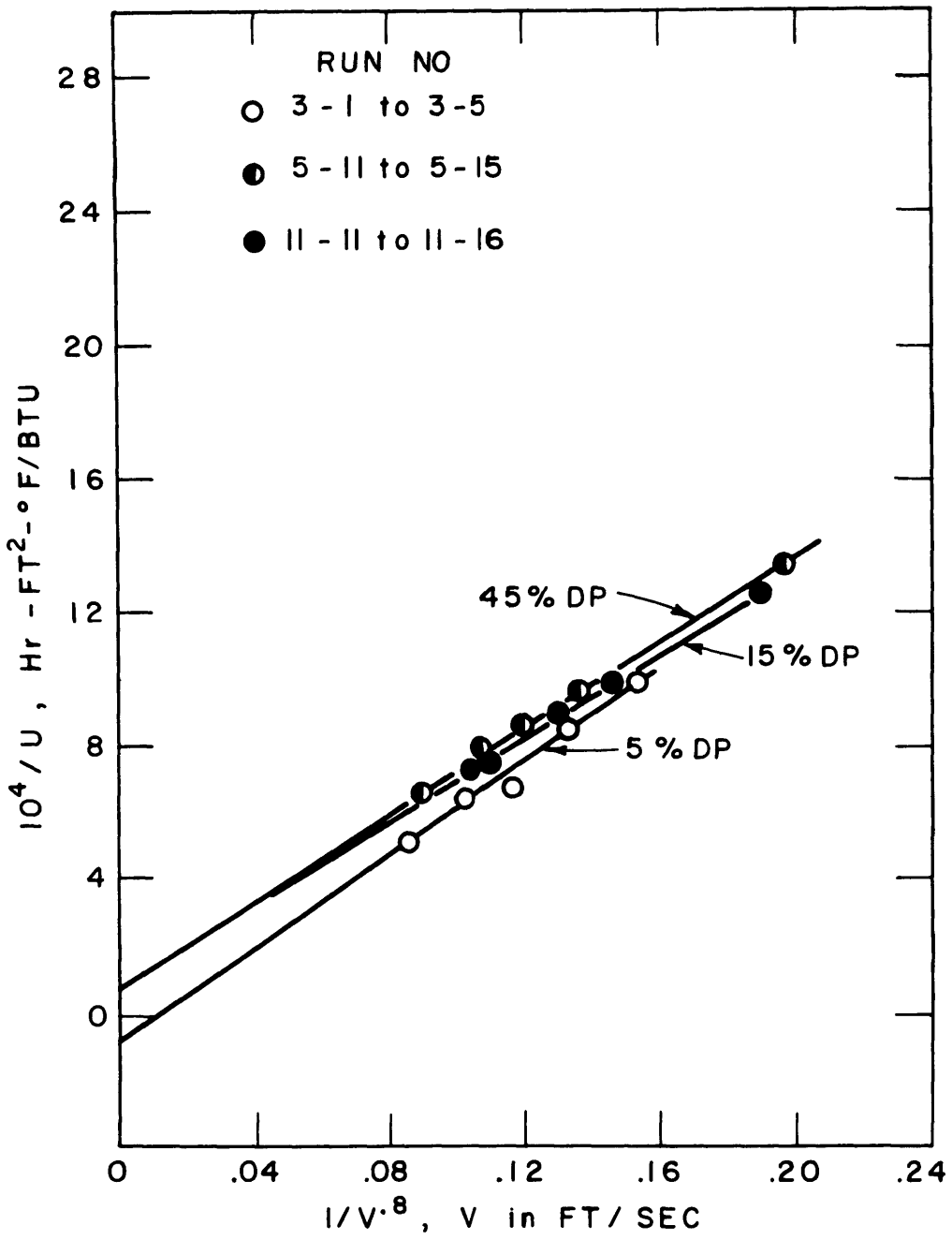

FIG. 39 TYPICAL WILSON PLOTS OF SANTOWAX WR, TH6 DATA

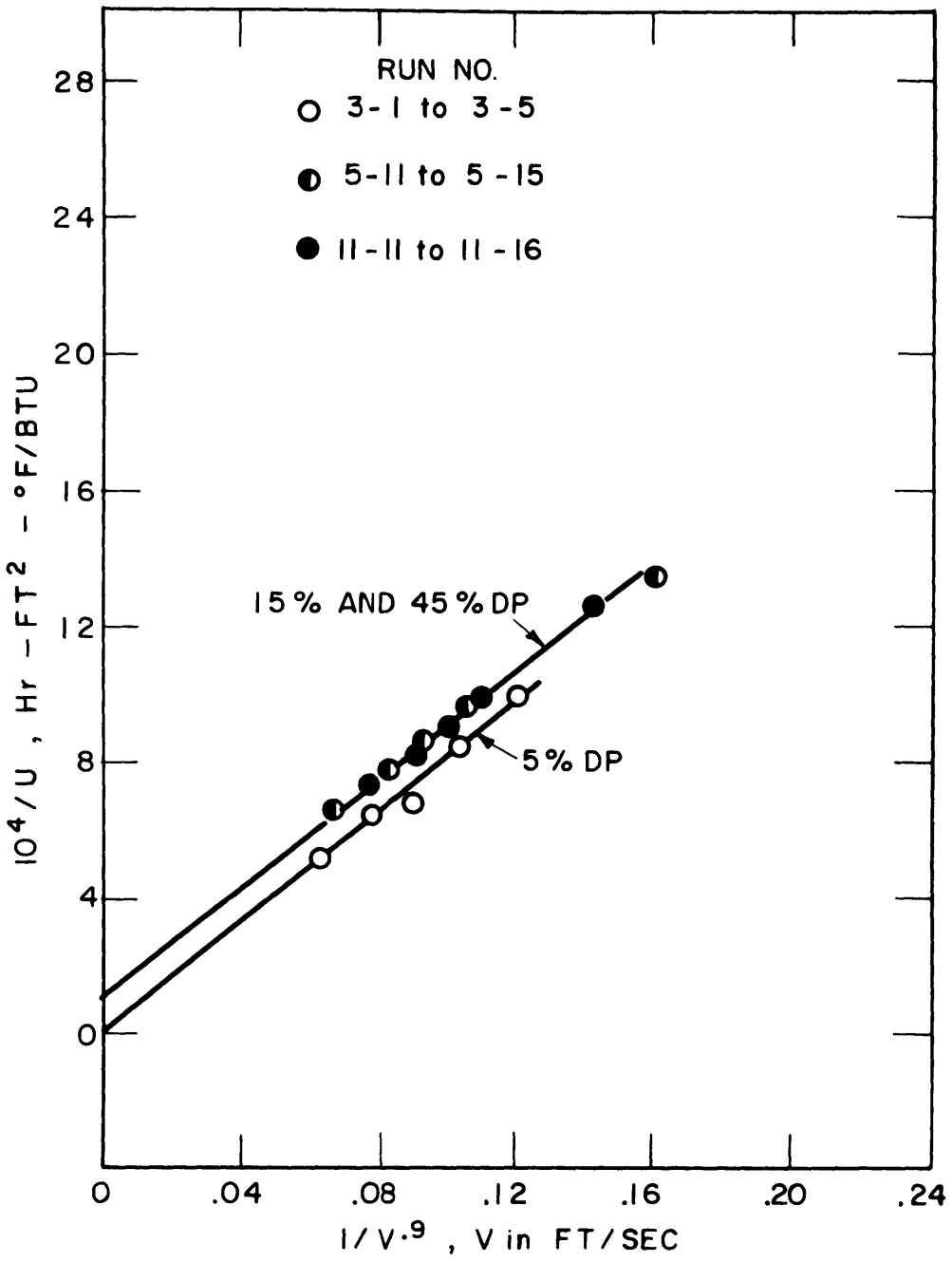

FIG. 40 TYPICAL WILSON PLOTS OF SANTOWAX WR, TH6 DATA

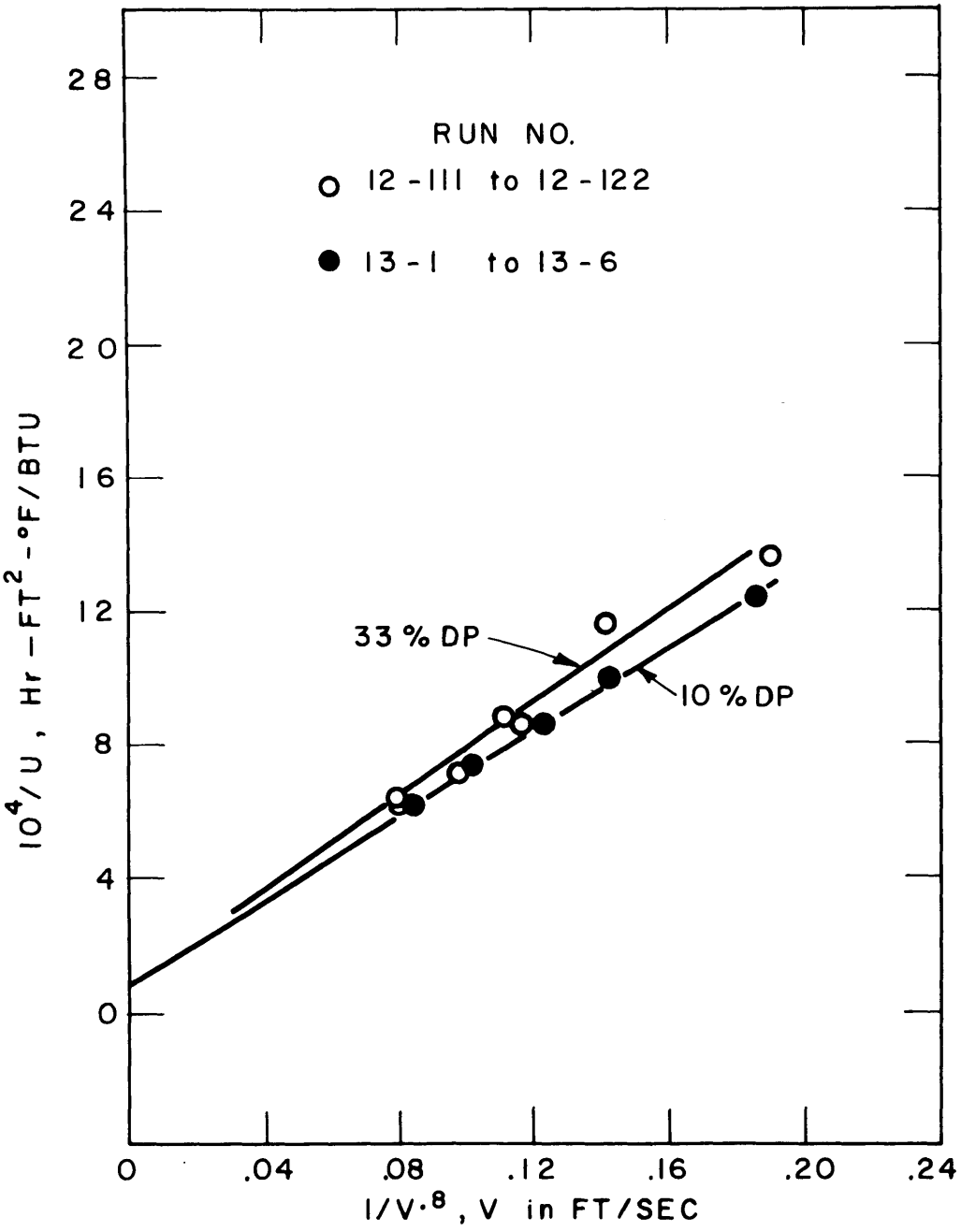

FIG. 41 TYPICAL WILSON PLOTS OF SANTOWAX WR, TH7 DATA.

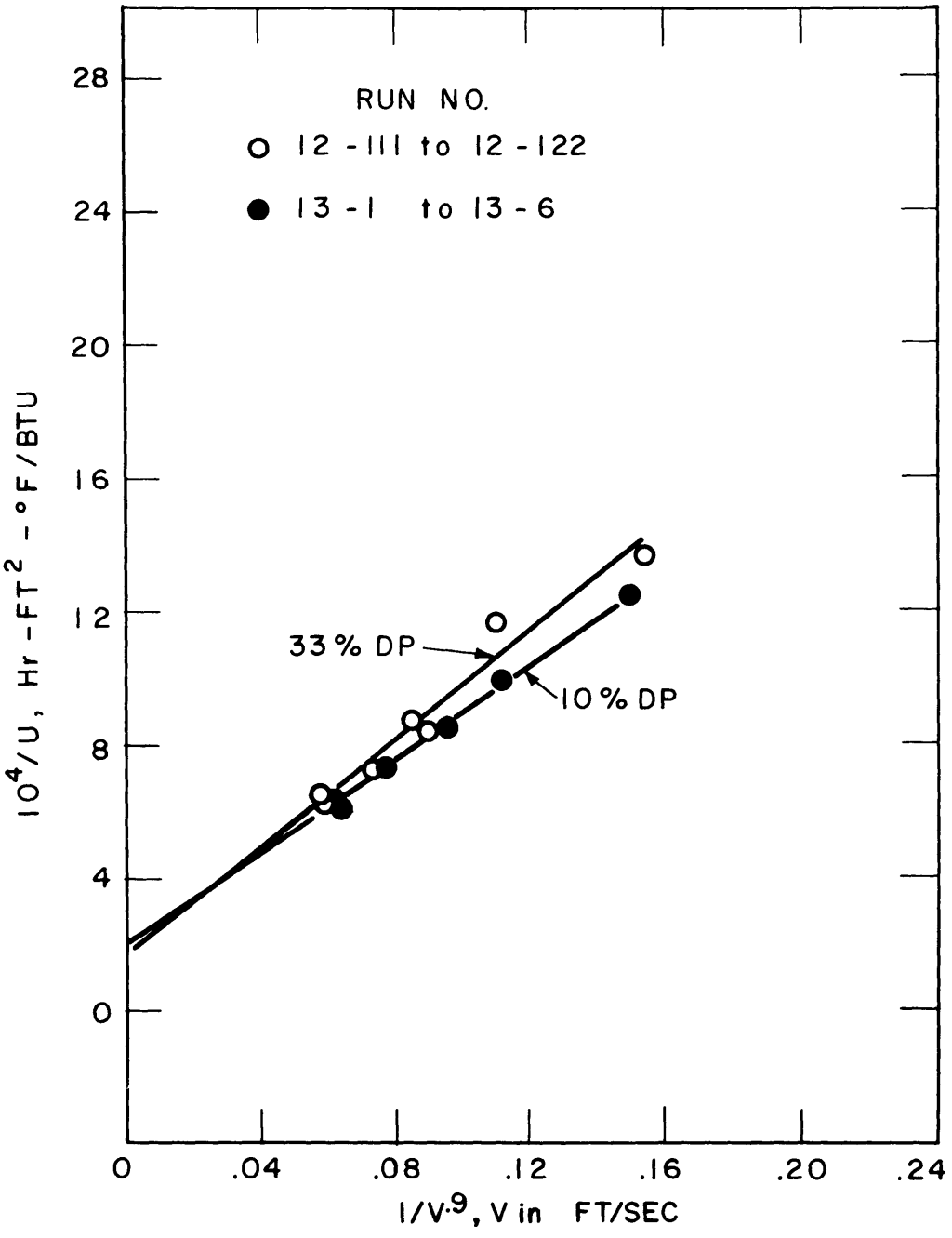

FIG. 42 TYPICAL WILSON PLOTS OF SANTOWAX WR, TH7 DATA

b. For the Santowax WR, TH6, data, a value of b = 0.8 is slightly preferred because these intercepts fall on both sides of 1/U = 0.

c. For the Santowax WR, TH7, data, the value of b = 0.8 gives intercepts closer to 1/U = 0.

In conclusion, the Wilson plots indicate that there was no scale buildup on Test Heater 6, over a period of three years, and that a Reynolds Number exponent of 0.8 is slightly preferred for the correlation of the heat transfer data.

7.10 Nomenclature

A	area for heat transfer	ft^2
a,b,c,d,e	constants used in Equations (4) and (40)	
c_p	specific heat	BTU/lb_m-^oF
D	diameter	ft.
E	defined E_H/E_M	
E_H	Eddy diffusivity of heat, defined by Equation (5)	
E_M	Eddy diffusivity of momentum, defined by Equation (6)	
f	friction factor defined by Equation (23)	
f_F	Fanning friction factor = f/4	
G	mass velocity = ρV_m	$lb_m/hr-ft^2$
g_o	constant	4.17×10^8 lb_m-ft/lb_f-hr^2
h	heat transfer coefficient	$BTU/hr-ft^2-^oF$
h_f	film heat transfer coefficient	$BTU/hr-ft^2-^oF$
h_s	scale heat transfer coefficient	$BTU/hr-ft^2-^oF$
I	current	ampere
j	Colburn heat transfer factor defined by Equation (2)	
j^*	modified Colburn heat transfer factor defined by Equation (18)	
k	thermal conductivity of coolant	$BTU/hr-ft-^oF$
k_s	thermal conductivity of stainless steel tube wall	$BTU/hr-ft-^oF$

L	length	ft.
m	mass rate of flow	lb_m/hr
Q	heat produced in test heater	BTU/hr
Q_{down}	heat into coolant, downstream half of test heater	BTU/hr
Q_{in}	heat into coolant $\equiv Q - Q_{loss}$	BTU/hr
Q_{loss}	heat loss from test heater	BTU/hr
Q_{up}	heat into coolant, upstream half of test heater	BTU/hr
R	electric resistance	ohms
r	radius of tube	ft.
r_i	radius at wall, inside	ft.
r_o	radius at wall, outside	ft.
r_W	radius at wall	ft.
S	cross sectional area for flow	ft^2
T	temperature	^oF
T_B	temperature fluid bulk	^oF
$\overline{T_B}$	temperature defined by Equation (32)	^oF
$\overline{T_{B_{down}}}$	average bulk temperature, downstream half of test heater	^oF
$\overline{T_{B_{up}}}$	average bulk temperature, upstream half of test heater	^oF
T_c	temperature at center line of tube	^oF
T_W	temperature of heater wall	^oF
T_{Wi}	temperature wall, inside	^oF

T_{Wo}	temperature wall, outside	^{o}F
U	over-all heat transfer coefficient	$BTU/hr\text{-}ft^2\text{-}^{o}F$
V	velocity	ft/hr
V_m	velocity, mean fluid	ft/hr
y	distance from the wall in the radial direction	ft.

GREEK

β	$-1/\rho \frac{\partial \rho}{\partial T}$	$^{o}F^{-1}$
ΔE	voltage drop	volt
ΔP	pressure drop	lb_f/ft^2
ΔT_f	temperature drop across film	^{o}F
ΔT_m	$(T_{Wi}-T_B)$ = mean temperature difference for a given test heater section	^{o}F
μ	viscosity	$lb_m/hr\text{-}ft$
ρ	mass density	lb_m/ft^3
ρ_e	electric resistivity	ohm-ft
σ	one standard deviation	
τ	shear stress	lb_f/ft^2

SUBSCRIPTS

B	indicates properties at bulk temperature
f	indicates properties at a film temperature $\equiv 1/2\ (T_{Wi}+T_B)$
i	indicates inside
m	indicates mean properties or value

o	indicates outside
W	indicates located at wall or that properties evaluated at wall temperature

DIMENSIONLESS GROUPS

Gr	Grashof Number, $g_o \beta \Delta T_f D^3 \rho^2/\mu^2$
Nu	Nusselt Number, UD/k
Pr	Prandtl Number, $c_p \mu/k$
Re	Reynolds Number, $\rho V_m D/\mu$
St	Stanton Number, Nu/Pr Re = $h/c_p G$

NOMENCLATURE USED ON FIGURE 4 FROM REFERENCE (14)

dV/Z	124 Re_B
Ud/k	12 Nu
cZ/k	Pr/2.42

7.11 References

1. Makens, R. F., et. al., "Organic Coolant Summary Report," AEC Report No. 100-11401, December 1964.

2. Morgan, D. T. and Mason, E. A., "The Irradiation of Santowax OMP in the MIT In-Pile Loop," MITNE Report #22, October 5, 1961.

3. Sawyer, C. D. and Mason, E. A., "The Effects of Reactor Irradiation on Santowax OMP at 610°F and 750°F," MITNE 39, September 1963.

4. Silverberg, M. and Huber, D. A., "Forced Convection Heat Transfer Characteristics of Polyphenyl Reactor Coolants," NAA-SR-2796, Atomics International, January 1959.

5. Stone, J. P., et. al., "Heat Transfer Studies on Some Stable Organic Fluids in a Forced Convection Loop," Journal of Chemical and Engineering Data, 7, 519-529, October 1962.

6. Anonymous, "Proprietes Thermiques Des Polyphenyls," Final Report, April 1963, Grenoble.

7. McAdams, W. H., "Heat Transmission," Third Edition, McGraw-Hill, 1954.

8. Colburn, A. P., "A Method of Correlating Forced Convection Heat Transfer Data and a Comparison with Fluid Friction," Trans. AIChE, 29, 174-220, 1933.

9. Sieder, E. N. and Tate, G. E., Ind. Eng. Chem., 28, 1429-1436, 1936.

10. Bessouat, R., et. al., "Études Thermiques sur les Caloporteurs Organiques," Paper presented at 7th Nuclear Congress, Rome, June 1962.

11. Martinelli, R. C., Trans. ASME, 69, 947-959, 1947.

11a. McAdams, W. H., "Heat Transmission," Second Edition, McGraw-Hill, 1942.

12. Rohsenow, W. M. and Choi, H., "Heat, Mass and Momentum Transfer," Prentice-Hall, Inc., 1961.

13. Giedt, W. H., "Principles of Engineering Heat Transfer," D. Van Nostrand Company, Inc., 1957.

14. Dittus, F. W. and Boelter, L. M. K., "University of California Publications in Engineering," 2, p. 443, 1930.

15. McAdams, W. H., "Heat Transmission," First Edition, McGraw-Hill, 1933.

16. Sherwood, T. K. and Petrie, J. M., Ind. Eng. Chem., 24, 736-745, 1932.

17. Boelter, L. M. K., Martinelli, R. C. and Jonassen, F., Trans. ASME, 63, 447-455, 1941.

18. Swan, A. H., Memorandum on Operation of Test Heater 7, MIT Internal Memo, August 1965.

19. Moody, L. F., Trans. ASME, 66, 671-684, 1944.

20. Elberg, S. and Fritz, G., "Physical Properties of Organic Nuclear Reactor Coolants," Euratom Report No. 400e, 1963.

21. Chavanel, et. al., "Compilation Des Mesures De Densite Et Viscosite Du Terphenyle OM2 Irradie En Pile," Euratom Report No. 1.3-673, April 1964.

22. Swan, A. H., "A Discussion of the Correlation of Santowax OMP Heat Transfer Data," MIT Course 2.521 Term Paper, January 1963.

23. Driver-Harris Co., "Nichrome and Other High Nickel Electrical Alloys," Catalog R-46, 1947.

24. Bergles, A. E. and Rohsenow, W. M., "Forced-Convection Surface-Boiling Heat Transfer and Burnout in Tubes of Small Diameter," MIT Report No. 8767-21, May 25, 1962.

25. Ziebland, H. and Burton, J. T. A., "The Thermal Conductivity of Santowax R Between 155 and 400°C," AERE/X/PR2653, Harwell, June 1959.

26. Bowling, R. W., et. al., "Measurements of the Specific Heats of Santowax R, Para-, Meta, and Ortho-Terphenyl, Dyphenyl and Dowtherm A.-," United Kingdom Atomic Energy Authority, December 1960.

27. Swan, A. H., "MIT Laboratory Notebook," 3 Volumes, June 1964 to July 1965.

28. Gerke, R. H. J., Martini, W. R., et. al., "Proceedings of the Organic Cooled Reactor Forum," Oct. 6-7, 1960, NAA-SR-5688.

29. "Organic Reactor Heat Transfer Manual," NAA-SR-MEMO-7343, December 1962.

30. Mason, E. A., et. al., "In-Pile Loop Irradiation Studies of Organic Coolant Materials," MITNE 41, December 1963.

31. Grove-Palmer and Pass, H., "Heat Transfer Properties of Santowax WR," Nuclear Power, 4, 181-121, December 1959.

32. Ewing, C. T., et. al., "Heat Transfer Studies on a Forced Convection Loop with Biphenyl and Biphenyl Polymers," NRL Report 4990, November 13, 1957, also Ind. Eng. Chem., 50, 895-902, 1958.

33. Judd, R. L., "Design of an Organic Heat Transfer Experiment," R58CAP43, Canadian General Electric Company, Ltd.

34. Wilson, E. E., Trans. ASME, 37, 47, 1915.

35. Maurer, G. W. and LeTourneau, B. W., "Friction Factors for Fully Developed Turbulent Flow in Ducts With and Without Heat Transfer," ASME Paper No. 63-WA-98.

36. Allen, R. W. and Eckert, E. R. G., "Friction and Heat Transfer Measurements to Turbulent Pipe Flow of Water (Pr = 7 and 8) at Uniform Heat Flux," Transactions of ASME Journal of Heat Transfer, p. 301, August 1964.